FIELD SIMULATION OF WASTE IMPOUNDMENT SEEPAGE IN THE VADOSE ZONE: NON-REACTIVE SOLUTE TRANSPORT THROUGH A STRATIFIED, UNSATURATED FIELD SOIL

by
Kevin G. Flanigan

Robert S. Bowman
Daniel B. Stephens

Hydrology Report No. H89-8
(Formerly Open File Report No. 89-8)

NEW MEXICO TECH HYDROLOGY REPORT SERIES

HYDROLOGY PROGRAM
SOCORRO, NEW MEXICO 87801

September 1989

This report was also submitted by Kevin G. Flanigan as an Independent Study in partial fulfillment of the requirements of the M.S. Degree in Hydrology

Research sponsored by:
Generic Waste and Recovery Center of the United States Bureau of Mines Under Contract No. G1175132-3521

FIELD SIMULATION OF WASTE IMPOUNDMENT SEEPAGE IN THE VADOSE ZONE: NON-REACTIVE SOLUTE TRANSPORT THROUGH A STRATIFIED, UNSATURATED FIELD SOIL

by

Kevin G. Flanigan

Submitted in Partial Fulfillment of
the Requirements for the Degree of
Master of Science in Hydrology

New Mexico Institute of Mining and Technology
Socorro, New Mexico

September, 1989

ABSTRACT

A long-term field experiment was conducted to simulate seepage from a waste impoundment into the unsaturated zone. The field site is highly stratified and heterogeneous, being located in an old arroyo channel which has been diked off from runoff events. It consists of two major facies, an upper unit comprised of alluvial silts and sands with interspersed cobble layers, and a lower unit consisting of well sorted fine to coarse fluvial sands.

Water was applied through a drip emitter system covering an area of 10-m by 10-m at a flux of approximately 1×10^{-5} cm/s from January of 1987 to August of 1989. This flux was approximately one percent that of the lowest saturated hydraulic conductivity found at the site. Water movement was monitored by neutron logging and a system of tensiometers. Water movement was found to be controlled by the geology of the site, due to anisotropy and differences in hydraulic properties at stratigraphic interfaces.

Part of the experiment consisted of the injection of the non-reactive tracer bromide into the drip system. After more than one year of constant flux application the flow field was determined to be at steady-state and a 5870 L slug of bromide at a concentration of 435 ppm was added to the plot over a period of 6.3 days during late February and early March, 1988. The horizontal and vertical movement of

the bromide was monitored by the use of porous cup samplers. Bromide was detected as far as 6 meters outside the plot at a depth of 5.6 meters after approximately 150 days.

Directly beneath the plot (1.07 to 3.20 meters below the drip lines) complete bromide breakthrough curves were obtained and analyzed using the one-dimensional solute transport code CXTFIT (Parker and van Genuchten, 1984a). Transport parameters were determined, including an average dispersivity of 12.1 cm. This value agrees with results from other unsaturated field studies at the same scale.

Accelerated transport of the tracer was observed, with the average tracer velocity being about 1.3 times greater than the average pore water velocity determined from known experimental parameters. This accelerated flow appeared to be due to both the existence of mobile-immobile water flow, and anion exclusion, as verified by simulating the field experiment in unsaturated laboratory columns. Retardation factors for bromide in the range of 0.8 were obtained from the unsaturated columns, indicating significant anion exclusion. The breakthrough curves could be fitted by assuming that approximately 26% of the soil water in the plot existed as immobile water.

The data from this experiment may be useful for the validation of solute transport codes in the unsaturated zone.

TABLE OF CONTENTS

LIST OF FIGURES

LIST OF TABLES

NOMENCLATURE

SYMBOL	QUANTITY	DIMENSIONS
A	Area	L^2
c_m	Dimensionless solute concentration in the mobile water phase	---
c_{im}	Dimensionless solute concentration in the immobile water phase	---
C	Solute concentration	M/L^3
C_{im}	Solute concentration in the immobile water phase	M/L^3
C_f	Flux concentration	M/L^3
C_m	Solute concentration in the mobile water phase	M/L^3
C_o	Solute concentration of the applied tracer solution	M/L^3
C_r	Resident concentration	M/L^3
d	Average particle diameter	L
D	Coefficient of hydrodynamic dispersion	L^2/T
D_l	Coefficient of hydrodynamic dispersion in the longitudinal direction	L^2/T
D_m	Coefficient of hydrodynamic dispersion in the mobile zone	L^2/T
D'	Coefficient of mechanical dispersion	L^2/T
D^*	Coefficient of molecular diffusion in porous media	L^2/T
D_o	Coefficient of molecular diffusion in bulk water	L^2/T
f	Fraction of the sorption sites which equilibrate with the mobile liquid phase	---
J	Solute flux	M/L^2T
$J_{D'}$	Dispersive flux	M/L^2T
J_D^*	Diffusive flux	M/L^2T

J_i	Solute flux into elemental volume	M/L^2T
J_o	Solute flux out of elemental volume	M/L^2T
K_d	Linear isotherm distribution constant	L^3/M
L	Straight line path length	L
L_e	Effective path length	L
m	Constant	---
M_{ev}	Solute mass within elemental volume	M
M_i	Tracer input mass	M
M_r	Recovered mass	M
M_s	Solute mass undergoing reactions within elemental volume	M
n	Number of observed data points	---
P	Peclet number	---
P_c	Column Peclet number	---
P'	Peclet number of the mobile water phase	---
q	Specific discharge	L/T
Q	Flow rate	L^3/T
R	Retardation factor	---
R_m	Retardation factor of the mobile water phase	---
R_{im}	Retardation factor of the immobile water phase	---
R_s	Residual sum of the squares	---
S	Adsorbed concentration	M/M
S_T	Slope of the BTC at R pore volumes	M/L^3T
t	Time	T
T	Pore volumes	---
T_o	Duration of input tracer pulse	T

v	Pore water velocity	L/T
v_m	Pore water velocity of the mobile water phase	L/T
v'	Pore water velocity calculated from experimental parameters	L/T
x	Distance in x-direction	L
y	Distance in y-direction	L
z	Distance in z-direction	L
Z	Dimensionless distance	---
α	Dispersivity	L
α_{lm}	Longitudinal dispersivity in the mobile zone	L
α_m	Dispersivity in the mobile zone	L
β	Dimensionless transport parameter in the mobile-immobile water model	---
ϵ	Mass transfer coefficient between the mobile and the immobile water phases	T^{-1}
θ	Volumetric water content	L^3/L^3
θ_m	Volumetric water content in the mobile water phase	L^3/L^3
θ_{im}	Volumetric water content in the immobile water phase	L^3/L^3
ϕ	Fraction of mobile water	---
π	Constant	---
ρ	Density	M/L^3
τ	Tortuosity factor in saturated porous media	---
τ'	Tortuosity factor in unsaturated porous media	---
ω	Dimensionless mass transfer coefficient	---

ACKNOWLEDGEMENTS

Funds for this research were provided by the Generic Waste and Recovery Center of the United States Bureau of Mines under Contract No. G1175132–3521 to the New Mexico Institute of Mining and Technology.

The following individuals contributed to this research: Earl Mattson, Alva Parsons, Rolf Schmidt–Peterson, Dave Grabka, Ann Stark, Warren Cox, Ken Black, Bob Friesen and Grady Rhodes.

ACKNOWLEDGMENTS

Funds for this research were provided by the Generic Waste and Recovery Center of the United States Bureau of Mines under contract no. G1175132-3521 to the New Mexico Institute of Mining and Technology. I am the third Master's student to complete his program using results from this project.

I wish to express my gratitude to my advisors, Rob Bowman and Dan Stephens, for their support and guidance during my stay at New Mexico Tech.

Other graduate students who worked on the project while I was at Tech were Earl Mattson, Alva Parsons, Rolf Schmidt-Petersen, Dave Grabka, Ann Stark, and Warren Cox. And even though he dropped the ball, Ken Black carried it pretty well while he was here. Student workers who performed above the call of duty were Bob Friesen and Grady Rhodes.

Thanks are due my office mates Todd Stein, James Beach and Mike Wei for their encouragement in the face of adversity. Thanks also to the rest of the students and faculty of the Hydrology program.

I especially wish to thank my family for their strong emotional and financial support during my college career.

Also deserving of gratitude are the Magdalena Mountains for being so close and accessible. I might not have survived my stay in Socorro without their presence.

I. INTRODUCTION

The movement of solutes through the unsaturated and the saturated zones is a topic which has experienced increased interest in recent years. It has always been an important topic to soil scientists and agronomists, but with the increasing number of incidents of contamination of soil and groundwater by toxic and hazardous substances, it is becoming an important topic to the general public as well.

As the usage of chemicals for agricultural and industrial purposes increases, and the volume of waste material requiring disposal also increases, the potential for soil and groundwater contamination increases. This contamination can pose a serious threat to public health. Since groundwater moves slowly in both the saturated and the unsaturated zones, contaminated soils and aquifers may remain so for long periods of time. Remediation of these contaminated areas can be extremely costly. Groundwater may also transport contaminants to surface waters via stream-aquifer interaction, or via seeps and springs, further endangering public health.

For these reasons the movement of contaminants in the unsaturated zone requires further understanding so that prevention of groundwater contamination, instead of remediation, may be the goal of environmental professionals and government agencies.

Recent theories and experiments have suggested that stratification and heterogeneity in the unsaturated zone may cause multi-dimensional flow. Miller (1963) observed

lateral flow beneath a 3-m x 3-m irrigation test plot consisting of a fine layer of silty loam over a coarse textured layer of sand and gravel. Crosby et al. (1968, 1971) described significant lateral movement of water and pollutants from a septic tank drain field in a stratified sand. Rouston et al. (1979) reported extensive lateral movement of seepage from a waste storage tank in a stratified glacial-fluvial environment. Palmquist and Johnson (1962) observed lateral movement at textural interfaces in laboratory experiments utilizing glass beads of various sizes as the porous medium. Heerman (1986) conducted a laboratory experiment using a sand tank containing several alternating layers of fine and medium sand. Controlled unsaturated infiltration was introduced as a point source at a constant rate. He observed significant advance of the wetting front in the horizontal direction, with a faster rate of advance in the fine layers compared to the medium layers.

Other research has shown that anisotropy also contributes to multi-dimensional flow in the unsaturated zone. Stephens and Heerman (1988) demonstrated that the lateral movement observed in the experiment described above (Heerman, 1986) was due to anisotropy and the initial moisture content of the porous medium. Studies by Mualem (1984), and Yeh et al. (1985) also suggest that anisotropy is a function of the degree of saturation. This was also demonstrated by McCord and Stephens (1987)

in a field study conducted in a homogeneous field soil having little or no stratification.

In arid and semi-arid climates, the unsaturated zone may be on the order of 10's of meters thick. Leachate from mill tailing impoundments, landfills, and other waste repositories located in these climates may seep for long distances and long periods of time before reaching the water table. Understanding the direction and rate of this seepage are the goals of groundwater hydrologists applying numerical models to these situations. Previously, most unsaturated flow models contained provisions for flow occurring in only one direction - downwards. Recent codes contain provisions for multi-dimensional flow (VAM2D, P.S. Huyakorn, H.O. White, and L.L. Wadsworth, HydroGeoLogic, Inc., Herndon, VA; FEMWATER, G.T. Yeh, Oak Ridge National Laboratory Technical Report ORNL-5567; UNSAT2, S.P. Neumann and L.A. Davis, U.S. Nuclear Regulatory Commission Technical Report NUREG-CR-3390), but have not been tested against actual field data for validation of their predictions.

Few unsaturated solute transport field studies have been conducted due to the time and expense involved. Warrick et al. (1971) applied 3 inches of a calcium chloride solution to the surface of a 1-m^2 plot followed by 9 inches of solute-free infiltration water, and utilized porous cup samplers to obtain breakthrough curves for the chloride. The soil was a uniform clay loam. Van de Pol

(1974) conducted an experiment on an 8-m x 8-m plot under steady state flow conditions. He used chloride and tritium as tracers in a layered soil consisting of a silty clay over a medium sand. He observed significant anion exclusion of the chloride and some retardation of the tritium. Kies (1981) conducted a similar experiment on a 7-m x 7-m plot under steady state flow conditions. The soil consisted of various layers of silts and sands, with some clays. He used chloride, nitrate, and tritium as tracers, and followed their movement through the unsaturated zone into the saturated zone. He observed increasing velocities with depth, and substantial accelerated transport of the solutes. Jury et al. (1982) conducted a large-scale (80-m x 80-m) field experiment in a loamy sand. They applied a 1-cm pulse of bromide solution by a sprinkler system followed by 93-cm of precipitation over a 100 day period. They monitored the downward movement of the bromide via porous cup samplers. The purpose of their experiment was to validate the stochastic transfer function model of Jury (1982), which predicts one-dimensional solute transport. Bowman and Rice (1986) conducted a large-scale (48.8-m x 128-m) field experiment in an agricultural soil consisting of a sandy loam. They sprayed the field with a solution containing the moderately retarded herbicide bromacil and the tracer pentafluorobenzoic acid in between periodic irrigation floodings. They used destructive sampling techniques to

monitor the transport of the solutes, and observed significant accelerated transport of both species due to preferential flow paths.

On the campus of the New Mexico Institute of Mining and Technology, Socorro, New Mexico, a controlled, long term field experiment has been in progress since January of 1987 (Figures 1-1 and 1-2). The experiment utilizes a drip irrigation system to simulate the seepage of leachate from a waste impoundment into the unsaturated zone. The goals of this experiment were to: 1.) investigate the importance of lateral movement of seepage in the unsaturated zone due to soil stratification and heterogeneity. 2.) determine the capability of analytical and numerical models to predict water and tracer movement in the unsaturated zone. 3.) develop practical guidelines for sampling and characterizing hydraulic properties in the unsaturated zone. 4.) evaluate the dispersive and sorptive characteristics and other solute transport parameters of the site. This investigation does not attempt to address all of these goals.

The site chosen for the experiment lies in an arroyo bottom which has been diked off from runoff events. It is highly stratified and heterogeneous, with an upper zone of alluvial silts and sands containing interspersed cobble layers, and a lower zone of fluvial sands. Depth to the water table at the start of the experiment was approximately 24 meters. The site had never been

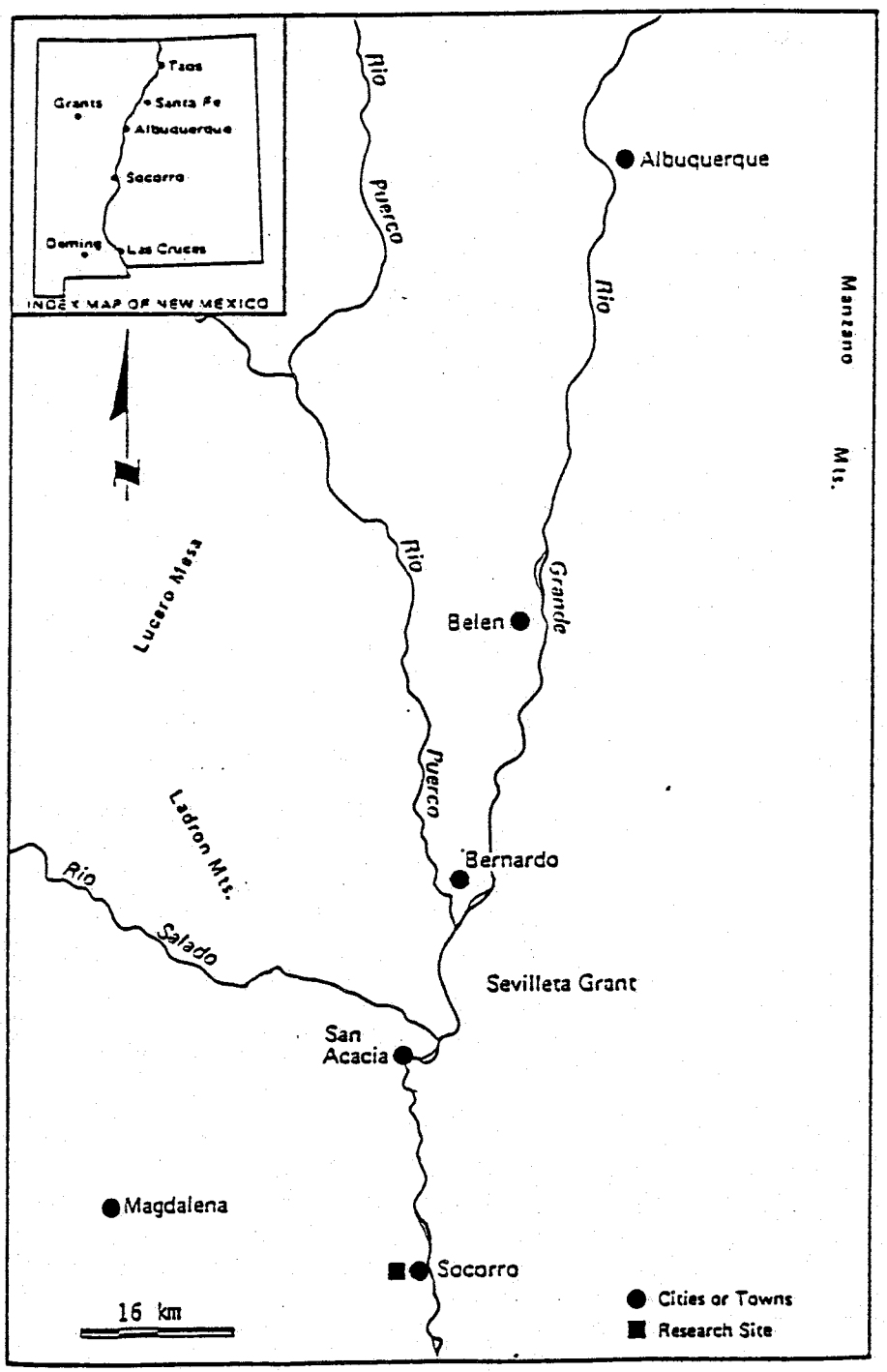

FIGURE 1-1. Index map.

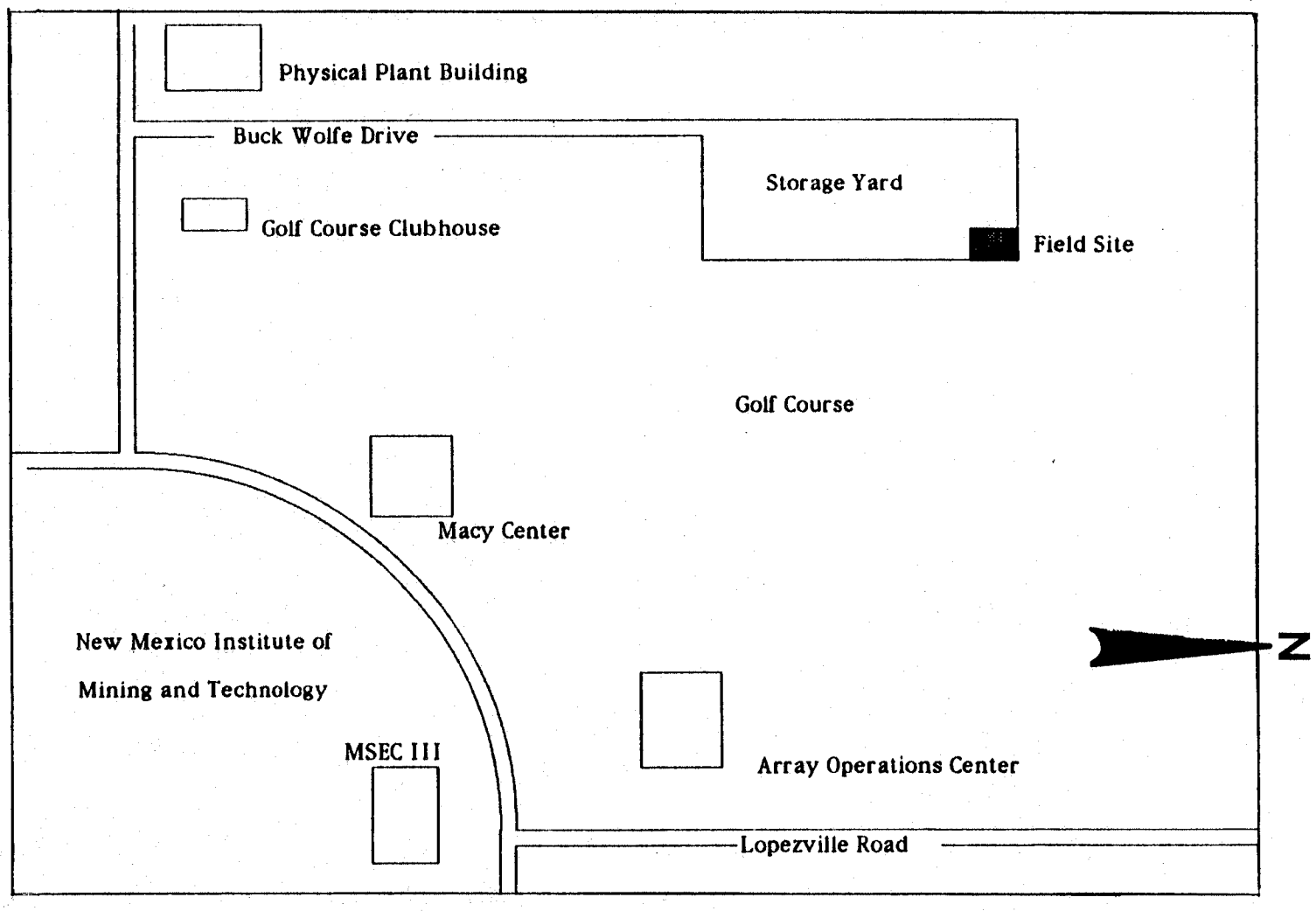

FIGURE 1-2. Site location map. (Not to scale).

irrigated prior to the experiment. Similar geological and hydrological conditions are common throughout the western half of the United States.

Part of this experiment consisted of the injection of a non-reactive tracer, anionic bromide, into the system and monitoring its movement in both the vertical and horizontal directions.

This report describes the solute transport experiment at the New Mexico Tech site, and the resulting observations. Following these observations, it became necessary to conduct unsaturated solute transport experiments in laboratory columns, using soil from the field site, to determine the nature of the transport mechanisms observed at the site. These experiments and results are also described in this report.

This chapter has provided an introduction to the experiment and discussed prior pertinent research. Chapter two provides a background in solute transport processes, particularly for the unsaturated zone. The third chapter describes the experiment, detailing the methodology. Chapter four discusses the resulting observations, and chapter five provides a summary and presents the conclusions drawn from the observations.

In a related report, Parsons (1988) provides details on the characterization of the hydraulic and geologic properties of the site, and applies a one-dimensional analytical model to the observed moisture movement.

Mattson (1989) provides detail on the experimental design and construction, and applies a two-dimensional analytical model to the observed moisture movement.

II. THEORETICAL

SOLUTE TRANSPORT PROCESSES

The movement of solutes through a porous medium is controlled by several different processes - advection, mechanical dispersion and molecular diffusion. Advection is the component of solute transport attributed to the bulk motion of the flowing groundwater. Advection is sometimes referred to as convection, but the use of this term should be discouraged since it implies transport due to temperature induced density gradients.

Mechanical dispersion is the mixing which occurs during fluid advection. It is important on both the microscopic and the macroscopic levels. On the microscopic scale mechanical dispersion results from three mechanisms. The first of these mechanisms is the difference of individual fluid particle velocities in a pore channel resulting from greater friction between particles adjacent to the pore surfaces than those particles in the center. The second is the difference in bulk fluid velocities between pore channels of different sizes. This results from differences in surface area and roughness of different pore channels. The third mechanism is related to the tortuosity, branching and interfingering of pore channels. This results in fluctuations in streamlines with respect to the average flow direction. These three mechanisms are illustrated in Figure 2-1.

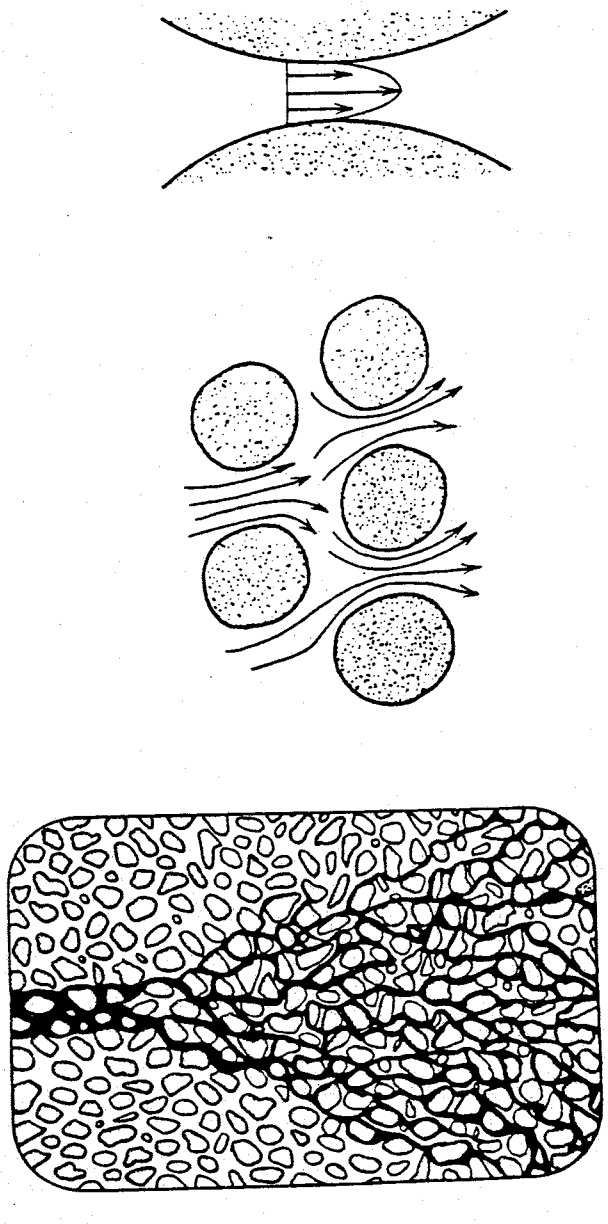

FIGURE 2-1. The three mechanisms of mechanical dispersion (from Freeze and Cherry, 1979).

Mechanical dispersion is quantified by the coefficient of mechanical dispersion, D', and can be described by

$$J_{D'} = - D'(\theta) \frac{\partial C}{\partial x} \qquad (2.1)$$

where $J_{D'}$ = the dispersive flux,

θ = the volumetric water content,

C = the solute concentration in the aqueous phase, and

x = the distance in the x-direction.

The coefficient of mechanical dispersion is a function of the fluid velocity, the degree of saturation, and the dispersivity, α. Various authors have found that they can be related by the empirical relationship

$$D' = \alpha v^m \qquad (2.2)$$

where m = constant, and

v = the pore water velocity:

$$v = q/\theta \qquad (2.3)$$

where q = the specific discharge.

Dispersivity is a characteristic property of the porous medium with dimensions of length (commonly expressed in centimeters). It is a function of the geotechnical

properties of the porous medium, i.e., grain size distribution, aggregation, etc.

The constant m is empirically determined and usually varies between 1 and 2. Yule and Gardner (1978) determined that, for an unsaturated soil, m is dependent on θ and the type of soil present. Scheidegger (1961) found that when molecular diffusion is neglected, m = 1. This is generally accepted to be true and the coefficient of mechanical dispersion is taken to be just

$$D' = \alpha v \tag{2.4}$$

Molecular diffusion results from random thermal-kinetic motion of ions or molecules. Molecular diffusion is quantified by the coefficient of molecular diffusion in a porous medium, D^*, and can be described by

$$J_D^* = - D^*(\theta) \frac{\partial C}{\partial x} \tag{2.5}$$

where J_D^* = the diffusive flux.

The coefficient of molecular diffusion in porous media, D^*, consists of

$$D^* = D_0 \tau \tag{2.6}$$

where D_0 = the coefficient of molecular diffusion in bulk water, and

τ = the tortuosity factor.

The tortuosity factor corrects for the obstructing effect of the porous medium and is defined as (Carman, 1937)

$$\tau = \left(\frac{L}{L_e}\right)^2 \qquad (2.7)$$

where L = the straight line path length for a diffusing molecule, and

L_e = the actual path length for a diffusing molecule.

The tortuosity factor commonly ranges from 0.01 to 0.5 for non-adsorbed ions in porous geologic materials (Freeze and Cherry, 1979).

Molecular diffusion and mechanical dispersion are collectively called hydrodynamic dispersion. Dispersion occurs in both the longitudinal (the direction of bulk fluid flow) and the transverse (at right angles to the bulk fluid flow) directions (Figure 2-2). Dispersion is an important phenomenon because it results in the spreading and dilution of solute, or contaminant, in ground water. The contaminant will therefore occupy a greater volume of the porous medium than would be predicted solely from advective transport (Figure 2-2). Dispersion will cause a contaminant to arrive at a point of interest (such as the water table or a well) prior to the arrival time calculated from purely advective transport. Hydrodynamic dispersion

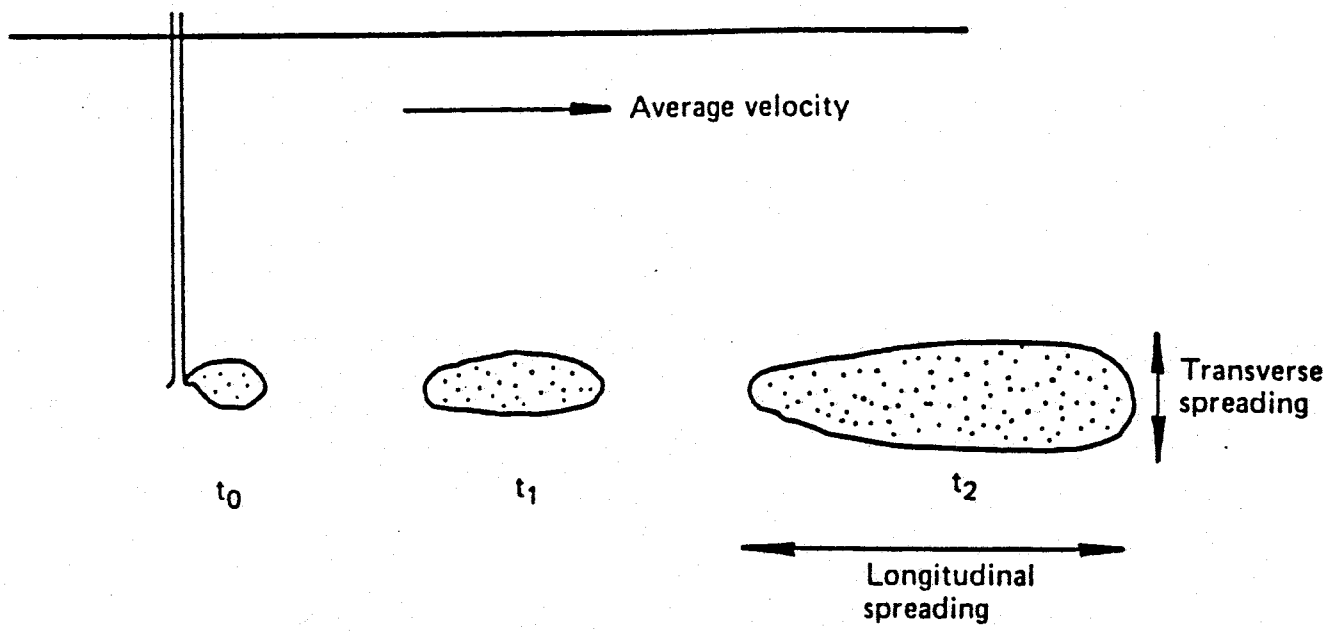

FIGURE 2-2. Longitudinal and transverse dispersion (from de Marsily, 1986).

is quantified by the coefficient of hydrodynamic dispersion, D, where

$$D = D' + D^* \qquad (2.8)$$

Molecular diffusion is generally neglected in the field of solute transport in porous geologic materials since it it is typically one or two orders of magnitude smaller than mechanical dispersion at velocities commonly seen in field and laboratory studies. This point is illustrated in Figure 2-3. The quantity vd/D^* in Figure 2-3 is called the Peclet number (P), where d is the average particle diameter. At pore water velocities commonly seen in the saturated zone, the values of P are well within the portion of the curve where mechanical dispersion dominates. At pore water velocities commonly seen in the unsaturated zone, the values of P range from the portion of the curve where transition conditions exist to that portion where mechanical dispersion dominates. In this example, the Peclet number defines the ratio between the rate of transport by advection to the rate of transport by molecular diffusion.

Hydrodynamic dispersion is the result of both microscopic and macroscopic processes. On the macroscopic scale dispersion results from the presence of large scale heterogeneities within a porous medium. The existence of macroscopic dispersion was first demonstrated by Skibitzkie

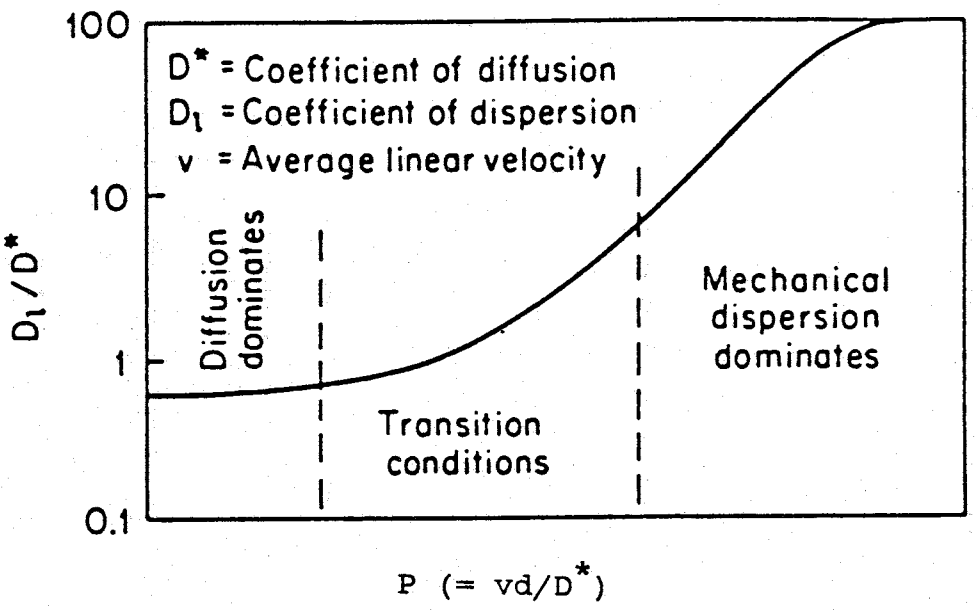

FIGURE 2-3. Relation between the porous medium Peclet number and the ratio of the longitudinal hydrodynamic dispersion coefficient to the coefficient of molecular diffusion in a uniform sand (from Freeze and Cherry, 1979).

and Robinson (1963) with a dye tracer experiment performed in a heterogeneous sand box. They demonstrated that lenses of high permeability material interspaced within a matrix of lower permeability material caused the spreading of a stream of dye as the dye and water moved through the sand box (Figure 2-4). The amount of macroscopic dispersion exhibited by a porous medium is dependent upon the size and amount of these heterogeneities, and more specifically, the variation of hydraulic conductivity within these areas of heterogeneity.

THE ONE-DIMENSIONAL ADVECTION-DISPERSION EQUATION

The derivation of the equation governing solute transport in porous media (commonly known as the advection-dispersion equation) is based upon the law of conservation of mass applied to an elemental volume (Figure 2-5),

$$\Delta M_{ev} = J_o - J_i \pm \Delta M_s \qquad (2.9)$$

where ΔM_{ev} = the net rate of change of mass of solute within the elemental volume,

J_o = the flux of solute out of the elemental volume,

J_i = the flux of solute into the elemental volume, and

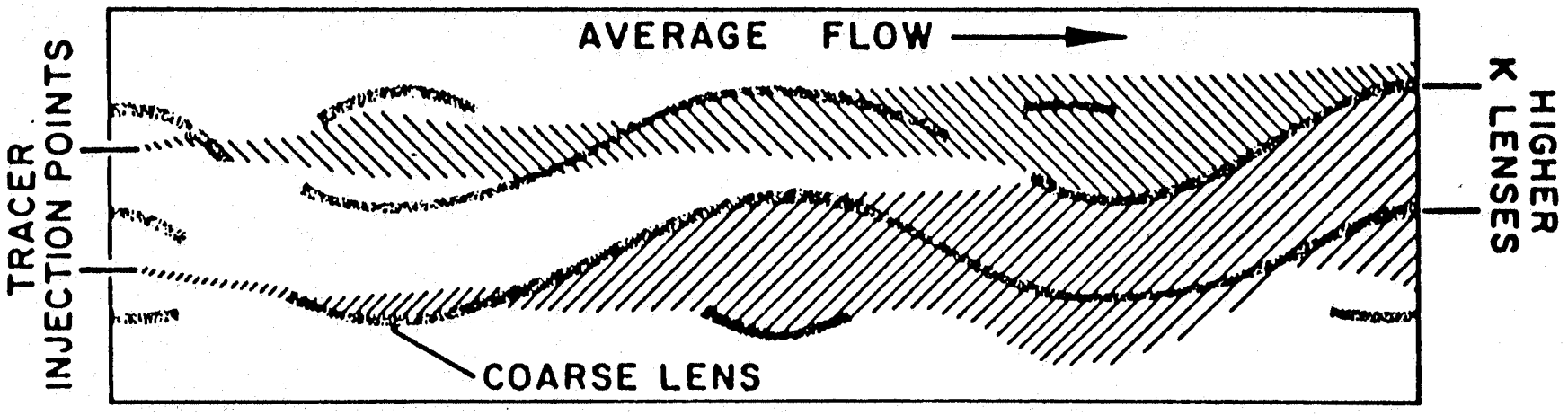

FIGURE 2-4. Demonstration of macroscopic dispersion by Skibitzkie and Robinson, 1963 (from Anderson, 1984).

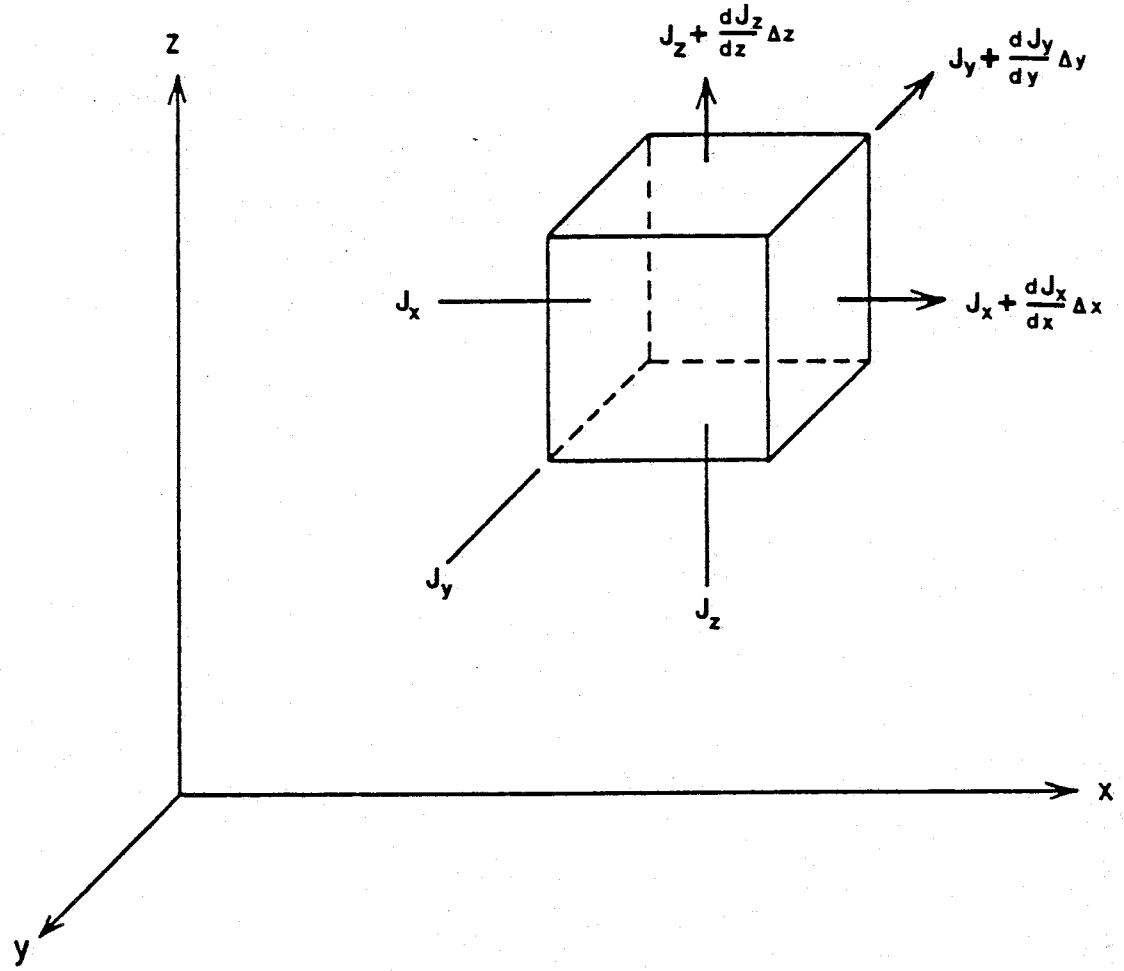

FIGURE 2-5. Elemental volume (adapted from Freeze and Cherry, 1979).

ΔM_s = loss or gain of solute mass due to reactions within the elemental volume.

Assuming that the porous medium is homogeneous and isotropic, the flow is steady-state, and that Darcy's law is applicable, the advection-dispersion equation (for one dimension) may be derived as follows.

Consider transport due to mixing first. For the X-direction

$$J_o = J_i + \frac{\partial J}{\partial x}\Delta x \qquad (2.10)$$

The rate of change of solute mass in the elemental volume, ΔM_{ev}, is

$$\Delta M_{ev} = (J_i - J_o)\Delta y \Delta z \qquad (2.11)$$

Substituting 2.10 into 2.11 yields

$$\Delta M_{ev} = \left[J_i - (J_i + \frac{\partial J}{\partial x}\Delta x)\right] \Delta y \Delta z$$

or

$$\Delta M_{ev} = - \frac{\partial J}{\partial x}\Delta x \Delta y \Delta z \qquad (2.12)$$

Now the volume of water within the elemental volume may be written as

$$\theta(\Delta x \Delta y \Delta z)$$

The total amount of solute within the elemental volume then is

$$C\theta(\Delta x \Delta y \Delta z)$$

where C = solute concentration.

Then ΔM_{ev} may also be written as

$$\Delta M_{ev} = \frac{\partial(C\theta)\Delta x \Delta y \Delta z}{\partial t} \qquad (2.13)$$

Equating 2.12 and 2.13 yields

$$\frac{\partial(C\theta)\Delta x \Delta y \Delta z}{\partial t} = -\frac{\partial J}{\partial x}\Delta x \Delta y \Delta z$$

or

$$\frac{\partial(C\theta)}{\partial t} = -\frac{\partial J}{\partial x} \qquad (2.14)$$

Now the solute flux, J, may also be defined as

$$J = -D_l(\theta)\frac{\partial C}{\partial x} \qquad (2.15)$$

Where D_l is the coefficient of hydrodynamic dispersion in the longitudinal direction.

Substituting 2.15 into 2.14 yields

$$\frac{\partial(C\theta)}{\partial t} = - \frac{\partial\left[-D_l(\theta)\frac{\partial C}{\partial x}\right]}{\partial x}$$

or

$$\theta\frac{\partial C}{\partial t} = D_l(\theta)\frac{\partial^2 C}{\partial x^2} \qquad (2.16)$$

Now consider transport due to advection. The flux of solute into and out of the elemental volume is $(qC)_i$ and $(qC)_o$, respectively. The net rate of change of solute mass in the elemental volume due to advection is

$$\frac{\partial(C\theta)}{\partial t}\Delta x\Delta y\Delta z = [(qC)_i - (qC)_o]\Delta y\Delta z \qquad (2.17)$$

Now

$$(qC)_o = (qC)_i + \frac{\partial(qC)}{\partial x}\Delta x \qquad (2.18)$$

Substituting 2.18 into 2.17 yields

$$\frac{\partial(C\theta)}{\partial t}\Delta x\Delta y\Delta z = \{(qC)_i - [(qC)_o + \frac{\partial(qC)}{\partial x}\Delta x]\}\Delta y\Delta z$$

or

$$\theta\frac{\partial C}{\partial t} = - q\frac{\partial C}{\partial x} \qquad (2.19)$$

The total transport is then obtained by combining 2.19 and 2.16 to yield

$$\theta \frac{\partial C}{\partial t} = D_l(\theta) \frac{\partial^2 C}{\partial x^2} - q \frac{\partial C}{\partial x} \qquad (2.20)$$

For the case where θ is constant, dividing by θ yields

$$\frac{\partial C}{\partial t} = D_l \frac{\partial^2 C}{\partial x^2} - v \frac{\partial C}{\partial x} \qquad (2.21)$$

Equation 2.21 is the common form of the one-dimensional advection-dispersion equation for non-reactive solute transport. This derivation ignores decay and/or production of solute due to such processes as radioactive decay, chemical precipitation and dissolution, or utilization by microbes. For the case of solutes which adsorb onto the solid matrix of the porous medium, another term must be introduced into the equation. Adsorption is the adhesion of a solute ion from the aqueous phase onto the solid surface with which it is in contact.

If we let S be the adsorbed concentration (mass of solute per unit mass of porous medium), then $\partial S/\partial t$ is a source or sink.

At constant θ we may write

$$\frac{\partial C}{\partial t} = D_l \frac{\partial^2 C}{\partial x^2} - v \frac{\partial C}{\partial x} - \frac{\partial S}{\partial t} \qquad (2.22)$$

To achieve dimensional consistency, and to express the adsorbed concentration as an equivalent solution concentration, the term $\partial S/\partial t$ must be multiplied by ρ/θ

$$\frac{\partial C}{\partial t} = D_l \frac{\partial^2 C}{\partial x^2} - v\frac{\partial C}{\partial x} - \frac{\rho \partial S}{\theta \partial t}$$

or

$$\frac{\partial C}{\partial t} + \frac{\rho \partial S}{\theta \partial t} = D_l \frac{\partial^2 C}{\partial x^2} - v\frac{\partial C}{\partial x} \qquad (2.23)$$

For the particular case where the solute adsorption is described by a linear isotherm (an isotherm is a plot of S vs. C)

$$S = K_d C \qquad (2.24)$$

where K_d is the slope of the linear isotherm.

Substituting 2.24 into 2.23 yields

$$\frac{\partial C}{\partial t} + K_d \left[\frac{\rho \partial C}{\theta \partial t}\right] = D_l \frac{\partial^2 C}{\partial x^2} - v\frac{\partial C}{\partial x}$$

or

$$\left[1 + K_d\left(\frac{\rho}{\theta}\right)\right]\frac{\partial C}{\partial t} = D_l \frac{\partial^2 C}{\partial x^2} - v\frac{\partial C}{\partial x} \qquad (2.25)$$

Introducing the term R, the retardation factor, where

$$R = 1 + K_d(\frac{\rho}{\theta}) \qquad (2.26)$$

and substituting into 2.25 yields

$$R \frac{\partial C}{\partial t} = D_l \frac{\partial^2 C}{\partial x^2} - v \frac{\partial C}{\partial x} \qquad (2.27)$$

The value of R is indicative of adsorption (R > 1), non-reactive solute transport (R = 1), or anion exclusion (R < 1). Anion exclusion is an electrochemical phenomenon exhibited mainly by soils with relatively high clay content. Anionic solutes are repelled by the negatively charged clay particles so that their concentrations are greater in the fast moving region of the velocity profile than in the slow moving region close to the solid particles. The net effect is accelerated transport of anionic solutes, resulting in their faster breakthrough.

Many different analytical solutions to Equation 2.27 are available. These solutions provide a means of determining transport parameters such as the coefficient of hydrodynamic dispersion and the pore water velocity from solute distribution data. The solutions differ depending upon the type of boundary and initial conditions which are applied. The type of boundary and initial conditions which best describe the experiment determines which analytical solution is to be used in analysis of data from either a laboratory column experiment or a field experiment.

Commonly used inlet boundary conditions are of two types: a first- or concentration-type and a third- or flux-type. The first-type boundary condition is

$$C(0,t) = C_0 \tag{2.28}$$

where C_0 = the concentration of the applied solution, and

t = time after solute application.

This condition assumes that the concentration is continuous across the solution-porous media boundary and that this concentration can be specified. This is not always possible in practice. Equation 2.28 assumes purely advective movement of solute into the porous medium. A more accurate description is provided by the third- or flux-type boundary condition

$$vC_0(0,t) = vC - D_1\frac{\partial C}{\partial x} \tag{2.29}$$

This condition includes both advective and dispersive movement of solute into the porous medium. This inlet boundary condition has been shown to be most correct in terms of conservation of mass (Parker and van Genuchten, 1984b). The lower boundary condition can be described by

$$\frac{\partial C}{\partial x}(\infty,t) = 0 \tag{2.30}$$

and the initial conditions by

$$C(x,0) = 0 \qquad (2.31)$$

Solutions to the one-dimensional advection-dispersion equation distinguish between two different concentration types (Parker and van Genuchten, 1984b). Resident concentration (C_r) is the mean fluid concentration of solute within a given volume of porous medium. Flux concentration (C_f) is the average solute concentration in the flowing fluid passing through a unit cross-sectional area. The two are related by

$$C_f = C_r - \frac{D_1}{v}\frac{\partial C_r}{\partial x} \qquad (2.32)$$

It is not clear which concentration mode is correct to use in experiments in which breakthrough curves (solute concentration vs. time or distance) are obtained by means of porous cup samplers (also known as suction lysimeters) or other extraction systems. The observed data are probably not strictly resident concentrations nor strictly flux concentrations (Parker and van Genuchten, 1984b).

Lapidus and Amundson (1952) developed a solution to the one-dimensional advection-dispersion equation (Equation 2.27) given Equations 2.28, 2.30, and 2.31

$$\frac{C_r}{C_0}(x,t) = \frac{1}{2}\mathrm{erfc}\left[\frac{Rx - vt}{2(D_1 Rt)^{0.5}}\right] + \frac{1}{2}\exp\left[\frac{vx}{D_1}\right]\mathrm{erfc}\left[\frac{Rx - vt}{2(D_1 Rt)^{0.5}}\right] \qquad (2.33)$$

Due to a failure to satisfy mass balance requirements, van Genuchten and Wierenga (1986) recommend this solution not be used for evaluating resident concentrations in semi-infinite field profiles, but rather that it be used for estimating flux concentrations at any point in the profile.

If the following dimensionless variables are introduced

$$T = \frac{vt}{L} \tag{2.34}$$

and

$$P_c = \frac{vL}{D_1} \tag{2.35}$$

where T = the number of pore volumes leached through the column, and

P_c = the column Peclet number,

then 2.33 may be written as

$$\frac{C_r}{C_0}(T) = \frac{1}{2}\text{erfc}\left[\left(\frac{P_c}{4RT}\right)^{0.5}(R - T)\right] \tag{2.36}$$

$$+ \frac{1}{2}\exp(P_c)\,\text{erfc}\left[\left(\frac{P_c}{4RT}\right)^{0.5}(R + T)\right]$$

Lindstrom et al. (1967) developed a solution to the one-dimensional advection-dispersion equation (Equation 2.27) given Equations 2.29, 2.30, and 2.31

$$\frac{C_r}{C_0}(T) = \frac{1}{2}\text{erfc}\left[\left(\frac{P}{4RT}\right)^{0.5}(R - T)\right] + \left(\frac{PT}{\pi R}\right)^{0.5}\exp\left[-\frac{P}{4RT}(R - T)^2\right]$$

$$- \frac{1}{2}(1 + P + \frac{PT}{R})\text{erfc}[(\frac{P}{4RT})^{0.5}(R + T)] \qquad (2.37)$$

This solution correctly evaluates in-situ resident concentrations in semi-infinite field plots and satisfies mass balance requirements. Solutions 2.33 and 2.37 will converge at large values of distance x, since the inlet boundary conditions (the only difference between the conditions) will have less influence at greater distances.

The two solutions listed above (Equations 2.33 and 2.37) are applicable only to the case where the solute is applied continuously at the inlet position. This is known as a step-type input. For a pulse- or slug-type input (an input of finite mass and duration) Equations 2.36 and 2.37 must be replaced by

$$\frac{C_r}{C_0}(T) = \begin{cases} \frac{C_r}{C_0}(T) & 0 < t \leq t_1 \\ \frac{C_r}{C_0}(T) - \frac{C_r}{C_0}(T') & t > t_1 \end{cases} \qquad (2.38)$$

where t_1 is the time at which the solute input ends, and

$$T' = v(t - t_1)/L$$

An equation frequently used to describe solute transport data is

$$\frac{C_r}{C_0}(x,t) = \frac{1}{2}\text{erfc}[\frac{Rx - vt}{2(D_I Rt)^{0.5}}] \qquad (2.39)$$

This equation provides a close approximation to the two solutions listed above (Equations 2.33 and 2.37) at relatively large values of P_c ($P_c > 20$).

For further information on the various boundary conditions and solutions available to the one-dimensional advection dispersion equation it is suggested that the reader see van Genuchten and Alves (1982).

SOLUTE TRANSPORT IN UNSATURATED POROUS MEDIA

In the unsaturated zone water is under pressure which is less than atmospheric. This subatmospheric pressure is called matric potential or suction and is equivalent to a negative pressure potential. The gradient of this potential causes water to flow from where matric potential is higher to where it is lower, all other potentials being equal.

As a soil desaturates some of the pores become air filled with a resulting decrease in hydraulic conductivity. Therefore, tortuosity increases with desaturation since the empty pores must be bypassed. This results in smaller values of τ (the tortuosity factor, equation 2.7) than would be found in saturated flow conditions. The coefficient of molecular diffusion in porous media is also a function of the volumetric water content in unsaturated soils, and equation 2.6 may now be written as

$$D^* = D_0 \tau'(\theta) \qquad (2.40)$$

where τ', the tortuosity factor in the unsaturated zone, decreases with decreasing θ. These factors result in a lower coefficient of molecular diffusion in porous media in the unsaturated zone than in the saturated zone. However, diffusion can represent a higher proportion of hydrodynamic dispersion in the unsaturated zone since fluid velocities are generally much lower.

Under unsaturated conditions the coefficient of hydrodynamic dispersion is a function of the pore structure, the pore water velocity, and the volumetric water content. Wilson and Gelhar (1974) found that the coefficient of hydrodynamic dispersion determined under unsaturated conditions may surpass the value determined under saturated conditions for the same porous medium.

A decrease in water content of a soil results in an increase in the amount of air-filled pores and an increase in the matric potential of the remaining water. Conceptually, water may become partitioned into two phases: a flowing mobile phase and a stagnant immobile phase (Coats and Smith, 1964). The stagnant immobile water may consist of water trapped in dead-end pores, as non-moving water in soil aggregates, water held tightly around individual soil particles or as isolated regions unconnected with the mobile phase. Solutes may be transported by the mobile phase with some solute diffusing into and out of the

immobile phase. A transport model based on the above was initially developed by Coats and Smith (1964) for the petroleum engineering field and later extended to water and solute movement in the unsaturated zone by van Genuchten and Wierenga (1976)

$$\theta_m R_m \frac{\partial C_m}{\partial t} + \theta_{im} R_{im} \frac{\partial C_{im}}{\partial t} = \theta_m D_m \frac{\partial^2 C_m}{\partial x^2} - v_m \theta_m \frac{\partial C_m}{\partial x} \qquad (2.41)$$

$$\theta_{im} R_{im} \frac{\partial C_{im}}{\partial t} = \epsilon (C_m - C_{im}) \qquad (2.42)$$

where θ_m = the volumetric water content of the mobile phase,

θ_{im} = the volumetric water content of the immobile phase ($\theta_m + \theta_{im} = \theta$),

C_m = the solute concentration in the mobile phase,

C_{im} = the solute concentration in the immobile phase,

D_m = the coefficient of hydrodynamic dispersion in the mobile phase,

v_m = the pore water velocity of the mobile phase,

ϵ = the mass transfer coefficient between the mobile and the immobile phase [T^{-1}],

R_m = the retardation factor of the mobile phase, and

R_{im} = the retardation factor of the immobile phase.

For the case where the solute is not adsorbed onto the porous geologic medium, R_m and R_{im} are equal to 1. Equation 2.41 is the classical advection-dispersion

equation for the mobile water phase, while 2.42 describes the transfer of solute into and out of the immobile water phase. This diffusion-controlled transfer is assumed to be proportional to the difference in concentration between the two phases. While the above mobile-immobile water model may be applied to the saturated zone, it is much more appropriate for, and applicable to, the unsaturated zone. This is due to the fact that as a soil becomes increasingly saturated, the relative amount of dead-end pores and other regions associated with immobile water decreases.

In previous studies (Nielsen and Biggar, 1961) of solute transport through unsaturated porous media it was found that the resulting breakthrough curves exhibited earlier breakthrough than was expected and an asymmetrical tailing. The above model has been found to match these phenomena quite well (van Genuchten and Wierenga, 1977; De Smedt et al. 1986).

The value of the mass transfer coefficient, ϵ, depends upon both the solute chemical and the porous medium. It involves the coefficient of diffusion of the solute in water, the concentration gradient, and the pore cross sectional area through which the diffusion takes place. Small values of ϵ mean that solute is being exchanged slowly between the immobile and the mobile water phases. This results in extended tailing and a decrease in the peak of the breakthrough curve.

The fraction of mobile water is defined as

$$\phi = \frac{\theta_m}{\theta} = \frac{\theta_m}{\theta_m + \theta_{im}} \tag{2.43}$$

As ϕ decreases, the amount of immobile water increases, and the advective transport is confined to a smaller cross-sectional area of the porous medium, resulting in a faster pore water velocity, and hence, a faster solute velocity. This results in a quicker breakthrough of the solute. Factors affecting ϕ include soil type and structure (aggregation, pore size distribution, etc.), the presence of soil layers exhibiting different hydraulic properties, and the method of water application.

If the following dimensionless variables are introduced into 2.41 and 2.42

$$P' = \frac{v_m L}{D_m} \tag{2.44}$$

$$Z = x/L \tag{2.45}$$

$$c_m = \frac{C_m}{C_o} \tag{2.46}$$

$$c_{im} = \frac{C_{im}}{C_o} \tag{2.47}$$

$$\omega = \frac{\epsilon L}{v_m \theta_m} \tag{2.48}$$

they may be written in dimensionless form as (for a non-reactive tracer where $R_m = R_{im} = 1$)

$$\phi \frac{\partial c_m}{\partial T} + (1-\phi) \frac{\partial c_{im}}{\partial T} = \frac{1}{P'} \frac{\partial^2 c_m}{\partial Z^2} - \frac{\partial c_m}{\partial Z} \qquad (2.49)$$

$$(1-\phi) \frac{\partial c_{im}}{\partial T} = \omega (c_m - c_{im}) \qquad (2.50)$$

where T is the number of pore volumes (2.34), also equivalent to $v_m t\phi/L$.

Solutions to 2.49 and 2.50 have been developed for various boundary conditions by Coats and Smith (1964), van Genuchten and Wierenga (1976) and De Smedt and Wierenga (1979). They will not be presented here due to their length and complexity.

De Smedt and Wierenga (1984) found that at large times and/or distances of solute transport, the following approximation may be made

$$D = \frac{\theta_m}{\theta} D_m + \frac{\theta_{im}^2 v^2}{\theta_m \theta \epsilon} \qquad (2.51)$$

This equation relates the mobile-immobile water model to the classical one-dimensional advection-dispersion model. The overall hydrodynamic dispersion coefficient consists of true dispersion in the mobile phase and an apparent dispersion due to solute exchange between the

immobile and the mobile phases. This equation suggests that in the presence of mobile-immobile water dispersion can increase significantly. This was confirmed by De Smedt et al. (1986). De Smedt and Wierenga (1984) reported that in a porous medium consisting of glass beads with an average diameter of 0.01 cm, the dispersivity was about 20 times greater for unsaturated flow versus saturated flow.

If all terms in Equation 2.51 are divided by v the following equation results (De Smedt et al., 1986)

$$\alpha = \alpha_m + \left(\frac{\theta_{im}}{\theta}\right)^2 \frac{v_m}{\epsilon} \qquad (2.52)$$

where α_m = the dispersivity in the mobile zone = D_m/v_m
This equation relates the overall dispersivity of the unsaturated soil to the mobile zone dispersivity, and is valid at large times and/or distances of solute transport.
For a further review of the current understanding of the processes of mass and solute transport in the unsaturated zone it is suggested that the reader see Nielsen et al. (1986).

DETERMINING TRANSPORT PARAMETERS

Various methods are available for determining the transport parameters which govern solute movement through

geologic porous media. Determination of these parameters is important for predictive purposes. The important parameters to be determined include the coefficient of hydrodynamic dispersion, the pore water velocity, the retardation factor, the fraction of immobile water present, and the mass transfer coefficient. The latter two parameters listed above pertain only to the mobile-immobile water model described earlier (Equations 2.48 and 2.49), while the first three pertain to both the mobile-immobile water model and the classical advection-dispersion model (Equation 2.27).

All of the methods available for determining transport parameters utilize the observed concentration distribution over time and distance and are based on analytical solutions of existing solute transport models.

The most commonly used technique for determining transport parameters is that of applying a least-squares analysis to the breakthrough curve. In this approach the transport parameters are adjusted until a least-squares fit of the observed data is obtained. The goal is to minimize the residual sum of the squares, R_s

$$R_s = \sum_{i=1}^{n} [c_e(L,T_i) - c(L,T_i)]^2 \qquad (2.52)$$

where n = the number of observed data points,

$c_e(L,T_i)$ = the observed data points at distance L and pore volumes T_i, and

$c(L,T_i)$ = the calculated data points at distance L and pore volumes T_i.

Existing methods which utilize this approach include the relatively simple graphical approach of Elprince and Day (1977), the computer code CFITM developed by van Genuchten (1980), and the computer code CXTFIT (Parker and van Genuchten, 1984a), a refined version of CFITM. The computer codes are the most convenient and accurate method to use. They consist of entering guessed values of transport parameters (some of which may be known) into the program which then adjusts these input parameters until a least-squares fit of the observed data is obtained. CXTFIT has the capability of determining transport parameters based upon both the classical one-dimension advection-dispersion model and the mobile-immobile water model.

Another relatively simple method of determining transport parameters is the method of trial and error. This method utilizes Equation 2.39, which in dimensionless quantities may be written as

$$\frac{C_r}{C_0} = \frac{1}{2}\text{erfc}\left[\left(\frac{P}{4RT}\right)^{0.5}(R - T)\right] \qquad (2.53)$$

By determining the number of pore volumes (T) at which the breakthrough curve reaches a reduced concentration (C_r/C_0)

of 0.5, an approximate value of the retardation factor (R) is obtained. Because erfc(0) = 1, the above expression reduces to $C_r/C_0 = 0.5$ at R = T. A value of the Peclet number (P), and subsequently, the coefficient of hydrodynamic dispersion (D_l), may then be determined by trial and error by using different values of P to calculate reduced concentrations from the above expression until the calculated breakthrough curve matches the observed breakthrough curve. The disadvantages to this method include the time and effort involved, and the relative inaccuracies of the results.

Another relatively simple method of determining P and R is a graphical technique. Differentiating Equation 2.53 with respect to T, evaluating the resulting equation at T = R, and solving for P yields (Rifai et al., 1956)

$$P = 4\pi R^2 S_T^2 \qquad (2.54)$$

where S_T^2 = the slope of the breakthrough curve at R pore volumes.

An estimate of R is first obtained as discussed in the above paragraph. Next the slope of the breakthrough curve at R pore volumes is graphically determined, and P may then be calculated from Equation 2.54.

Other methods for determining solute transport parameters include the method of moments (Turner, 1972), an inverse

technique (van Genuchten et al., 1987), and various stochastic approaches.

For further information on some of the above discussed methods, as well as two other relatively simple techniques, it is suggested that the reader see van Genuchten and Wierenga, 1986.

SOLUTE TRANSPORT IN UNSATURATED FIELD AND LAB STUDIES

During the past years a significant number of unsaturated solute transport experiments have been conducted - both in in-situ field soils and in soils in repacked laboratory columns. Existing laboratory studies are much more numerous than field studies, due to the cost, time, and complexity involved in field studies.

The first solute transport experiment conducted in the field was by Slichter (1905). Although this experiment was conducted in the saturated zone, it is important to mention it here due to its historical implications. His main goal was the determination of groundwater velocities by the injection of an electrolyte into an upstream well and monitoring the breakthrough at various downstream wells. He became interested in the shape of the resulting breakthrough curves and attempted to explain these shapes by a crude dispersion-diffusion theory.

Unsaturated solute transport studies in in-situ field soils consist of applying tracer to the soil and monitoring its movement through the use of soil-water samplers, also called suction lysimeters, and/or by destructive sampling techniques. The experiments generally consist of two types: steady-state or transient. Steady-state conditions exist when, at any point in the flow field, the magnitude and direction of the flow velocity are constant with time. In field experiments this may be achieved through uniform (temporal and spatial) application of water to the soil. Transient, or non-steady, conditions exist when, at any point in the flow field, the magnitude and direction of the flow velocity changes with time. In field experiments this may be achieved by simply utilizing natural precipitation events, by applying a ponded depth of water at the soil surface, or by other means.

In recent years unsaturated solute transport studies in in-situ field soils have been conducted by Warrick et al. (1971), Van de Pol (1974), Kies (1981), Jury et al. (1982), Elabd et al. (1988), Jaynes et al. (1988), and others.

In laboratory unsaturated solute transport experiments, soil is repacked into columns to which tracer is added at the top and the effluent is collected at the outlet, or bottom end. Movement of tracer and leaching solution is facilitated by placing the lower end of the column under a vacuum. The magnitude of the vacuum should be such that unit gradient flow conditions are established within the

column and a uniform soil moisture content exists with depth along the column. This magnitude depends on the hydraulic properties of the soil and the applied solution flux rate.

Some of the first laboratory column experiments were conducted by Biggar and Nielsen (1962). Since then, numerous laboratory experiments consisting of unsaturated solute transport through repacked soils and glass beads in both short and relatively long columns have been conducted. Recently, Wierenga and van Genuchten (1989) and Springer et al. (1989) have conducted intermediate-scale unsaturated solute transport experiments utilizing "columns" consisting of highway culverts or caissons one to three meters in diameter and up to six meters long.

One of the aspects of solute transport in unsaturated porous media which requires further research is a phenomenon known as the scale dependence of dispersivity. As the length, or scale, over which solute transport occurs increases, so does the measure of dispersivity. For saturated conditions this scale dependence has been well documented and is believed to be a function of the amount of large scale heterogeneities present in the porous medium. For unsaturated conditions there is insufficient data with which to draw the same conclusions. Table 2-1 presents a listing of dispersivities determined from various field scale unsaturated solute transport

TABLE 2-1 Measured dispersivities from various unsaturated field solute transport experiments.

AUTHOR(S)	SCALE (cm)	DISPERSIVITY (cm)
Warrick et al. (1971)	180.0	2.70
Van de Pol (1974)	15.0	2.76
	31.5	4.45
	36.5	5.30
	46.5	6.02
	65.0	5.75
	77.5	4.11
	92.0	2.87
	119.0	3.10
	149.0	2.61
Kies (1981)	25.0	9.10
	60.0	11.73
	100.0	14.96
	200.0	23.45
Elabd et al. (1988)	50.0	1.23
	150.0	0.71
	350.0	2.05
	550.0	1.16

experiments. The values in Table 2-1 are shown on a log-log plot in Figure 2-6. As can be seen from this figure, there is no clear trend between the scale, or distance of transport, and the measured dispersivities.

Table 2-2 presents a listing of dispersivities determined from unsaturated solute transport experiments conducted in laboratory columns utilizing repacked soils or glass beads as the porous medium. This table also contains the values determined by Wierenga and van Genuchten's (1989) and Springer et al.'s (1989) intermediate-scale experiments. These values were presented in this table, and not Table 2-1, since the experiments utilized repacked soils, not in-situ field soils. Figure 2-7 presents the values from Table 2-2 in graphical form, on a log-log plot. While there may be some indication of correlation between scale and dispersivity in this figure, there is also a substantial scattering of the data points. Figure 2-8 presents the values from both Table 2-1 and Table 2-2 in one plot.

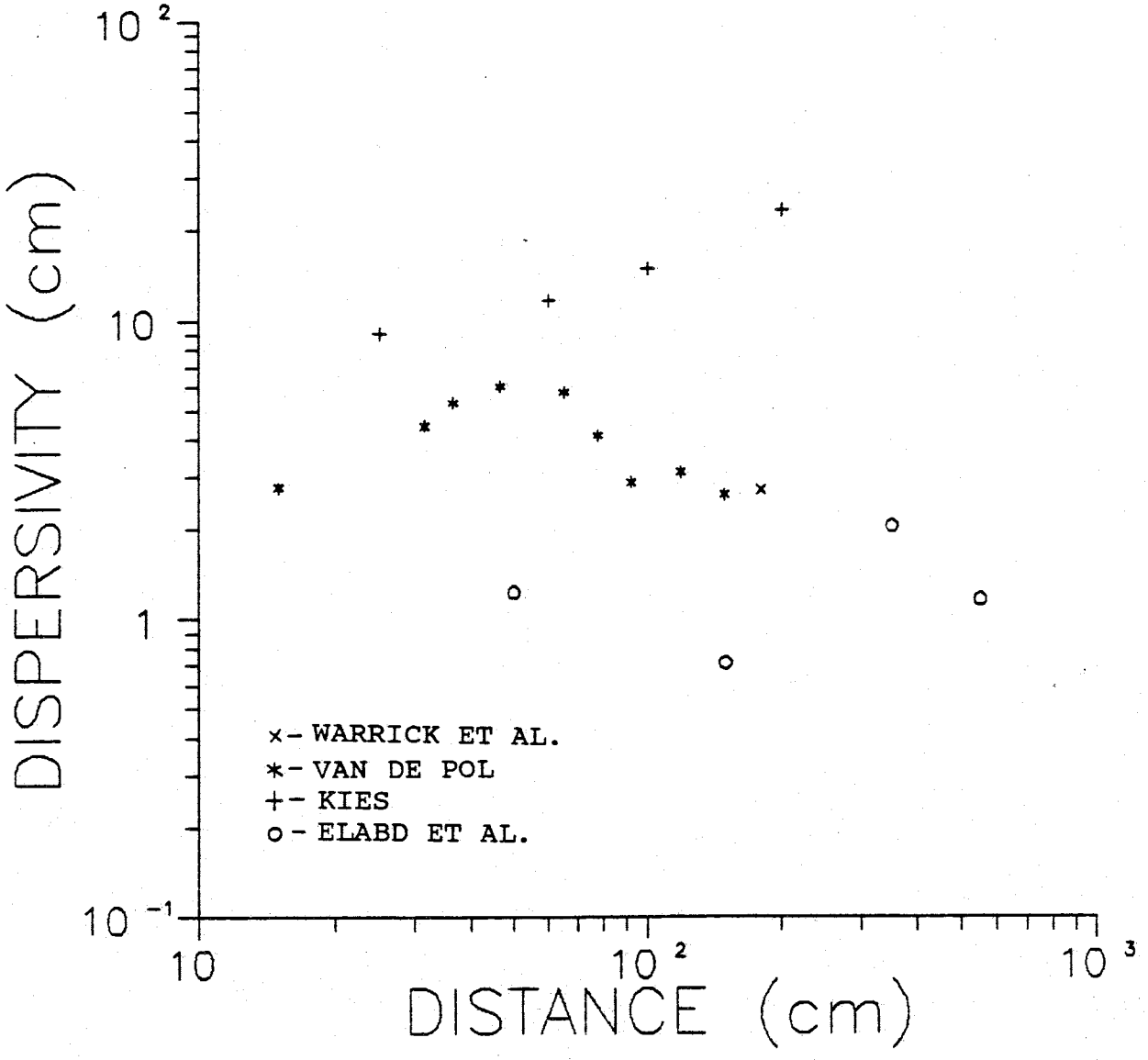

FIGURE 2-6. Dispersivity versus transport distance from various unsaturated solute transport field studies listed in Table 2-1 (after McElroy, 1987).

TABLE 2-2 Measured dispersivities from various unsaturated laboratory column solute transport experiments.

AUTHOR(S)	SCALE (cm)	DISPERSIVITY (cm)
Nielsen and Biggar (1962)	30.0	0.22
	30.0	0.34
	30.0	0.12
	30.0	1.57
	30.0	0.10
Elrick et al. (1966)	10.7	0.04
	10.7	0.76
Krupp and Elrick (1968)	10.0	0.02
Gupta et al. (1973)	54.0	0.007
Gaudet et al. (1977)	94.0	0.14
	94.0	0.10
	94.0	0.11
	94.0	0.10
Hildebrand and Himmelbau (1977)	79.0	0.15
van Genuchten et al. (1977)	30.0	0.33
	30.0	0.73
	30.0	0.67
	30.0	0.66
	30.0	1.31
Yule and Gardner (1978)	23.0	0.22
De Smedt and Wierenga (1979)	30.0	0.02
Mansell et al. (1979)	10.0	0.37
	10.0	0.72
	10.0	0.15
	10.0	0.31
De Smedt and Wierenga (1984)	30.0	0.03
	30.0	0.03
	30.0	0.03
	30.0	0.02
	30.0	0.02
	30.0	0.08
James and Rubin (1986)	48.5	0.015
	48.5	0.014
	48.5	0.012
	48.5	0.015
	48.5	0.023

TABLE 2-2. (Continued)

AUTHOR(S)	SCALE (cm)	DISPERSIVITY (cm)
McElroy (1987)	30.0	0.47
	63.0	3.1
	126.0	4.1
	252.0	1.2
Schulin et al. (1987)*	50.0	2.95
	42.0	3.86
Boyle et al. (1988)	27.0	0.58
	27.0	0.67
	27.0	0.79
	30.0	0.65
	27.0	0.57
	27.0	0.43
Wierenga and van Genuchten (1989)	28.7	0.67
	28.7	0.64
	28.7	0.95
	28.7	0.94
Wierenga and van Genuchten (1989)@	82.0	2.12
	125.0	4.49
	220.0	1.78
	320.0	6.69
	400.0	6.95
	500.0	2.88
Springer et al. (1989)@	36.0	9.8
	36.0	13.3
	36.0	19.8
	36.0	13.2
	113.0	2.7
	113.0	4.9
	113.0	3.1
	113.0	2.9
	188.0	1.2
	188.0	1.6
	188.0	1.6
	188.0	2.6
	264.0	7.0
	264.0	4.6
	264.0	4.3
	264.0	4.3
	339.0	1.0
	339.0	1.5
	339.0	2.8
	415.0	0.8
	415.0	1.5

TABLE 2-2. (Continued)

AUTHOR(S)	SCALE (cm)	DISPERSIVITY (cm)
Springer et al. (1989)[@] (Continued)	415.0	1.0

* Columns consisted of intact, undisturbed cores.
@ Large, repacked caisson experiments.

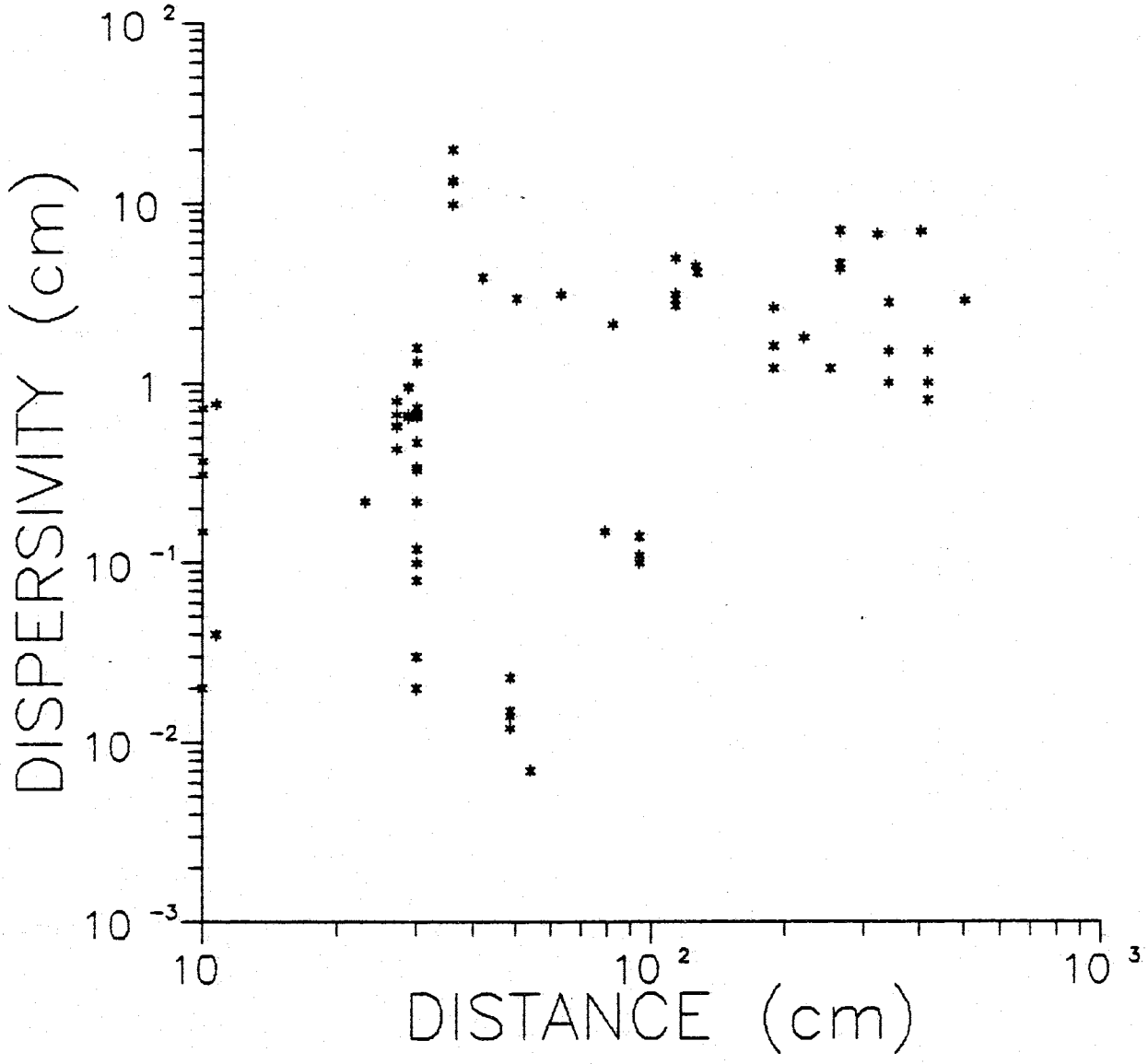

FIGURE 2-7. Dispersivity versus transport distance from various unsaturated solute transport column studies listed in Table 2-2 (after McElroy, 1987).

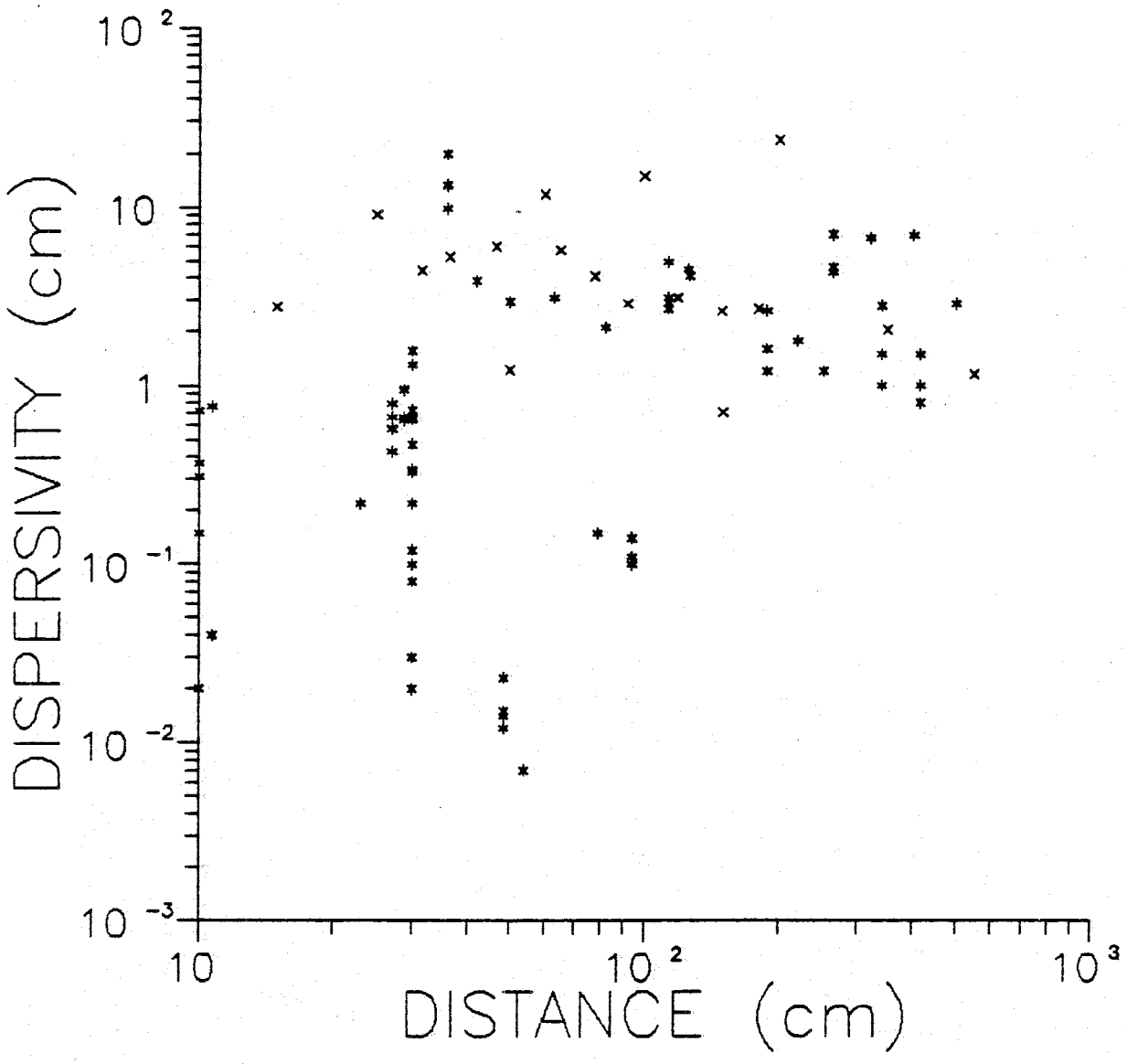

FIGURE 2-8. Dispersivity versus transport distance from various unsaturated solute transport field and column studies listed in Tables 2-1 (stars) and 2-2 (crosses) (after McElroy, 1987).

III. MATERIALS AND METHODS

FIELD SIMULATION OF WASTE IMPOUNDMENT SEEPAGE IN THE VADOSE ZONE

Since January of 1987 a field experiment has been in operation on the campus of the New Mexico Institute of Mining and Technology to simulate unsaturated seepage through a waste impoundment into the vadose zone. Water was applied through a drip irrigation system at a rate which was roughly one percent that of the lowest saturated hydraulic conductivity of the site. Water movement was monitored with a neutron moisture probe and a network of tensiometers. The site is highly stratified, consisting of an upper zone of alluvial silts and sands containing interspersed cobble layers, and a lower zone of fluvial sands.

EXPERIMENT DESIGN

The seepage experiment was designed and constructed during the summer and fall of 1986. Details are provided by Mattson (1989). A 30 meter by 30 meter site was cleared and levelled, and the water monitoring instrumentation was installed. The center 10-m x 10-m area of the site was excavated to a depth of about 60 cm below the land surface. This area was surveyed and levelled by pick and shovel and a 2-cm layer of sand was placed as bedding for the drip lines. Twenty-one polyethylene drip lines (Model No. 164,

Agrifim Irrigation Inc., Fresno, CA) with an inside diameter of 0.52 inches were then laid down running east-west (Figure 3-1). The one gallon per hour (3.785 l/hr) emitters in the drip lines formed a 50-cm spaced grid to provide a uniform distribution of water to the soil. The drip lines were connected to two 3/4 inch PVC manifold headers on the east and west sides. The headers ran north-south and were encased in wood lined trenches which provided protection and access for maintenance. Water flow entered the east manifold between drip lines 10 and 11 and was divided to the northern and southern halves of the system. The western header ensured even distribution of pressure, and uniform water application from the emitters, throughout the system.

A plastic sheet was placed over the lines to prevent evaporation of the applied water. A layer of hay was then installed to provide insulation, and the excavation was backfilled with the previously excavated soil to slightly above the original surface elevation. A second plastic sheet was placed about 2-cm below the surface to prevent infiltration of precipitation (Fig. 3-2). Depth to the water table at the site was approximately 24 meters when the experiment commenced.

Water was applied at the rate of 1×10^{-5} centimeters per second by means of a positive displacement pump (Model No. 5-BBV, Sherwood, Detroit, MI) controlled by an electric timer (Model No. BB-4, Sherwood) and a custom made control

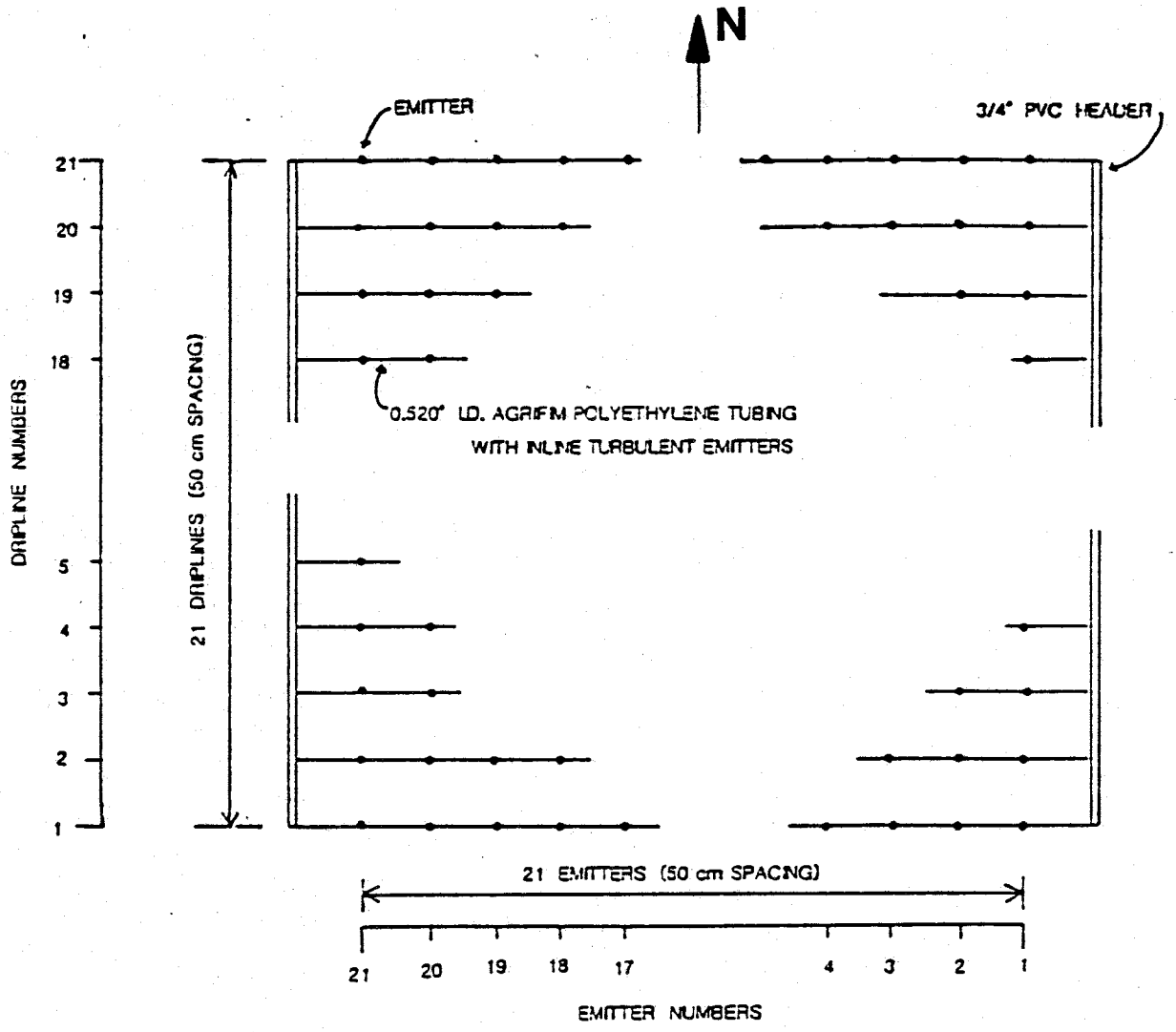

FIGURE 3-1. Schematic showing the dripline system (from Mattson, 1989).

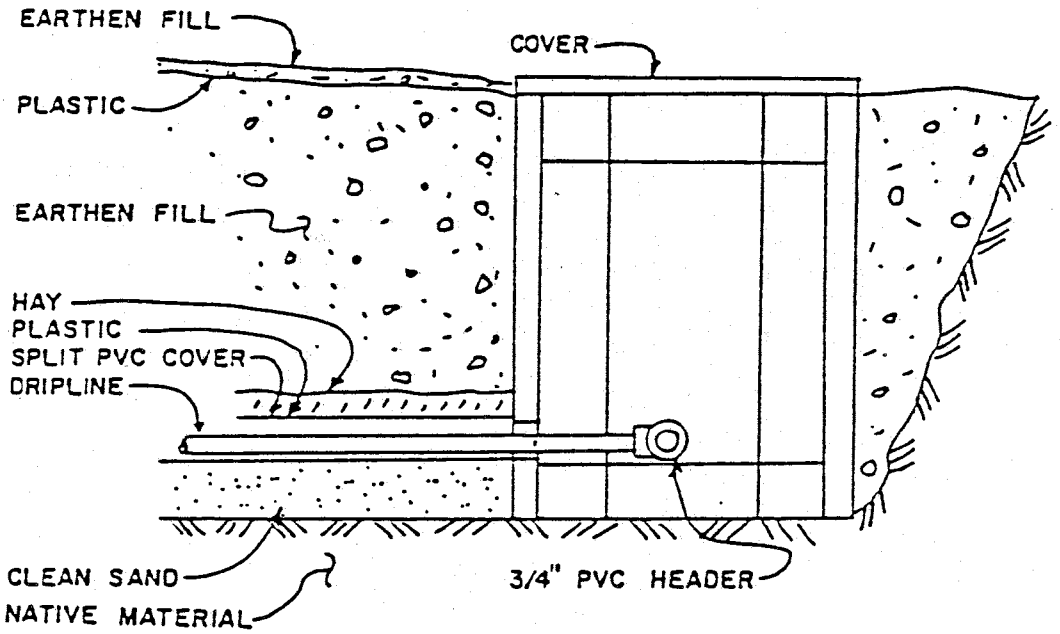

FIGURE 3-2. Cross-section through the simulated impoundment and manifold trench (from Mattson, 1989).

box. Water was fed to the drip line system for approximately one minute per hour by the timer system. A system of floats in a water tank ensured that a constant volume of water was delivered to the drip lines during each cycle in the following manner: the pump was turned on by the timer and ran until the water level in the tank reached a bottom float and activated a switch which turned the pump off. Approximately 30 minutes after the pump was off, the timer opened a solenoid gate valve (Model No. EV-100, Rain Bird Sales, Inc., Glendora, CA) which allowed water from the city water line to flow into the tank. The valve remained open until the water level in the tank reached an upper float and activated a switch which closed the valve. During the refilling of the tank, the timer also turned on a small chemical feed pump (Model No. 2500C, MEC-O-MATIC Co., St. Paul, MN) which delivered a small amount of a 1:13 solution of muriatic acid (31.45%) to tap water into the tank. This was done to keep the pH of the water delivered to the drip lines around 6.5, so that dissolved minerals would not precipitate out and clog the emitters. The acid was originally delivered to the water tank during that part of the cycle when the pump was running, but was changed to the refilling part of the cycle midway during the experiment. In both cases, the amount of acid added to the tank was proportional to the amount of water pumped during that cycle.

The water application system is shown in Figure 3-3. Several totalizing flow meters were installed in the water supply system to monitor distribution of water to the drip lines. A small trailer at the site served as a field office and equipment room. A computerized data logger (Model No. CR7, Campbell Scientific, Inc., Logan, UT) in the field office recorded climatic factors such as precipitation, wind speed, air temperature, and various system parameters such as in-line water pressure, pumping duration and water temperature.

Water movement through the soil was monitored by a neutron moisture probe (Model 503DR, CPN Corp., Pacheco, CA), and tensiometers. The tensiometers were constructed using 1/2 inch PVC pipe, one bar standard ceramic porous cups (SoilMoisture Equipment Corp., Santa Barbara, CA), and rubber septa. Pressure heads were recorded by inserting a hypodermic needle connected to a pressure transducer system (Tensimeter, Soil Measurement Systems, Tucson, AZ) through the rubber septum.

The tensiometers and neutron probe access tubes were installed at twenty-one stations in a symmetrical distribution throughout the site (Fig. 3-4), prior to the construction and installation of the water application system. Each station contained a 2-in diameter by 30-ft (9.1-m) long aluminum tube which served as an access tube for the neutron moisture meter. Tensiometers were installed in duplicate nests of 8 each, to depths of 1 to 5

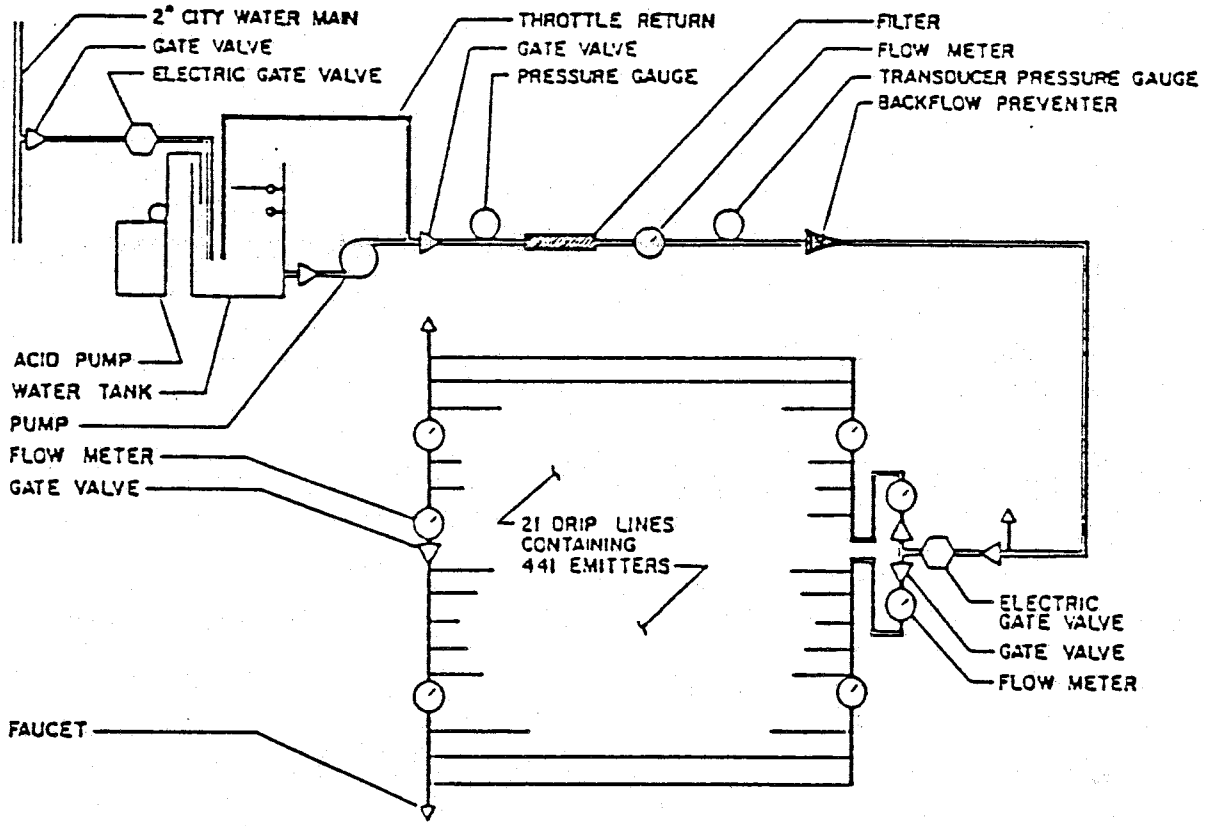

FIGURE 3-3. Schematic showing the water application system.

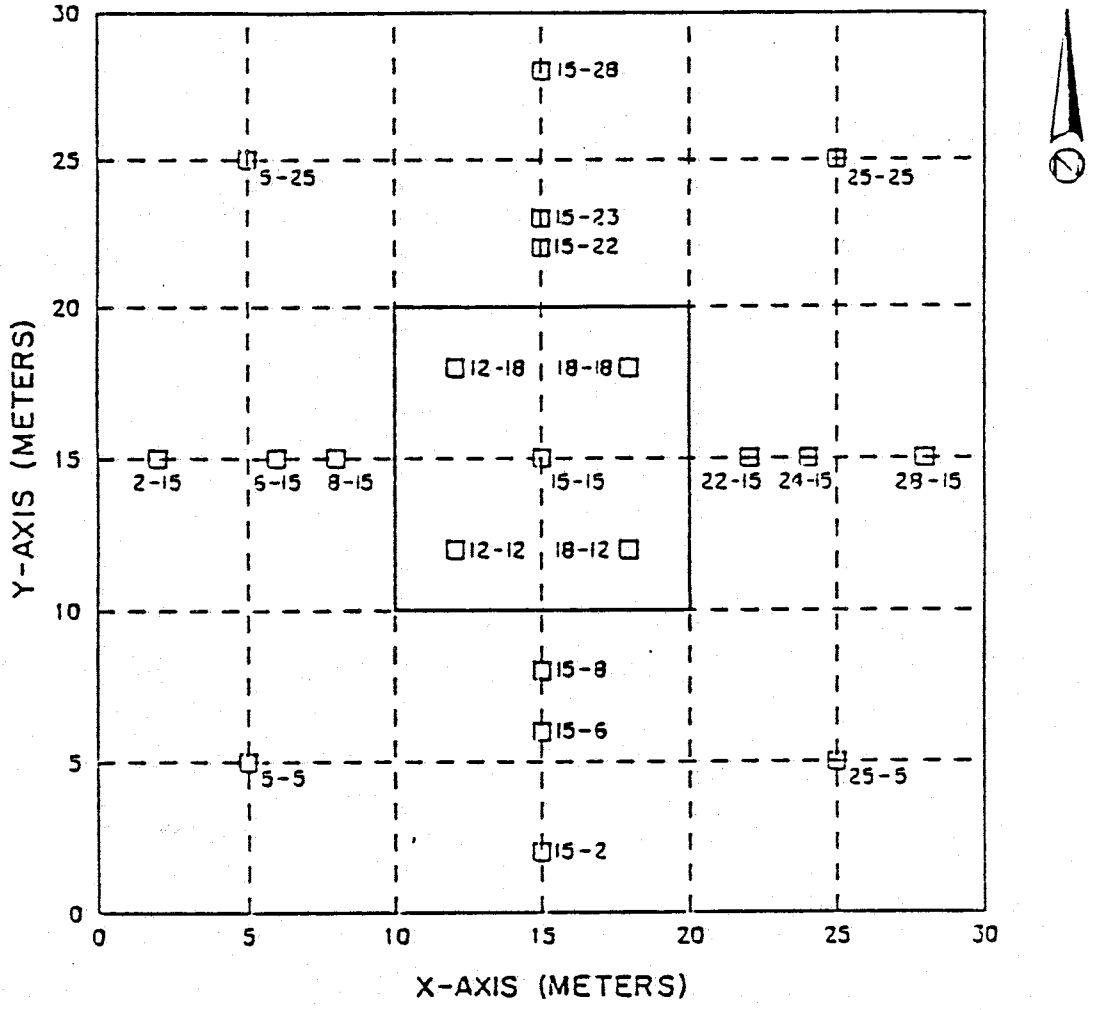

FIGURE 3-4. Diagram showing the location of instrument stations at the field site. Each square represents a neutron probe access tube and one or two tensiometer nests. The grid origin is at the southwest corner of the site. The heavy lines in the center outline the wetted area.

meters. Due to the stony nature of the soil, it was not possible to use hand tools to install this instrumentation. An auger drill rig (Model B-53, Mobil Drill, Indianapolis, IN) was used to drill 8 inch diameter boreholes into which the instrumentation was placed. Native soil was used as backfill with compaction being achieved both with the drill rig and by hand. For the access tubes inside the plot a layer of bentonite was placed just below the level of the driplines to prevent preferential flow of water along the instrument bodies. For the access tubes outside of the plot a bentonite layer was placed just below the ground surface to prevent flow of precipitation along the instrument bodies.

Calibration of the neutron probes used at the site was accomplished utilizing destructive soil samples obtained at, and adjacent to, the site (Mattson, 1989). Volumetric moisture contents were first measured by the probe. Soil samples directly adjacent to the access tube were then collected by either hand augering, split spoon sampling, or by utilizing Shelby tubes. Gravimetric moisture contents of the samples were determined in the laboratory, and, by knowing the bulk density of the samples, their volumetric moisture contents were calculated.

The instrumentation was monitored weekly prior to initiation of the experiment in order to provide background information on conditions at the site. After water application commenced, data was collected daily, bi-weekly,

and then weekly as the experiment progressed. Neutron probe readings were initially taken in half-foot increments, and later at one-foot increments. These readings were then converted to meters below a datum, which was established at an elevation of 0.86 meters above the drip lines. All geological cross-sections, wetting front movement, and tensiometric data were then referenced to this datum. Water application began on January 29, 1987, and was scheduled for cessation in September of 1989.

SITE GEOLOGY

During installation of the monitoring instrumentation, over 150 disturbed soil samples were collected at regular depth intervals using a split-spoon sampler, and 76 100-cm^3 core samples were collected by hand auger. These soil samples were analyzed in the lab for various geotechnical and hydraulic properties including porosity, field moisture content, bulk density, grain size distribution, saturated hydraulic conductivity, and soil moisture characteristic (Parsons, 1988). Geologic cross-sections of the east-west and north-south transects were determined by correlating visual characteristics (such as soil type, color, grain size, etc.) of the collected soil samples. Figure 3-5 shows these soil profiles with the vertical scale exaggerated to illustrate textural contrasts in more detail.

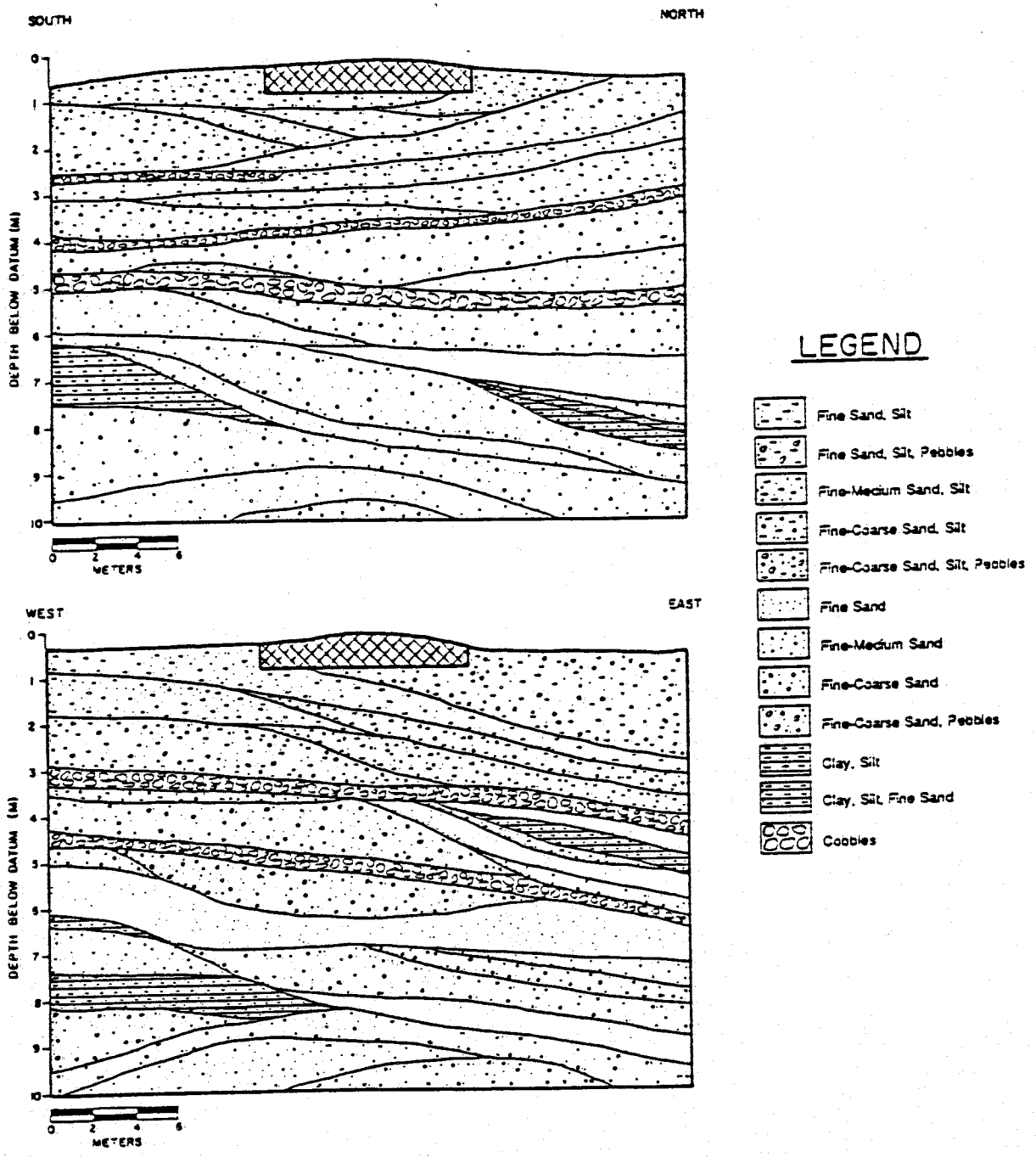

FIGURE 3-5. Geologic cross sections determined by correlation of collected soil samples. The vertical scale is exaggerated to illustrate the textural differences in more detail. The hatched area represents the drip irrigation system.

The cross-sections exhibit the highly stratified nature of the site. The soil profile consists of two general soil zones: an upper zone consisting of silty sands and pebbles interbedded with cobble layers to a depth of about 4 to 5 meters below the land surface; and a lower zone consisting of layers of clean, fine sand and fine to coarse sand and pebbles. The upper zone is alluvial in nature, and was derived as debris flow from the Socorro Range to the west of the site. The lower zone is fluvial in nature, and was deposited in ancient times by the Rio Grande to the east of the site. Details on the geologic and hydraulic characterization of the site are provided by Parsons (1988).

BROMIDE TRANSPORT EXPERIMENT AT THE SITE

In late February and early March of 1988 a solute transport experiment was conducted at the site. This experiment consisted of injecting a bromide solution into the drip irrigation system and monitoring the movement of the bromide using soil water samplers.

EXPERIMENT DESCRIPTION

A 2000-gallon capacity water tanker truck was attached to the system to serve as a reservoir for the bromide solution. The tanker truck fed directly into the water

tank shown in Figure 3-3 via a 3/4 inch PVC line. Feed from the tanker truck replaced that from the city water line during the period of tracer injection. Flow was controlled by a gravity valve (Model No. 18N22-W, Magnatrol Valve Corp., Hawthorne, NJ) operated by the electric timing system described earlier.

The truck was filled with tap water using a hose, with the bromide solution mixed in at this time. The bromide (as calcium bromide, $CaBr_2.H_2O$) was first mixed with water in a 5 gallon jug, and this solution was then poured into the truck as it was being filled. The amount of bromide used for the solution was carefully measured, and the volume of water placed in the truck was measured with a totalizing flow meter. Prior to the initial injection the solution was thoroughly mixed using a small gasoline engine pump. Several samples of the solution were taken before the start of the experiment. The initial concentration was determined to be 435 ppm, as measured using high performance liquid chromatography.

Approximately 24 hours before the start of the experiment the drip lines were emptied of water by attaching a pressure pump to the faucet opening on the east side of the drip line system and forcing the water contained in the lines out the faucet openings on the west side of the system. This was done so that no dilution of the solution would take place within the drip line system. The water

tank was then drained of tap water and filled with the bromide solution.

The injection of the bromide solution commenced at 1000 hours on February 25, 1988. The electric timer began controlling operations at this time. As with the regular system, the timer operated the positive displacement pump on the hour, and operated the gravity valve controlling refill of the water tank with solution from the tanker truck on the half-hour.

The bromide solution was injected for a period of 151 hours between February 25, and March 2, 1988. The total amount of solution injected was approximately 1550 gallons as measured by the totalizing flow meter directly downstream from the water tank. This is equivalent to a flux rate of solution application of 1.08×10^{-5} cm/s.

MONITORING INSTRUMENTATION

The movement of the bromide tracer was monitored by the use of soil water samplers, also called suction lysimeters in the literature. The entire unsaturated zone at the site was not instrumented since it is approximately 20 meters deep. Rather the samplers were placed to optimize the amount of area instrumented with the limited number of instruments available. This involved placing four samplers at an outer zone of approximately 6 meters horizontally distant and 6 meters below the plane of the drip lines, on each side of the plot; placing four at the perimeter of the

wetted area; and placing six at various depths and locations below the drip lines.

The soil water samplers (Figure 3-6) consisted of a length of 2 inch diameter PVC pipe with a porous ceramic cup (No. 653X01-B2M2, SoilMoisture Equipment Corp., Santa Barbara, CA.) epoxied to one end. The other end was sealed with a rubber stopper through which two 1/4 inch tubes passed. One of these tubes reached to the bottom of the instrument and was used to withdraw the collected sample from the instrument. The other tube ended just below the rubber stopper and was used to apply pressure or vacuum to the instrument.

Prior to field placement of the instruments, approximately 1/2 liter of 6N hydrochloric acid followed by 1 liter of distilled, de-aired water was pulled through the porous cups via application of a vacuum. The instrument bodies were also rinsed with the acid and the distilled, de-aired water. This was done to decontaminate the instruments and to ensure that samples obtained from the field did not contain any instrument induced species.

Table 3-1 presents a list of the samplers, their depths below the drip lines, their coordinates, and their installation dates. Figure 3-7 shows the locations of the samplers.

The instruments inside and adjacent to the drip line wetted area (with the exception of samplers G, H and I) were placed in 3-in diameter hand-augered holes ranging in

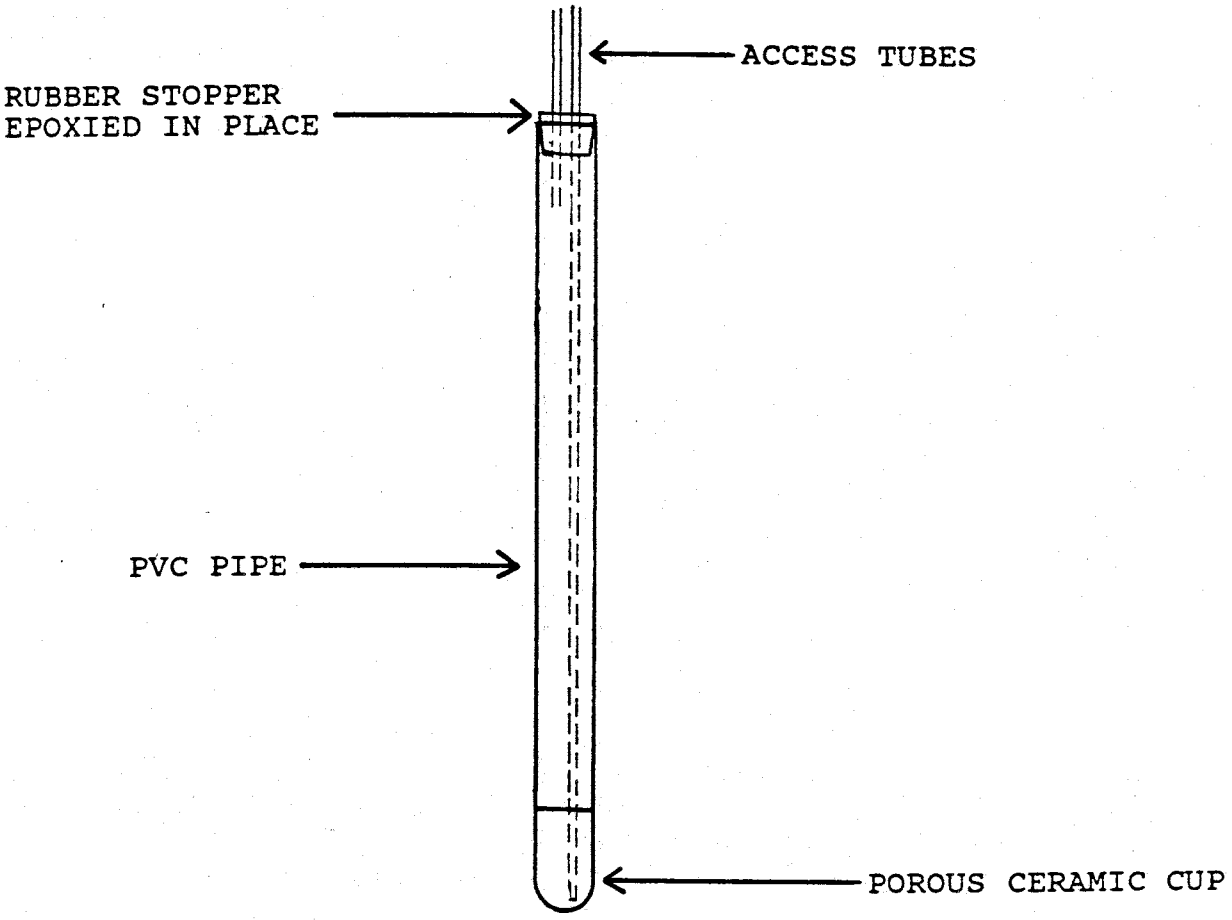

FIGURE 3-6. Soil water sampler.

TABLE 3-1. SOIL WATER SAMPLERS

SAMPLER	LOCATION[1]	z(M)	x(M)	INSTALLATION DATE
A	(14.47,9.75)	1.14	0.98	2/26/88
B	(14.47,9.75)	1.59	1.12	2/28/88
C	(14.44,11.84)	0.83	N/A	2/26/88
D	(14.44,11.84)	1.38	N/A	2/26/88
F	(14.54,20.92)	1.37	0.93	3/6/88
G	(15.69,16.90)	1.07	N/A	8/30/86
H	(15.00,16.98)	2.44	N/A	8/30/86
I	(14.42,16.82)	3.20	N/A	8/30/86
J	(11.37,10.18)	2.47	0.67	3/28/88
K	(14.34,14.79)	1.58	N/A	4/10/88
L	(14.54,5.27)	6.21	5.67	6/1/88
M	(26.03,14.99)	5.42	5.89	6/2/88
N	(14.92,25.79)	6.31	5.69	6/2/88
O	(3.90,14.71)	6.12	5.87	6/3/88

1: X AND Y COORDINATES, WITH THE ORIGIN LOCATED AT THE SOUTHWEST CORNER OF THE SITE (FIGURE 3-7).
z = DEPTH BELOW SOURCE (DRIP LINES)
x = HORIZONTAL DISTANCE FROM EDGE OF WETTED AREA
N/A = NOT APPLICABLE

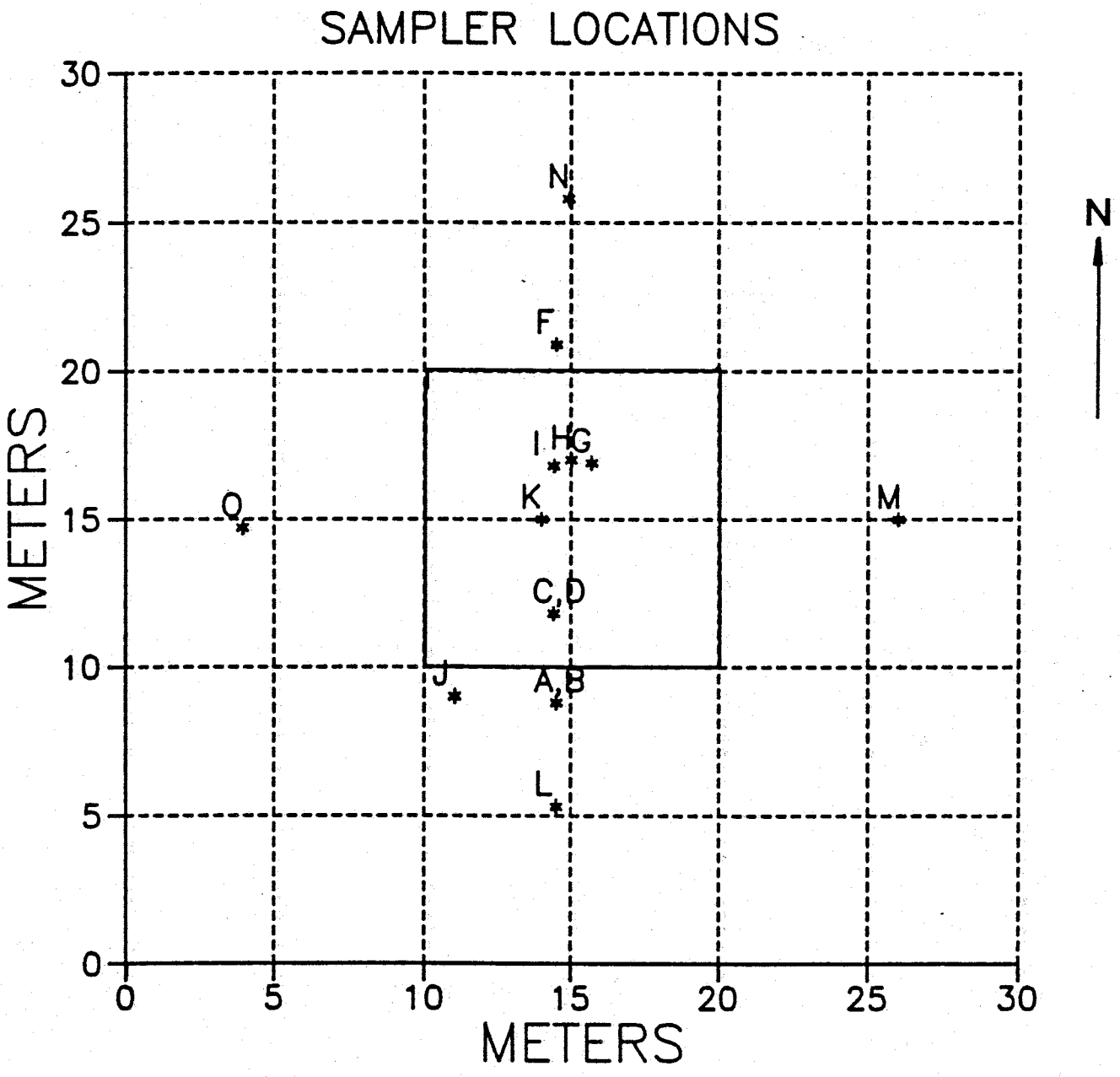

FIGURE 3-7. Location of soil water samplers for bromide tracer experiment.

depth from 1 to 3 meters below the drip lines. Silica flour (200 mesh) was placed around the porous cup downhole to prevent clogging of the cup by fines. Backfill consisted of soil from the borehole, which was tamped periodically during placement. Bentonite seals were placed above the porous cup, below the drip lines and below the ground surface to prevent preferential flow of moisture along the instrument bodies. Samplers G, H, and I had been installed during construction of the site using the drill rig with an 8-inch auger. Samplers L, M, N, an O were installed a few months after injection of the bromide, also using the drill rig and 8-inch auger. The rest were installed shortly before, during, and shortly after the injection period.

Figures 3-8 and 3-9 are schematic cross sections of the field site, showing the various samplers and their spatial relationships to the drip line system and the facies zones.

Samples were collected from each sampler about every three days during the course of the experiment. Vacuum and pressure were applied to the samplers using a portable electric vacuum/pressure pump. Applied vacuum was in the range of 20 to 25 centibars of suction for the samplers inside and adjacent to the plot, and in the range of 60 to 70 centibars for the four samplers (L, M, N, and O) on the edges of the site. Vacuum was applied to the samplers for approximately 24 hours before samples were collected. The samples were collected by applying pressure to the

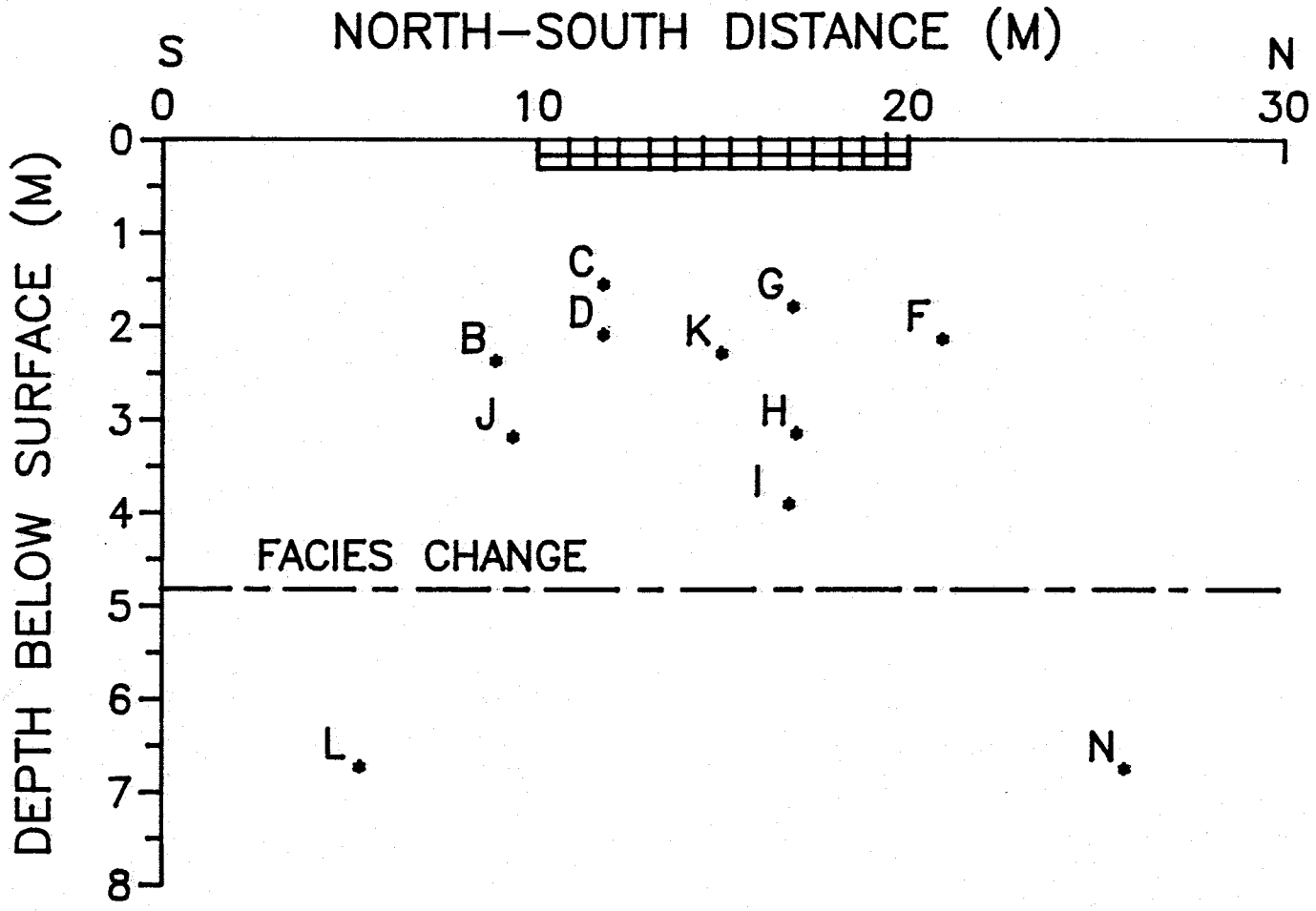

FIGURE 3-8. Cross sectional schematic showing the locations and depths of the soil water samplers along the north-south axis near the center of the plot.

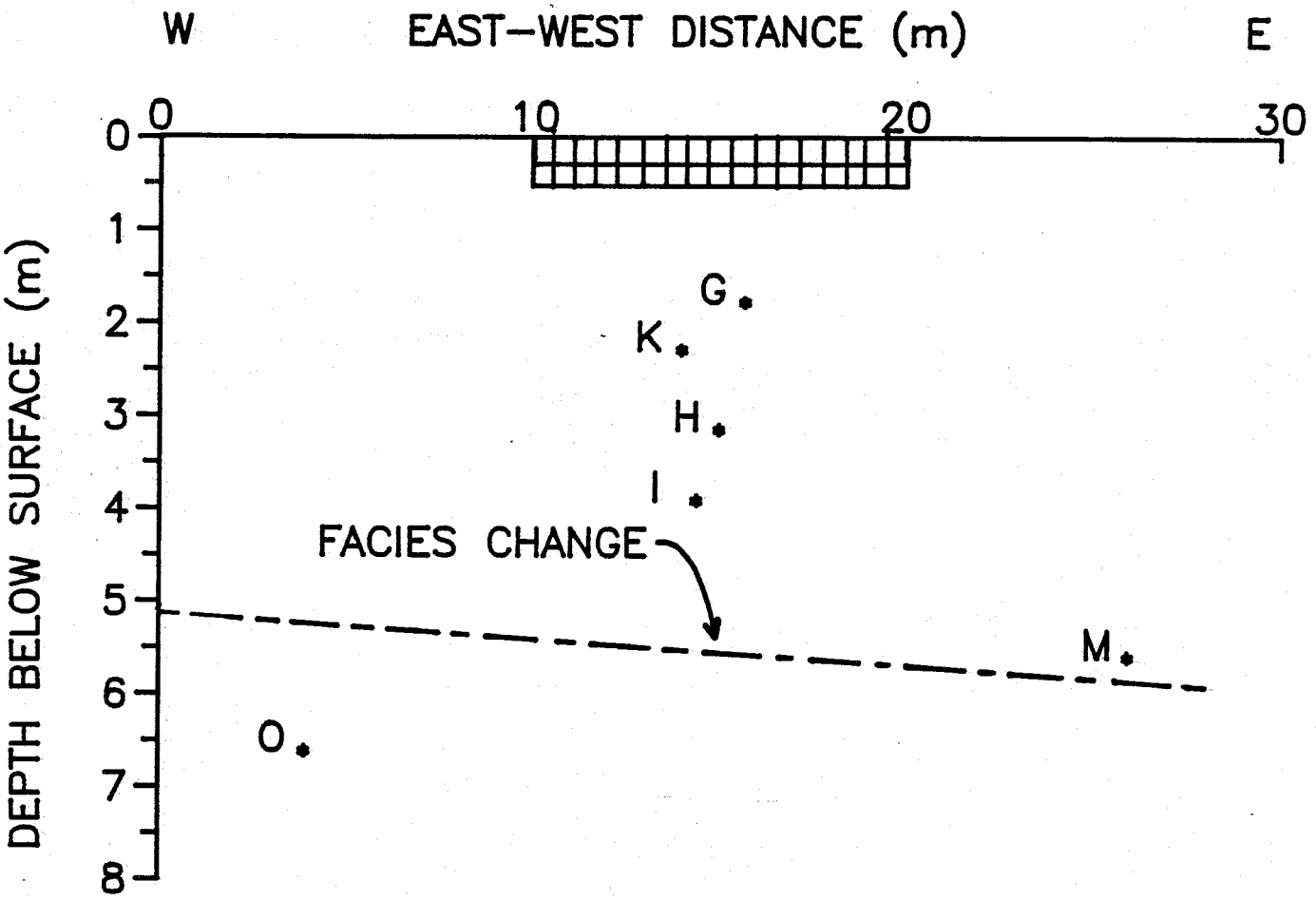

FIGURE 3-9. Cross sectional schematic showing the locations and depths of the soil water samplers along the east-west axis near the center of the plot.

instrument, forcing the soil water which had been drawn into the cup out through the tube which ran the length of the instrument, from the surface down to the porous cup. Volumes collected ranged from 20 to 200 milliliters. The samples were analyzed for bromide content using high performance liquid chromatography by the method outlined by Bowman (1984).

UNSATURATED COLUMN EXPERIMENTS

Two unsaturated column experiments using soil from the field site were conducted. The goal of these experiments was to simulate the field conditions as closely as possible so as to determine the suitability of bromide as a tracer of water movement at the site.

Figure 3-10 shows the unsaturated column experimental apparatus. The columns (Soil Measurement Systems, Tucson, AZ) were 30-cm long and 5-cm in diameter. Porous steel plates with a bubbling pressure of 250-cm were attached at the bottom end. Tensiometers were located 5-cm below the top and 5-cm above the bottom of the columns.

The soil for the columns came from the area of the plot where samplers G, H, and I are located. Figure 3-11 is a cross section which shows from which stratigraphic layers the soil was taken. It was desired to obtain soil from different layers in between the drip lines and samplers G,

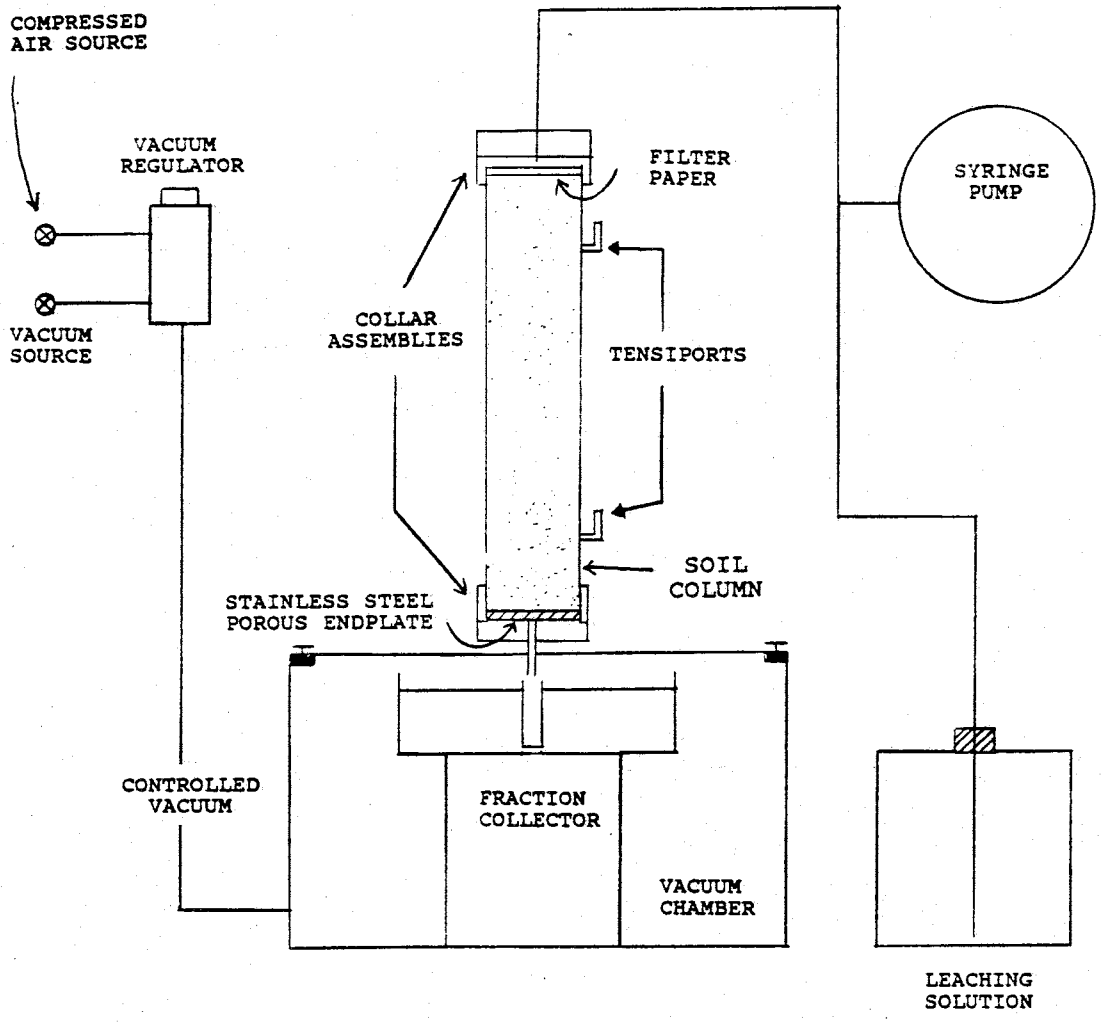

FIGURE 3-10. Schematic showing the apparatus used in the unsaturated column tracer experiments. (Modified from van Genuchten and Wierenga, 1986).

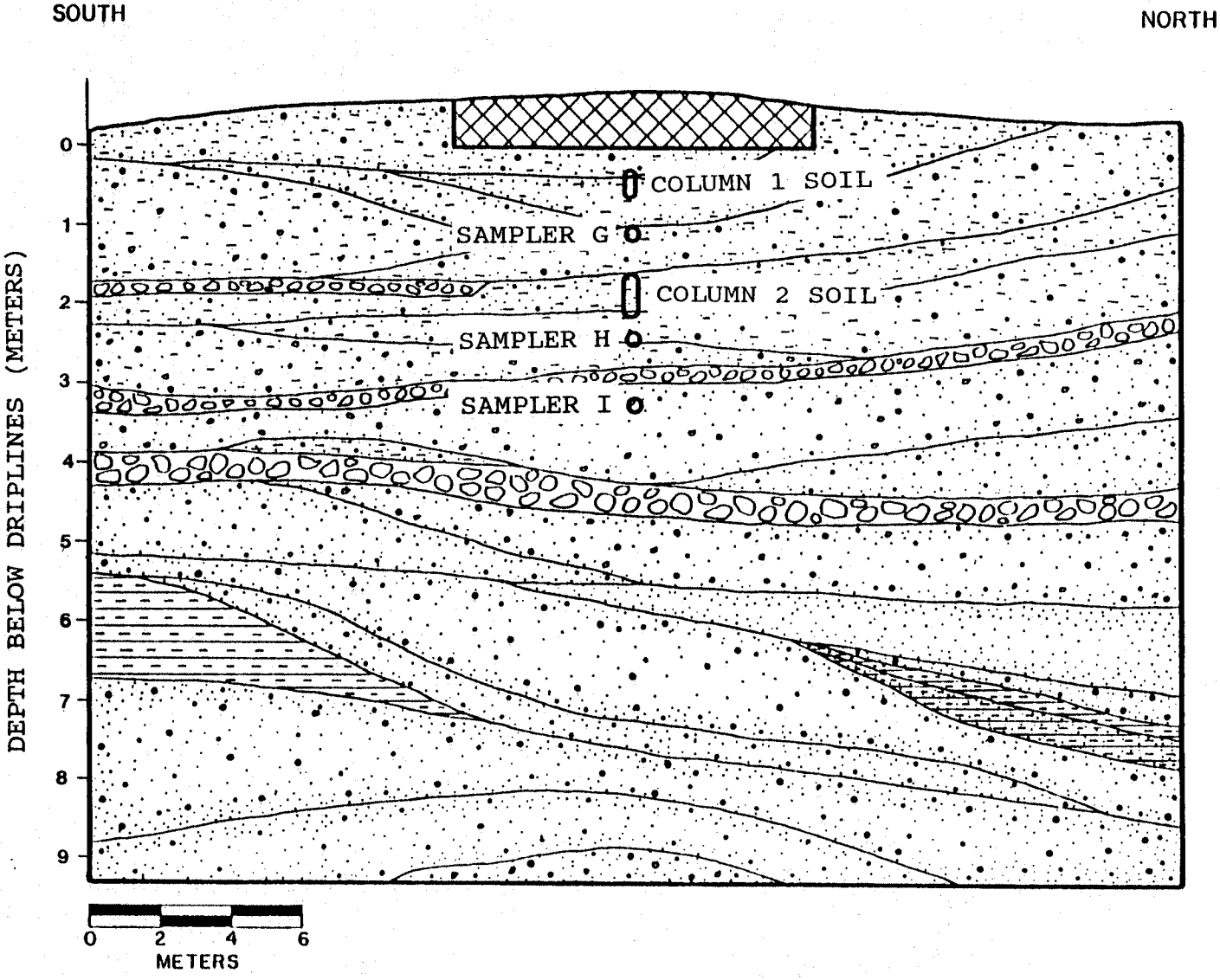

FIGURE 3-11. Cross section showing the locations of samplers G, H, and I, and the location from which the soil for the two unsaturated columns was taken.

H, and I. Both soil samples consisted of sands and silts, with a significant amount of pebbles and cobbles.

Repacked columns instead of intact cores were used due to the difficulty of obtaining intact cores from the field. Since the purpose of the unsaturated column experiments was to determine the amount of anion exclusion occurring at the site, it was not necessary to preserve the pore structure of the soil as would be the case with intact cores.

The soil was allowed to air dry and was then sieved through a 2-mm sieve. Sub-samples of the soil were oven dried and the gravimetric moisture content of the air dry soil was determined for use later as a correction factor in calculations. The columns were packed with the aid of a funnel and tube assembly to avoid any free fall of soil material and subsequent segregation of soil particles by size and mass. This was accomplished by keeping the tube filled with soil at all times, so that the soil flowed down the tube as a continuous unit. The soil was well mixed prior to filling the funnel and tube. An attempt was made to pack the columns to the same dry bulk density as found at the site. The mean dry bulk density of the upper alluvial facies is 1.50 g/cm^3 (Parsons, 1988). The achieved dry bulk densities were close to this value - 1.464 for column #1 and 1.414 for column #2.

The columns were attached to a vacuum chamber (Soil Measurement Systems) which contained a fraction collector (Retriever II, Isco, Inc., Lincoln, NE). A vacuum

regulator (Model Series 44, Moore Products Co., Spring House, PA) provided a constant vacuum in the chamber. A multichannel precision syringe pump (Soil Measurement Systems) was used to deliver a constant flux of solution to the top of the columns through 1/8th inch inside diameter tubing. Two-way check valves attached to the syringes allowed one loading and one discharge of the syringes per pump cycle. A piece of filter paper was place on top of the soil to provide distribution of solution across the width of the column.

Solution was applied once an hour at a flux of 9.2 x 10^{-6} cm/s, which was 92% of the field rate. Tap water was used as the leaching solution. The tap water had a pH of 7.8 and an electrical conductivity of 700 micromhos, compared to the field water unadjusted pH of 7.7 and electrical conductivity of 920 micromhos. A sufficient amount of tap water was stored in a container and used throughout the experiment to avoid any fluctuations in chemical content. The columns were leached continuously until the electrical conductivity of the effluent was constant. Then the vacuum was adjusted until approximate unit gradient conditions existed in the column, as indicated by the tensiometers. The difference in suction between the upper and lower tensiometers was between 5 and 10 millibars (with the upper tensiometer having the more negative reading), for each column. At this point the

volumetric moisture content along the length of the column was assumed to be approximately constant.

The columns were weighed before and after packing, and several times during the tracer experiment. The average of the wet weights was used to determine pore volumes (131.7 cm^3 for column #1, 112.4 cm^3 for column #2) and the volumetric moisture content of the columns (24.6% for column #1, 19.1% for column #2)

After unit gradient conditions were achieved a three-day pulse (0.355 pore volumes for column #1, 0.416 pore volumes for column #2) of tracer solution was injected into the columns. The tracer solution consisted of the leaching solution with bromide (100 parts per million) and tritium (450,000 counts per minute) added. Leaching with the stored tap water resumed after the tracer injection ended. Fractions were collected for 14 days after the end of the tracer injection at 16 hour intervals for the first four days. This was then changed to 4 hour intervals for the duration of the experiment.

The collected fractions were then analyzed for bromide content by high performance liquid chromatography, and for tritium content by liquid scintillation counting.

IV. RESULTS AND DISCUSSION

PROPAGATION OF THE WETTING FRONT

As described in the previous chapter, neutron logging was performed periodically throughout the duration of the experiment at the 21 positions where the neutron access tubes were installed. Figure 4-1 shows the change in soil moisture content with time for several depths at monitoring instrument station 15-15, in the center of the simulated impoundment. Using similar data over the monitored depth range, the location (depth) of the wetting front versus time can be determined, as shown in Figure 4-2 (also for station 15-15). The wetting front is defined as the point of maximum change in moisture content with depth or time. Also from this data the rate of advance of the wetting front can be determined as shown in Figure 4-3 (also for station 15-15).

It is important to note in Figure 4-3 how the rate of advance of the wetting front decreases dramatically upon reaching one of the cobble layers. In unsaturated flow water cannot enter into a stratigraphic layer consisting of larger material with correspondingly larger pores than the layer above until the water builds up sufficient pressure to penetrate the larger pores. During the time it takes for this pressure buildup to occur, water content increases and significant lateral flow may occur. Increased water contents and lateral flow may also occur when the wetting front reaches a layer with a lower unsaturated hydraulic

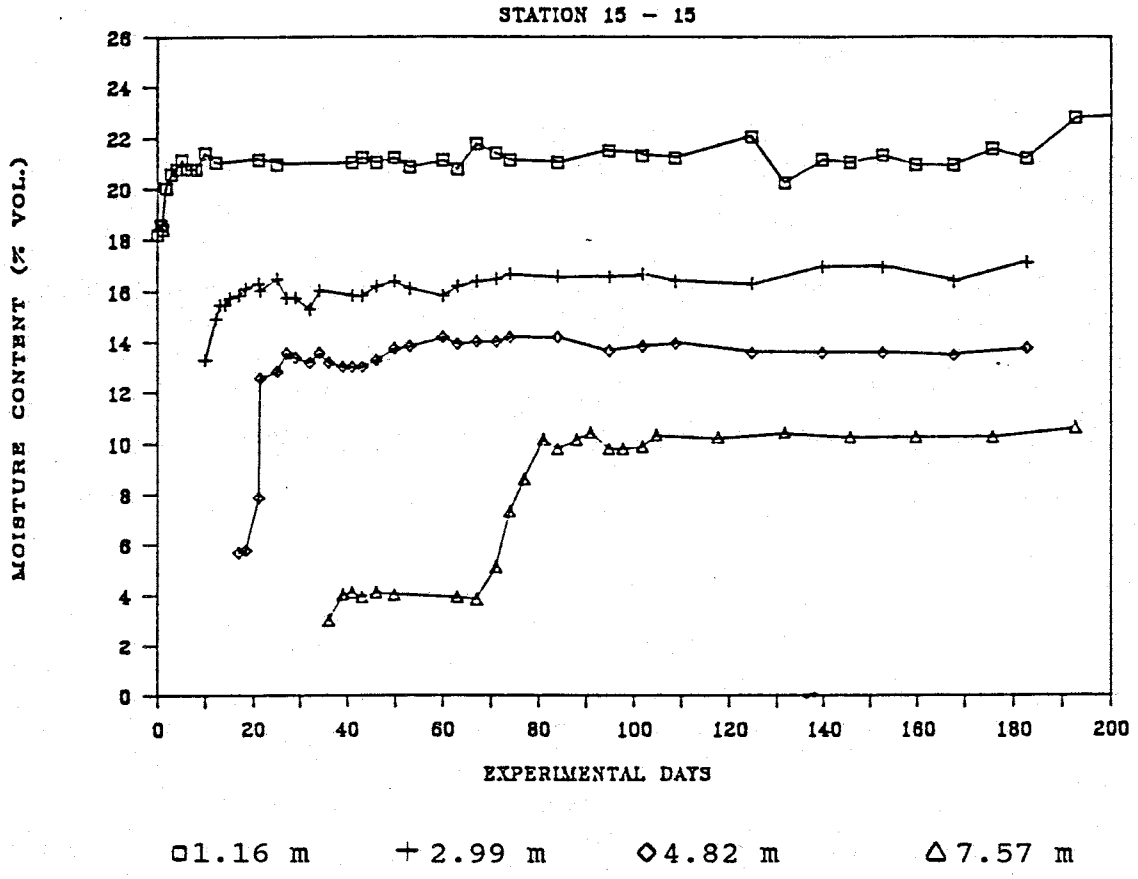

FIGURE 4-1. Variation of moisture content with time for various depths at station 15-15, which is at the center of the wetted area. The depths are meters below the datum, which is 0.86 meters above the driplines. The sharp increase in moisture content at a specific time shows when the wetting front reached a particular depth.

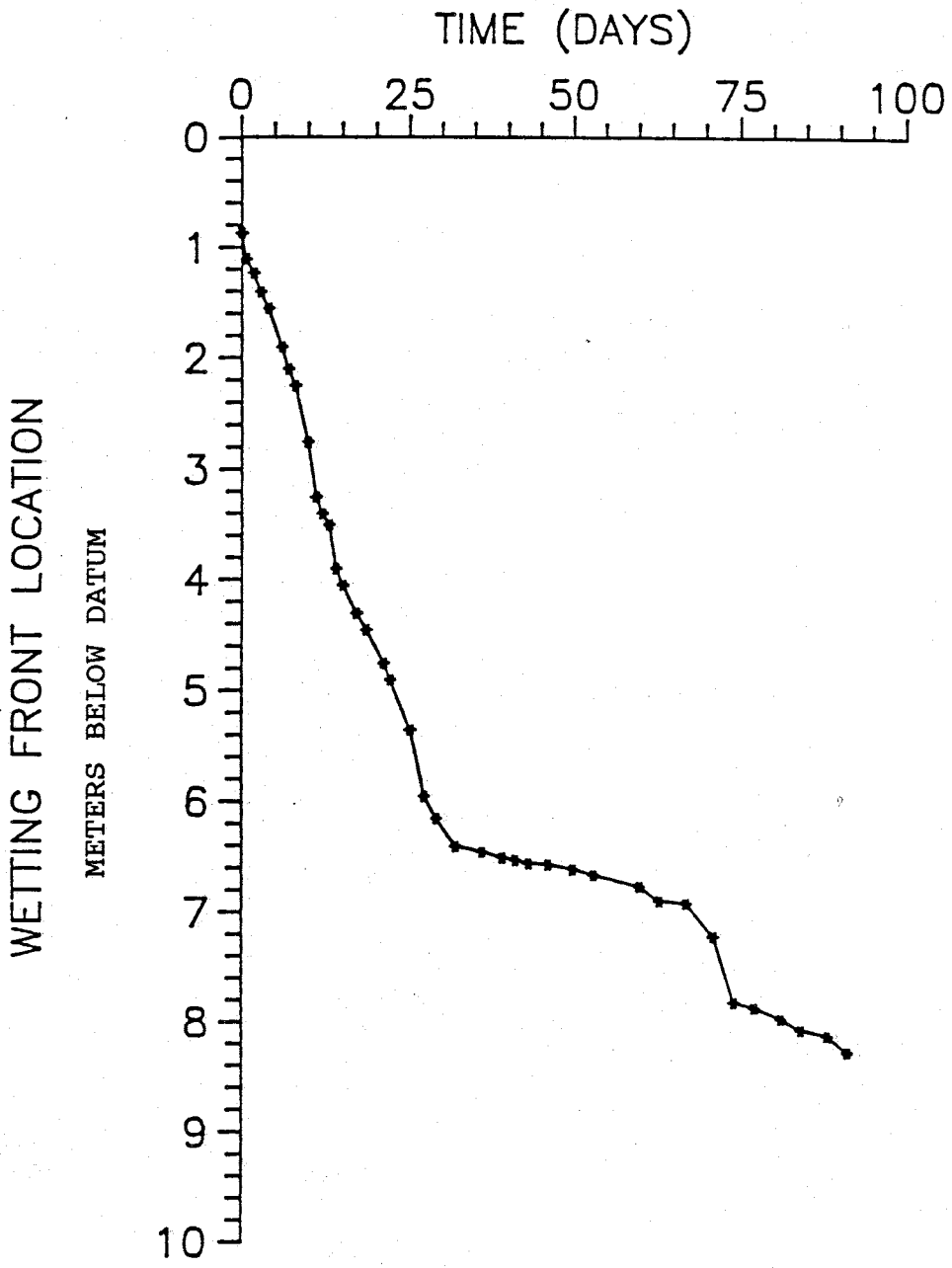

'IGURE 4-2. Depth of wetting front versus time at station 15-15.

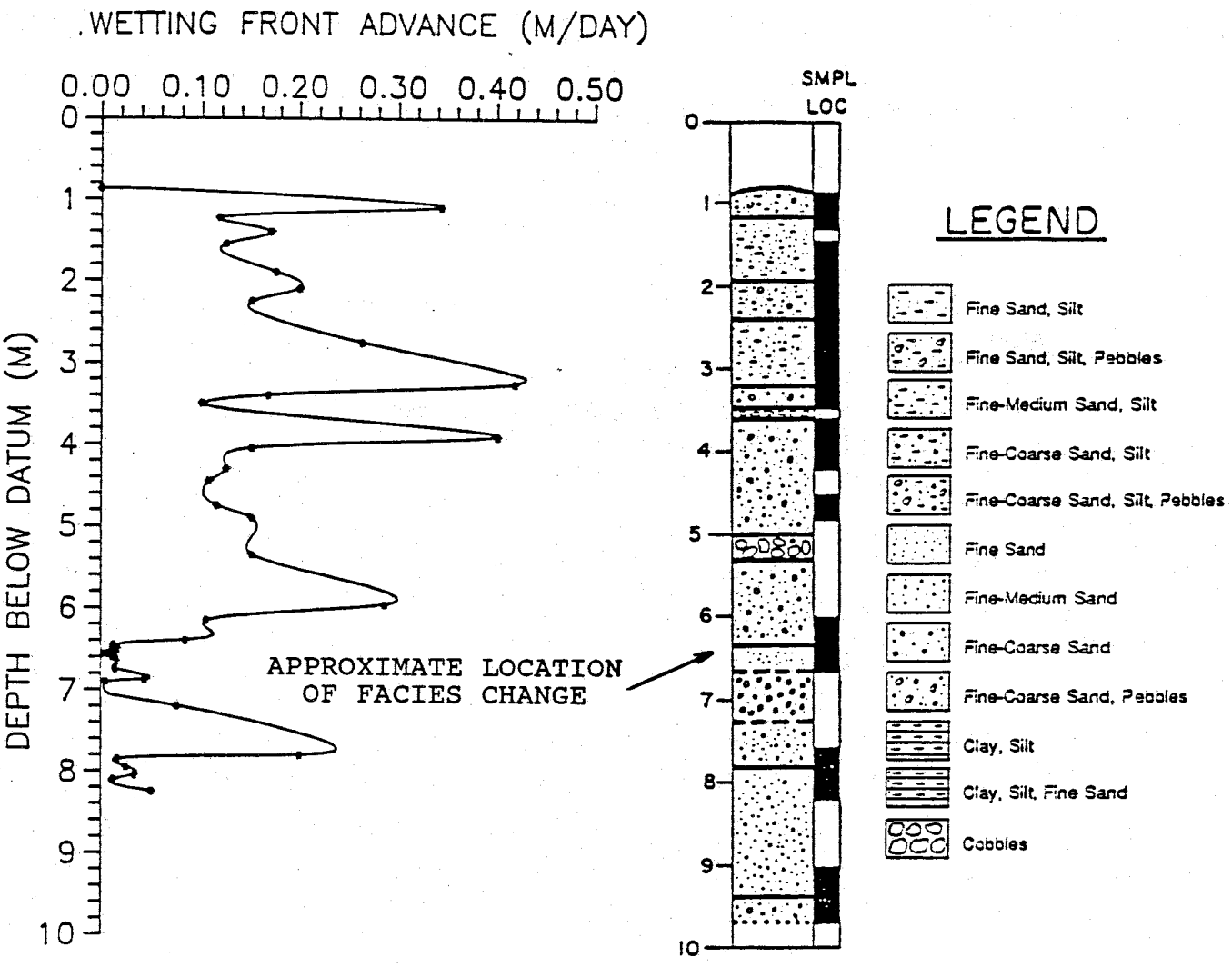

FIGURE 4-3. Rate of advance of wetting front versus depth at station 15-15. The data points are fitted by a cubic spline.

conductivity than the one above, since the water will not be able to flow as easily into the lower layer. This can be seen in Figure 4-3 at the 6.4 meter and 7.8 meter depths.

The extent to which lateral flow has occurred at the site is shown in Figure 4-4. After 153 days of water application the wetting front had progressed approximately 5 meters laterally from the edge of the simulated impoundment. Figure 4-5 shows moisture content contours for the alluvial facies and the fluvial facies after 329 days of water application.

These results demonstrate the existence and importance of lateral movement of seepage in the unsaturated zone, and how this lateral movement is controlled by the geology of the site, due to anisotropy and differences in hydraulic properties at stratigraphic interfaces. More detailed presentation and analyses of the wetting front propagation may be found in Parsons (1988) and Mattson (1989).

BROMIDE MOVEMENT THROUGH THE UNSATURATED ZONE AT THE SITE

As described in the Materials and Methods section, 14 soil water samplers were used to monitor the bromide movement through the unsaturated zone at the site. The bromide concentration in parts per million (ppm) versus time data is presented in Appendix A. Of particular

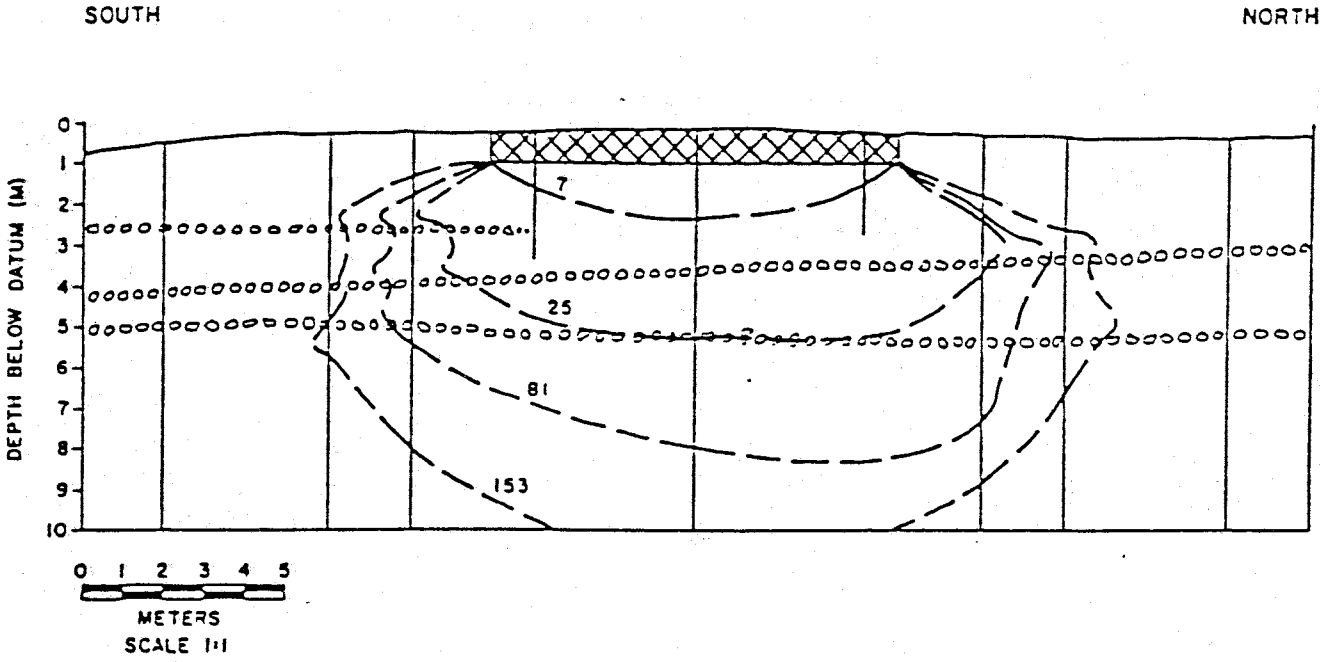

FIGURE 4-4. Cross section of site showing wetting front location at 7, 25, 81, and 153 days after the start of water application. Note the extent of lateral spreading.

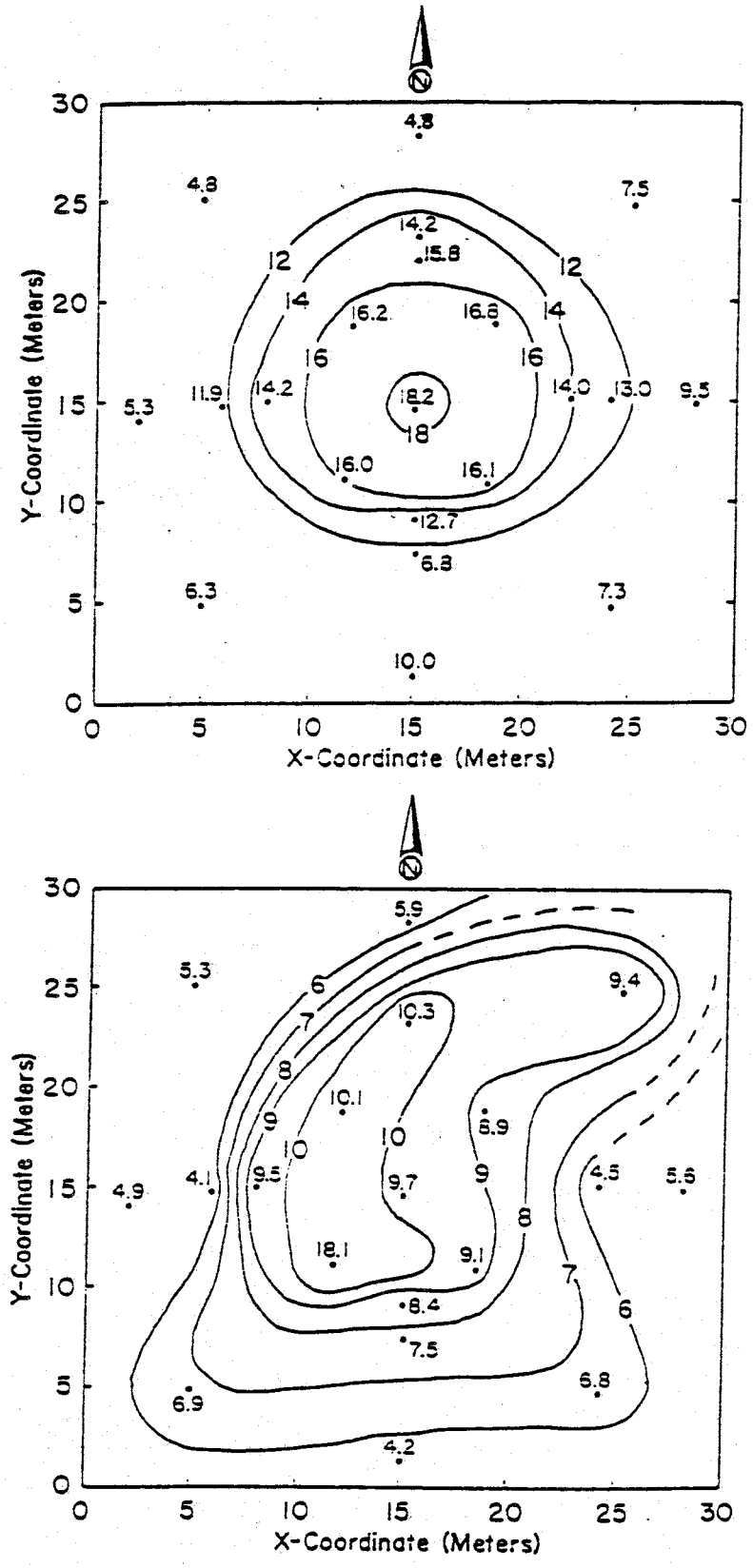

FIGURE 4-5. Moisture content contours at 2.25 (top) and 7.5 (bottom) meters below drip lines after 329 days of water application. The values of the contours are volumetric moisture content.

interest are samplers G, H, and I. The data from these samplers is important because it may be analyzed to determine transport parameters and transport mechanisms at the site. These samplers were nested at one location (Figure 3-7) at depths ranging from about 1 to 3.2 meters below the drip lines (Table 3-1).

BROMIDE BREAKTHROUGH BENEATH THE PLOT

Figure 4-6 presents the reduced bromide concentration (observed concentration divided by input concentration) versus time data for samplers G, H, and I. Plots of this type are known as breakthrough curves (BTCs).

Figure 4-7 presents the BTCs for the other samplers located beneath the plot - samplers C, D, and K. For various reasons none of these curves is complete. Sampler K was installed too late after the tracer injection to capture the first half of the curve. Although it appears as if the BTC for K includes a peak, it is not known if this is the actual peak or an anomaly. Comparison of BTC K with those of G, H, and I in Figure 4-6 shows that K's peak has a reduced concentration of about 0.18, while the lowest peak in Figure 4-6 is I's with a reduced concentration of about 0.23. Both of these peaks occur at about the same time, but what is noteworthy is that sampler I is about twice as deep as is sampler K. If this peak is real, then it serves to illustrate the degree of spatial variability existing at the site.

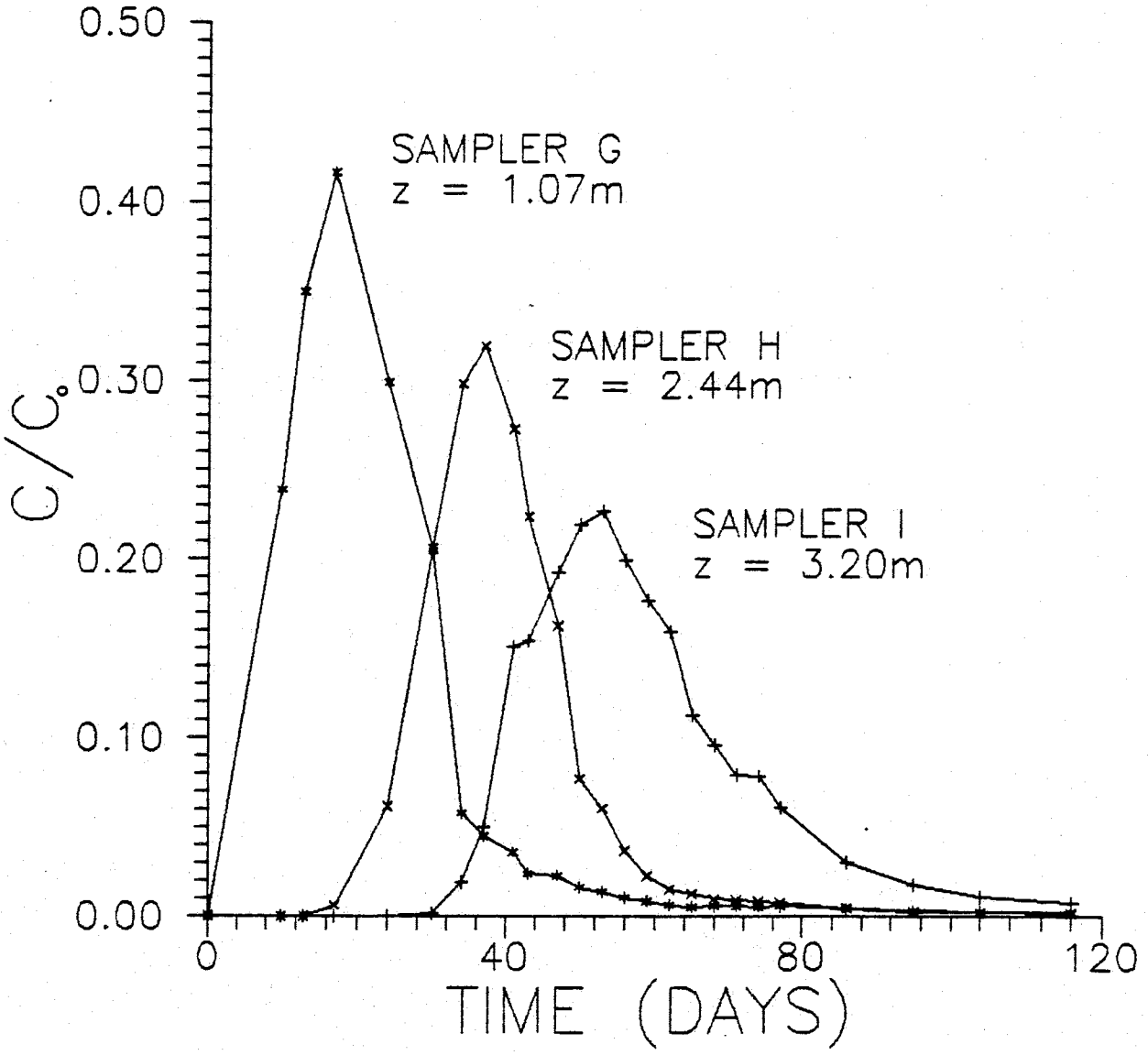

FIGURE 4-6. Bromide breakthrough curves for samplers G, H, and I, located at various depths below the driplines, beneath the plot. Z is the depth below the lines of each porous cup.

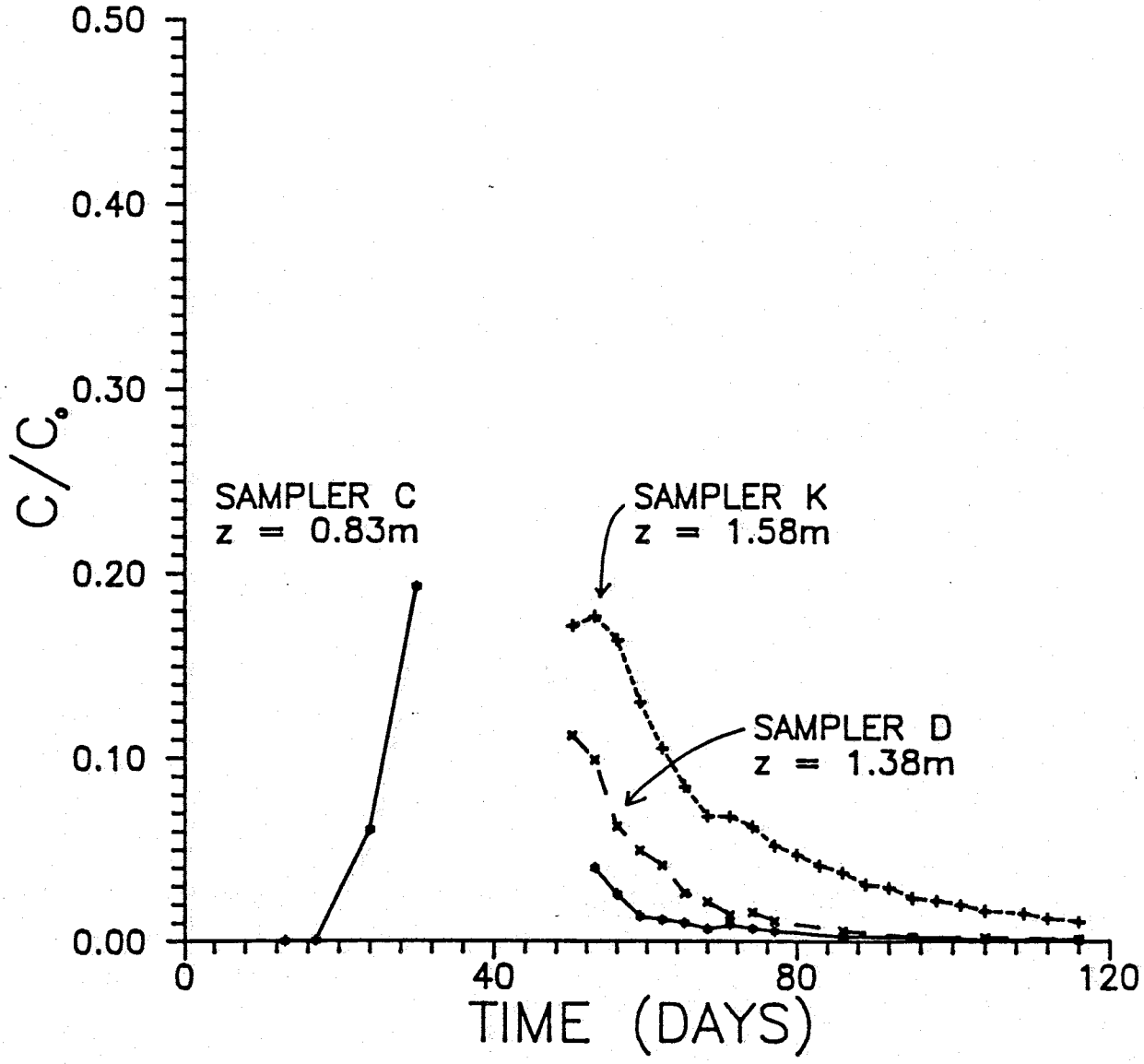

FIGURE 4-7. Bromide breakthrough curves for samplers C, D, and K, located at various depths below the driplines, inside the plot. These curves are incomplete due to reasons explained in the text.

Samplers C and D's BTCs are incomplete due to the clogging of their porous cups by fines. These samplers were installed initially without the use of silica flour. During the time it took to remove the instruments, rehabilitate the cups, and replace them (this time with silica flour around the cups), the bromide had passed the instruments' locations.

BROMIDE BREAKTHROUGH AT THE PERIMETER OF THE PLOT

Figure 4-8 presents the BTCs for samplers B, F, and J. These samplers are all located on the perimeter of the plot, being about 1-m horizontally distant, at various depths. The data from these samplers also serves to illustrate the degree of spatial variability existing at the site, since there is no correlation between the heights and times of the various peaks compared to the samplers' locations.

This group of samplers also included sampler A, which was nested with sampler B. Samples from A were collected at the same frequency as the other samplers, however, the bromide in the samples was undetectable by the HPLC due to masking effects by nitrate contamination. The source of this nitrate was never positively determined, but it is believed to have been due to decomposition of the layer of hay installed for insulation purposes when the site was constructed.

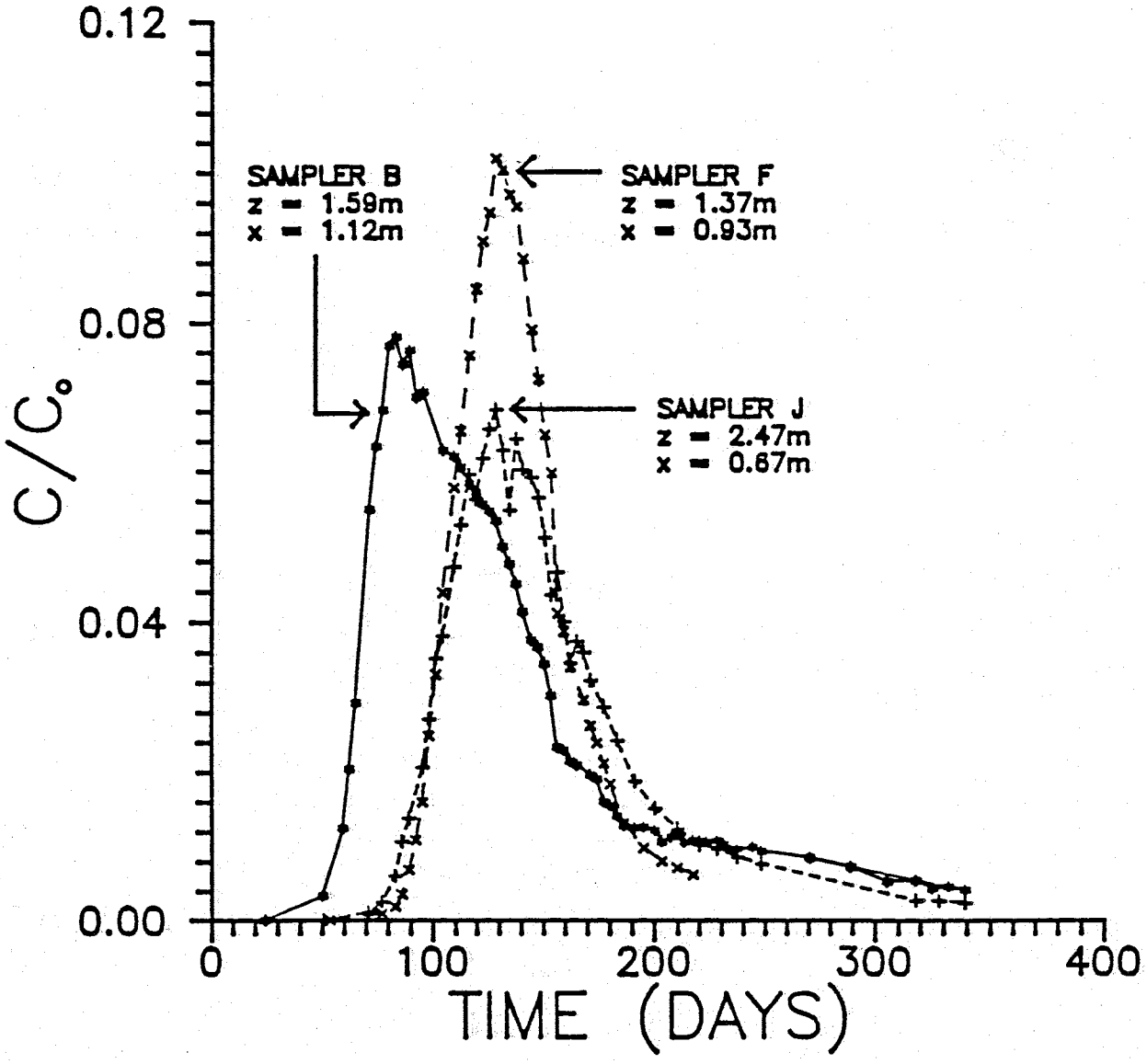

FIGURE 4-8. Bromide breakthrough curves for samplers B, F, and J, located at various depths below the driplines, on the perimeter of the plot. Z is the depth of the sampler cup below the plane of the driplines, and x is the horizontal distance from the edge of the plot.

BROMIDE BREAKTHROUGH AT THE OUTER ZONE

Figure 4-9 shows the bromide breakthrough for samplers L, M, N, and O. These samplers are all located about 6 meters from the plot (L on the south side, M on the east side, N on the north, and O on the west), and are between 5.5 and 6.5 meters below the plane of the driplines.

As can be seen from Figure 4-9 only sampler M saw significant quantities (more than 1.0 ppm) of bromide. Bromide began to arrive at this location in significant quantities about 140 days after injection. In contrast, bromide did not arrive at L until about 340 days after injection, and about 300 days after injection at N. At the end of the experiment, sampler O had still not seen significant quantities of bromide. These results are consistent with the observed behavior of the wetting front movement shown in Figures 4-4 and 4-5. Figure 4-4 shows significant lateral movement of the wetting front in the north and south directions, while Figure 4-5 shows water movement off to the north-east, and to a lesser extent, the south-west and south-east, in the fluvial facies.

Figures 4-10 and 4-11 show the locations of the outer zone samplers in relation to the stratigraphic layers at the site. All of these samplers are located in the fluvial facies, a meter or two below the interface between the piedmont slope facies and the fluvial facies. Samplers M, N, and O are located in layers of fine and medium fine sands. Sampler M is positioned just below a major cobble

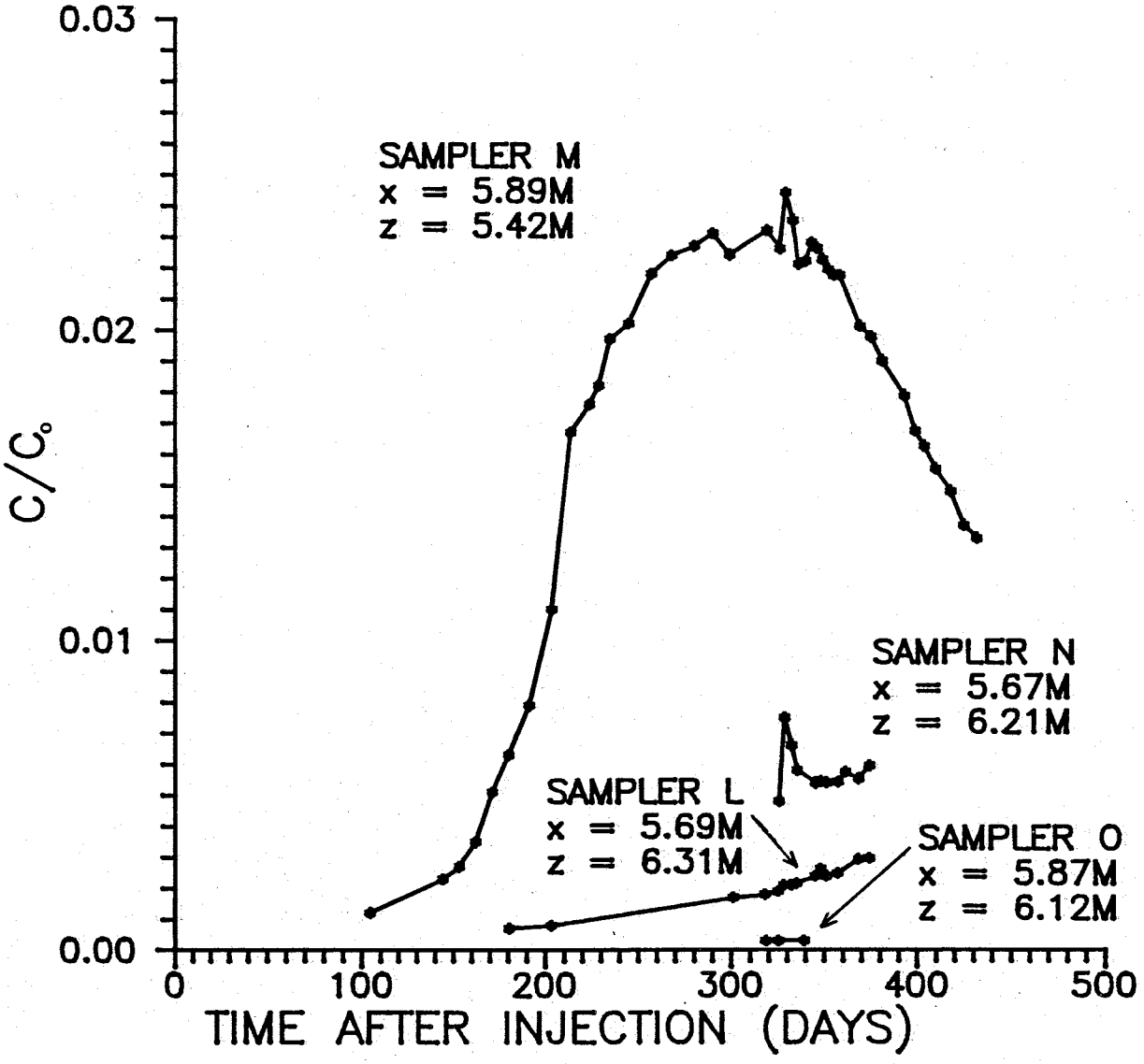

FIGURE 4-9. Bromide breakthrough curves for samplers L, M, N, and O, located about 6 meters below the plane of the driplines, and about 6 meters horizontally distant from the driplines, one on each side of the plot. Z is the depth of the sampler cup below the plane of the driplines, and x is the horizontal distance from the edge of the plot.

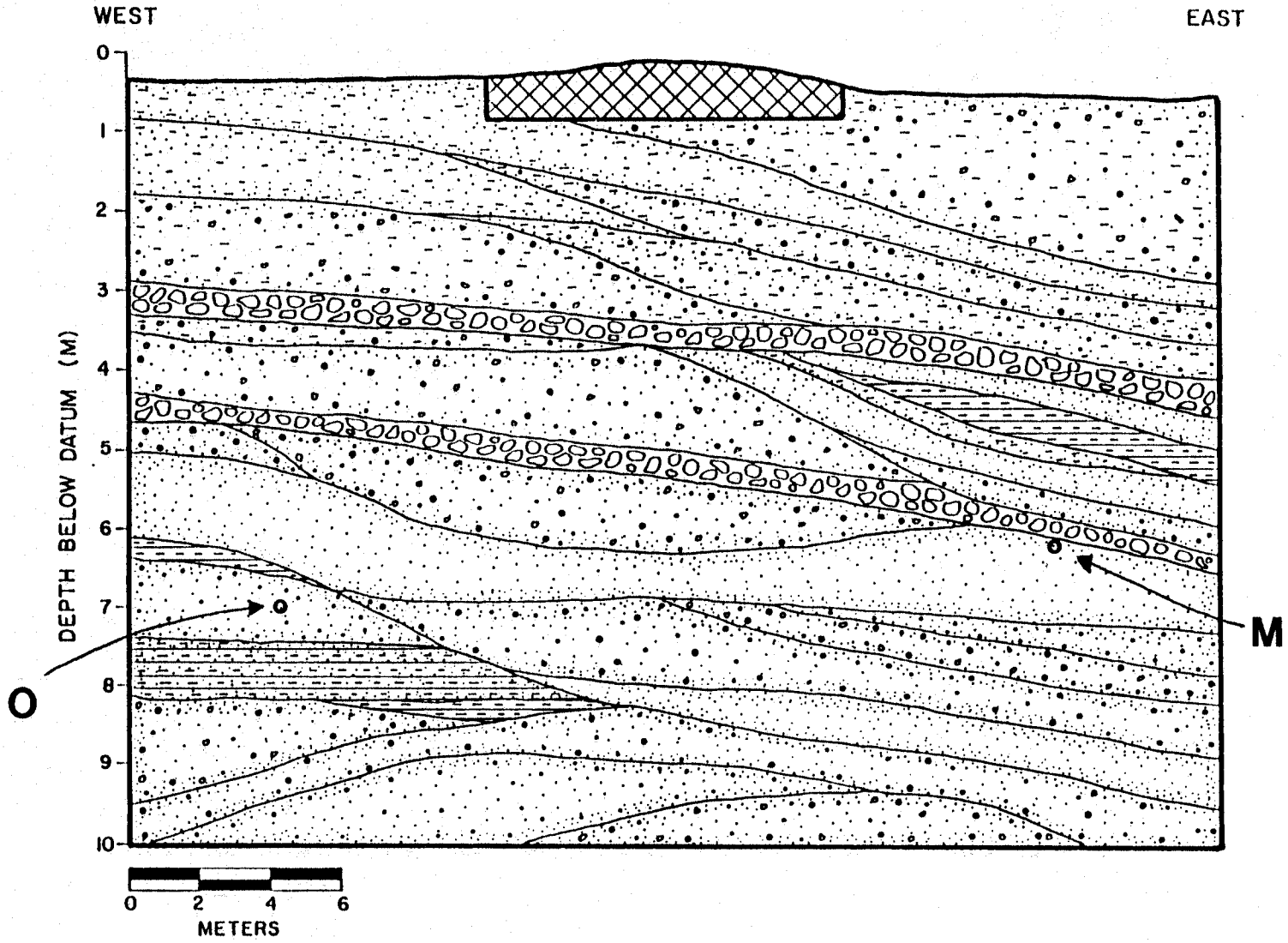

FIGURE 4-10. Location of samplers M and O, in relation to the stratigraphy of the site.

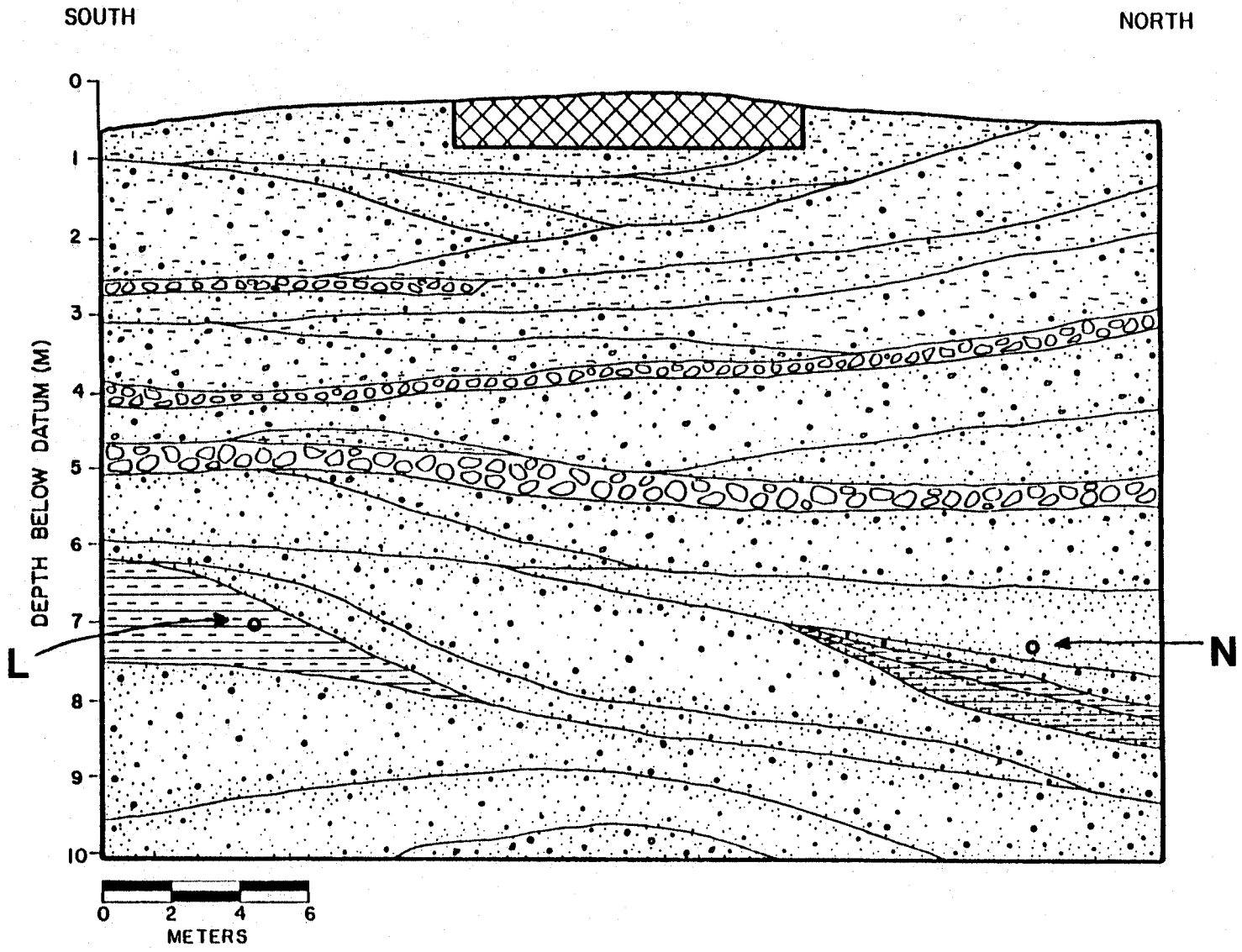

FIGURE 4-11. Location of samplers L and N, in relation to the stratigraphy of the site.

layer. Sampler L is located in a layer of clay and silt. The stratigraphic layers dip from west to east across the site. This dipping facilitates lateral movement of water in this direction due to the addition of gravitational forces to the stratigraphic effects on unsaturated flow discussed earlier (Chapter 3). This may explain why the bromide reached sampler M significantly sooner than the others.

Volumetric moisture contents at the location of sampler M are twice that of the other outer zone samplers. Neutron logging at station 28-15 (Figure 3-4), about 2.5 meters horizontally distant from sampler M, showed a volumetric moisture content of about 10%, while neutron logging at the stations similarly distant to the other outer zone samplers show volumetric moisture contents on the order of 5 to 6%, which is the background volumetric moisture content at these locations. While these other stations showed no evidence of the wetting front, it is inferred that the wetting front has reached the locations of samplers L and N, otherwise bromide would not have been detected at these positions.

MASS RECOVERIES

The percentage of mass recovered for each of the samplers located beneath the plot are presented in Table 4-1. These percentages were determined by calculating the area under the BTCs for each sampler, converting to mass recovered,

TABLE 4-1. FIELD SAMPLER MASS RECOVERIES

SAMPLER	PERCENT RECOVERED
C[1]	13.8
	6.2
	20.0
D	20.8
G	143.5
H	104.0
I	108.3
K	67.4

1: THE BTC FOR SAMPLER C CONSISTS OF TWO PARTS (REFER TO FIGURE 4-10)

and dividing by the input mass. The input mass was calculated as

$$M_i = QT_0C_0 \qquad (4.1)$$

where Q = applied flow rate to plot,

T_0 = duration of input pulse, and

C_0 = input solute concentration.

For the bromide tracer experiment the input mass was

$$M_i = (815.7 \text{ l/day})(6.29 \text{ days})(0.435 \text{ g/l})$$

or

$$M_i \approx 2232 \text{ g of bromide}$$

The applied flux of 815.7 l/day was determined to be the actual applied amount of water for the duration of the tracer experiment, as measured by the totalizing flow meter.

The area under the BTCs was converted to mass recovered as follows

$$M_r = AQ \qquad (4.2)$$

where A = area under the BTC (mg-days/l).

The area under the BTCs was determined by the use of a computer program called TRAP2. This code fits a polynomial to the BTC using cubic spline interpolation. It then performs numerical integration on this polynomial using Simpson's Rule to determine the area under the BTC. A listing of the FORTRAN code of TRAP2 is presented in Appendix E.

For the complete BTCs underneath the plot (samplers G, H, and I), the mass recoveries ranged from 143.5% for G, to 104.0% for H. Mass recoveries greater than 100% are possible due to such mechanisms as non-uniform flow and non-uniform distribution of solute. The mass recoveries for the incomplete BTCs underneath the plot (samplers C, D, and K), were calculated strictly as the area under the incomplete curves. No effort was made to interpolate where the unobserved portions of the curves would have been located.

BROMIDE AND TRITIUM MOVEMENT THROUGH UNSATURATED SOIL FROM THE SITE IN LABORATORY COLUMNS

The bromide BTCs from the two unsaturated solute transport laboratory column experiments are shown in Figure 4-12. There was some difficulty analyzing the collected fractions for bromide content by HPLC due to interference by (it was assumed) nitrate. Both curves were normalized

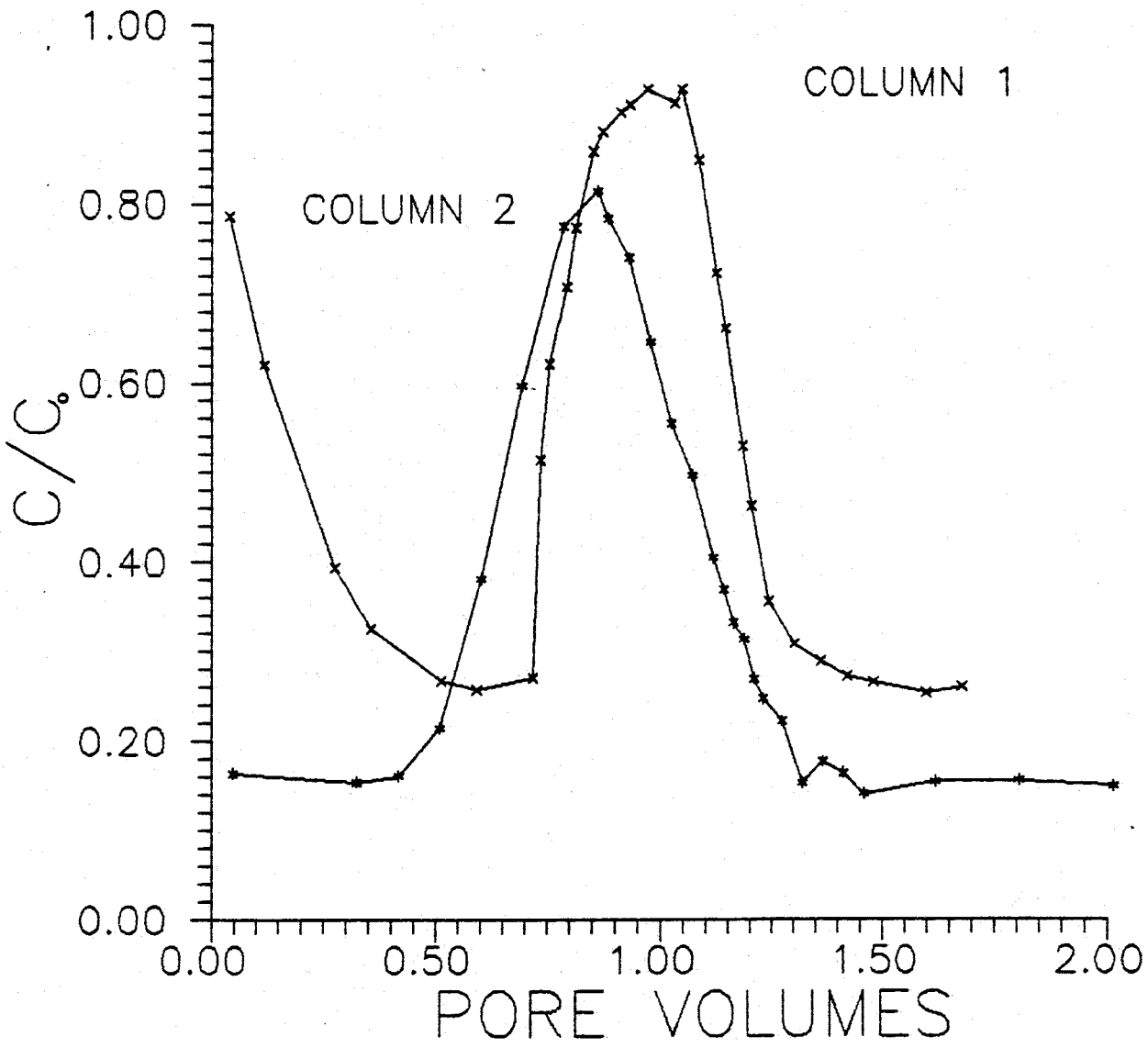

FIGURE 4-12. Actual bromide BTCs for columns #1 and #2.

by subtracting a constant value from each data point of the curves. These values were determined from the low point of each of the curves. The unusually high initial values of column 1 were also subtracted from that curve. The data from the two column experiments is listed in Appendix B.

The normalized bromide BTCs along with the tritium BTCs are shown in Figures 4-13 and 4-14. As is evident from the figures, a significant amount of anion exclusion occurred in the columns. In most soils tritium moves with the water as an ideal tracer. Since the bromide came through significantly faster than the tritium in the columns, anion exclusion is indicated.

This data was analyzed using the CXTFIT program developed by Parker and Van Genuchten (1984a). The program uses a nonlinear least-squares inversion method to fit transport parameters to observed data for a number of theoretical one-dimensional solute transport models. Only the one-dimension advection-dispersion equation (1-D ADE) model was fitted to the data, since there was no, or little, evidence of mobile-immobile water flow in the columns (i.e., little or no asymmetry or tailing); and this equation fit the observed data quite well. This model fits an analytical solution of the 1-D ADE (Equation 2.27) to the given data points. The analytical solution was based on the assumptions that the extracted samples represented flux-averaged concentrations; the initial bromide concentration in the soil was zero (Equation 2.31); the upper boundary

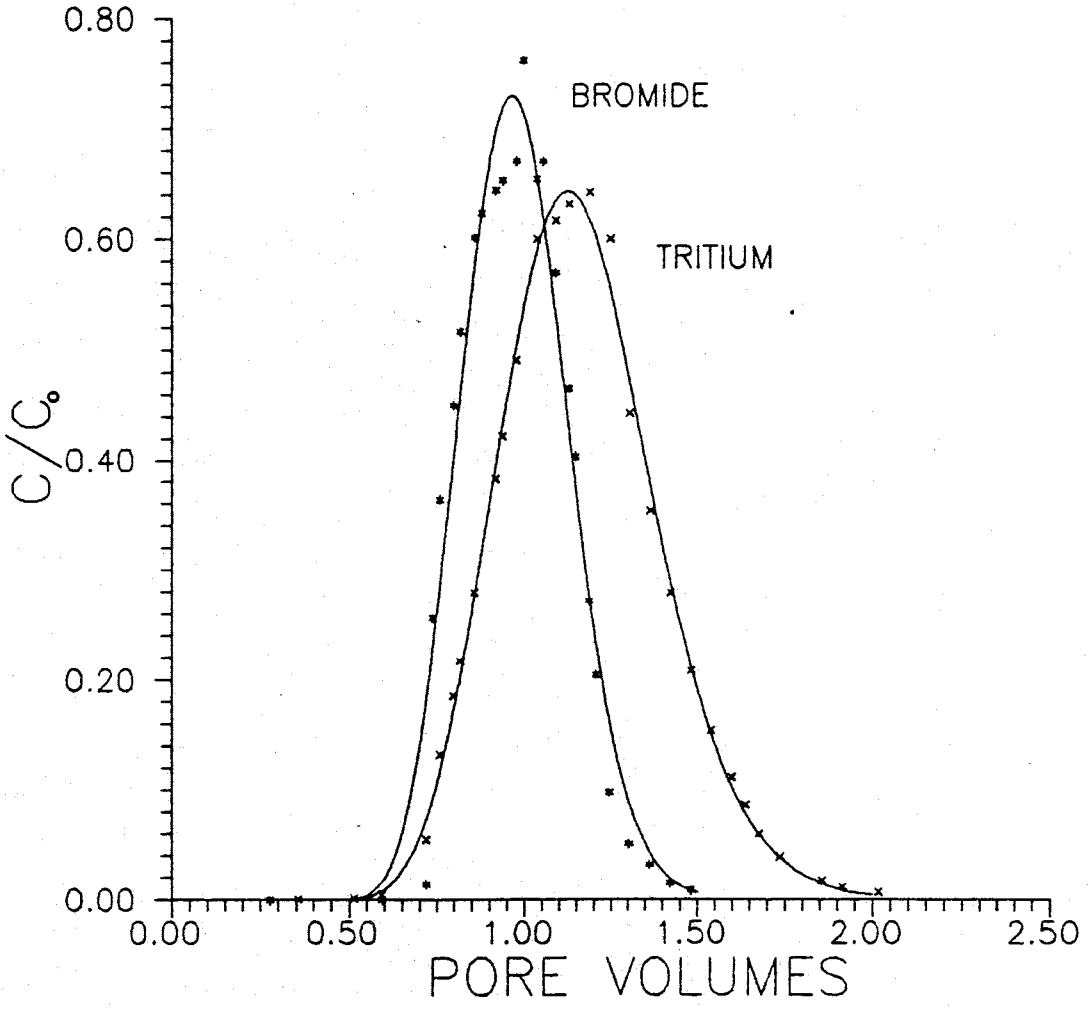

FIGURE 4-13. Tritium and normalized bromide BTCs for column #1. The symbols represent observed data points and the solid lines represent CXTFIT (model number 2) fitted BTCs. The retardation factor for bromide was determined to be 0.84, indicating anion exclusion.

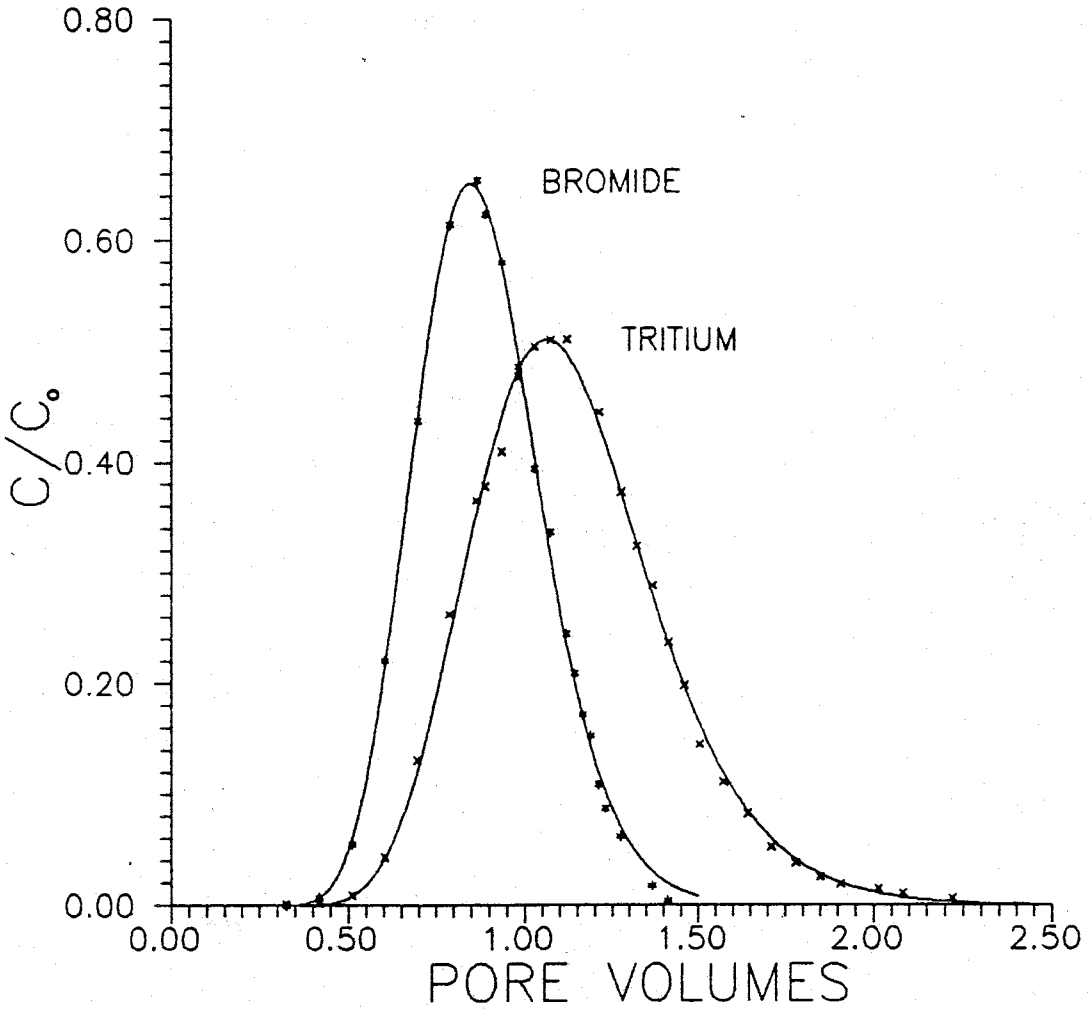

FIGURE 4-14. Tritium and normalized bromide BTCs for column #2. The symbols represent observed data points and the solid lines represent CXTFIT (model number 2) fitted BTCs. The retardation factor for bromide was determined to be 0.74, indicating significant anion exclusion.

condition was of the third-type (Equation 2.29); the system was semi-infinite (Equation 2.30); and tracer was applied as a pulse, resulting in the solution of the 1-D ADE having the form of Equation 2.38.

The values resulting from applying this model are presented in Table 4-2. In both cases (columns #1 and #2) the only parameter held constant while running the model was the pore water velocity, which was known from experimental measurements. The retardation factor, the coefficient of hydrodynamic dispersion, and the injection pulse were then fitted to the observed data.

This analysis indicated that the bromide had a retardation factor of 0.84 for column #1, and 0.74 for column #2, which is surprising, due to the low average clay content of the upper facies. The average D_{10} (10% of the particle are finer than this size, by weight) for the upper alluvial soil zone at the site is 0.067 mm (Parsons, 1988). Particles less than 0.002 mm are classified as clays according to the USDA soil classification system. This relatively high D_{10} value indicates that the clay content of the upper alluvial zone is quite small.

The fitted retardation for the tritium BTCs were 0.99 for column #1, and 0.97 for column #2, indicating that the tritium behaved as an ideal tracer.

TABLE 4-2. FITTED PARAMETERS OF THE LABORATORY COLUMN TRANSPORT EXPERIMENTS OBTAINED FROM CXTFIT USING THE CLASSICAL ONE-DIMENSION ADVECTION-DISPERSION EQUATION (EQUATION 2.27).

BROMIDE

COLUMN	L(cm)	v(cm/day)	R	T_0(PV)	D(cm²/day)	α_l
1	27.3	3.23	0.837	0.282	1.08	0.33
2	30.0	4.16	0.735	0.290	3.06	0.74

TRITIUM

COLUMN	L(cm)	v(cm/day)	R	T_0(PV)	D(cm²/day)	α_l
1	27.3	3.23	0.985	0.357	1.86	0.57
2	30.0	4.16	0.974	0.323	4.32	1.04

L = COLUMN LENGTH.
v = PORE WATER VELOCITY. FIXED PARAMETER.
R = RETARDATION FACTOR. FITTED PARAMETER.
T_0 = PULSE LENGTH IN PORE VOLUMES. FITTED PARAMETER.
D = COEFFICIENT OF HYDRODYNAMIC DISPERSION. FITTED PARAMETER.
α_l = LONGITUDINAL DISPERSIVITY = D/v.

BROMIDE TRANSPORT PARAMETERS AND TRANSPORT MECHANISMS AT THE SITE

The breakthrough data for samplers G, H, and I were analyzed using the CXTFIT code to determine the bromide transport parameters for the unsaturated zone in the area of these samplers. Both the 1-D ADE model and the 1-D ADE with mobile-immobile water model were used. The results for the 1-D ADE model are presented in Table 4-3.

Only samplers G, H, and I were analyzed with CXTFIT since the program is only applicable to the one-dimensional case. While samplers C, D, and K fit this criteria, there was insufficient data for these samplers to apply the model. While CXTFIT is strictly applicable to the case where the volumetric moisture content is constant with depth, it has been shown (Cassel et al., 1975; Wierenga, 1977) that the use of an average volumetric moisture content instead of the actual distribution is justified for use in the analytical modeling of one-dimensional solute transport.

Figure 4-15 shows the BTCs for samplers G, H, and I, with the fitted curves generated by applying CXTFIT. The particular CXTFIT model used for this analysis was No. 2: deterministic linear equilibrium adsorption with flux concentrations. The same initial and boundary conditions used for the column analysis were also used here. Flux concentrations were used since they gave a slightly better

TABLE 4-3. FITTED PARAMETERS OF THE BROMIDE TRANSPORT EXPERIMENT OBTAINED FROM CXTFIT USING THE CLASSICAL ONE-DIMENSION ADVECTION-DISPERSION EQUATION (EQUATION 2.27)

		FIXED		FITTED		
SAMPLER	z(m)	R	T_0(day)	v(cm/day)	D(cm²/day)	α_l
G	1.07	1.0	9.03	5.90	115.5	19.6
H	2.44	1.0	6.54	6.87	47.2	6.87
I	3.20	1.0	6.81	6.05	59.5	9.83
AVE.				6.27	74.1	12.1

z = DEPTH BELOW SOURCE.
R = RETARDATION FACTOR. ASSUMED TO BE EQUAL TO 1.0. FIXED PARAMETER.
T_0 = PULSE LENGTH. DETERMINED FROM MASS RECOVERY. FIXED PARAMETER.
v = PORE WATER VELOCITY. FITTED PARAMETER.
D = COEFFICIENT OF HYDRODYNAMIC DISPERSION. FITTED PARAMETER.
α_l = LONGITUDINAL DISPERSIVITY = D/v.

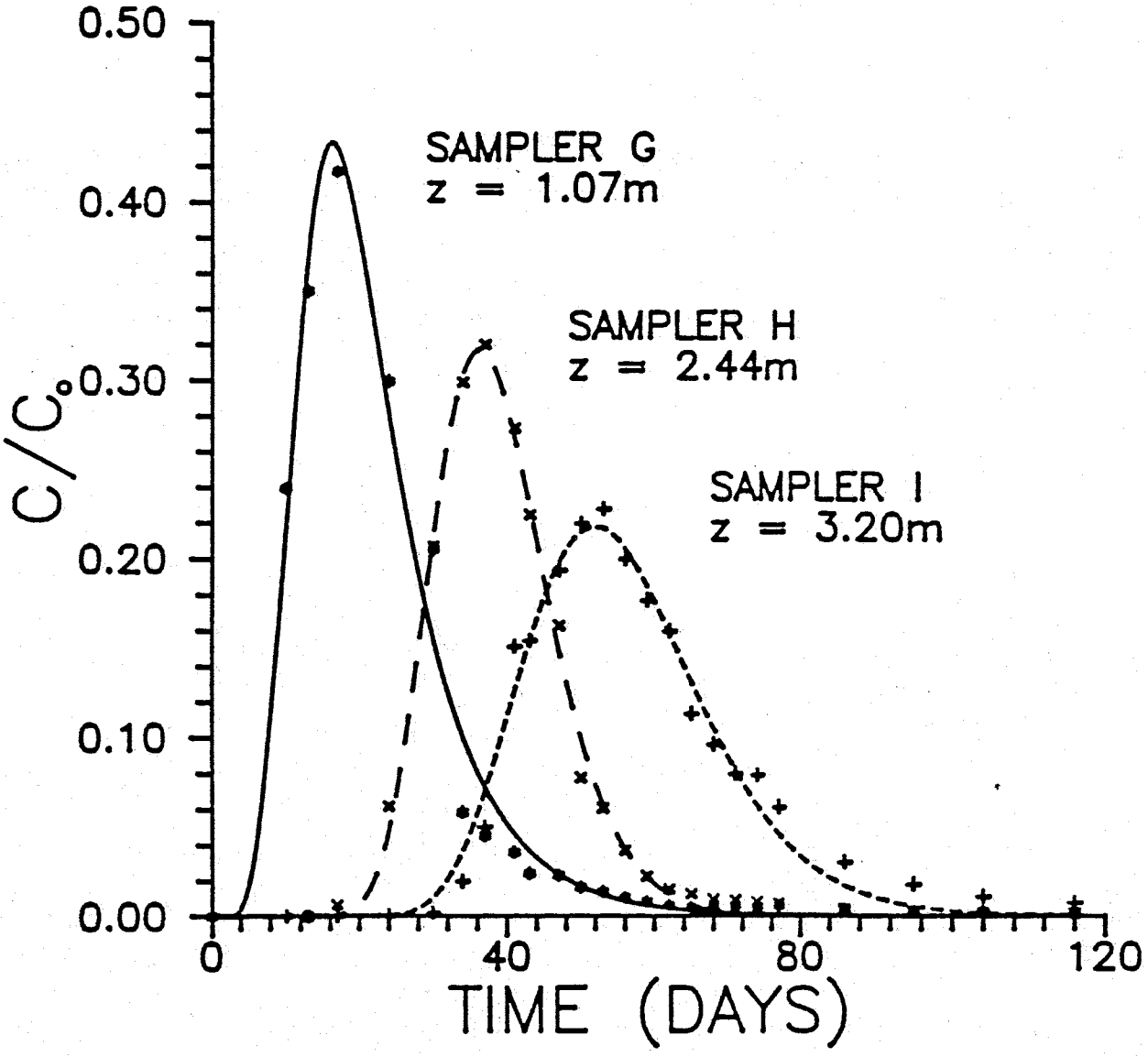

FIGURE 4-15. CXTFIT (model number 2) fitted BTCs for samplers G, H, and I. The symbols represent observed data points. Z is the depth below the driplines of each sampler cup.

fit to the observed data than resident volume-averaged concentrations when applying CXTFIT.

The fitted curves generally followed the data points quite well, with the exception of the tails. The extensive tailing exhibited by the three BTCs is characteristic of the mobile-immobile water model for unsaturated flow and solute transport, described earlier (Chapter 2).

For this case, bromide is considered to be a conservative tracer, and the retardation factor, R, was assumed to be equal to 1.0. This parameter was then held constant while running the program for each sampler. The other parameter held constant was the input pulse, T_0. This parameter was determined by dividing the calculated area under each BTC by the input concentration times the tracer application period. The parameters v and D were then fitted to the observed BTC data.

The fitted pore water velocities ranged from 6.87 cm/day for sampler H to 5.91 cm/day for sampler G. These values are substantially higher than those obtained using the known values of other experimental parameters to calculate the pore water velocities for each sampler. The average fitted pore water velocity is 6.27 cm/day, compared to an average calculated pore water velocity of 3.89 cm/day.

Dividing the flux to the section of the plot which contained these samplers by the measured volumetric moisture contents yields the values tabulated in Table 4-4.

TABLE 4-4. PORE WATER VELOCITIES DETERMINED FROM EXPERIMENTAL PARAMETERS

SAMPLER	z(m)	θ(cm^3/cm^3)	q(cm/day)	v'(cm/day)
G	1.07	0.188	0.685	3.64
H	2.44	0.174	0.685	3.94
I	3.20	0.168	0.685	4.08
AVE.		0.177		3.89

z = DEPTH BELOW SOURCE.
θ = VOLUMETRIC WATER CONTENT. SEE APPENDIX C FOR CALCULATION OF THESE VALUES.
q = APPLIED FLUX. SEE APPENDIX D FOR CALCULATION OF THIS VALUE.
v'= PORE WATER VELOCITY = q/θ.

The measured flux to this section of the plot was determined to be 0.685 cm/day. This value is calculated in Appendix D.

The calculated moisture contents are also presented in Table 4-4. They were determined from the neutron logging conducted periodically during the course of the tracer experiment. Figures 4-16, 4-17, and 4-18 present the time averaged volumetric moisture content observed at stations 15-15, 12-18, and 18-18, respectively. These stations surround the location of samplers G, H, and I. The error bars indicate the maximum and minimum readings observed. Readings were taken in 1-foot (.305 m) increments starting at a depth of 0.3-m below the drip lines. This uppermost value was not included in the calculations since the probe was influenced by the water remaining in the lines and the material of which the lines were constructed (polyethylene) in obtaining this value. The remaining values were then averaged to provide a spatially averaged value at each depth increment. These spatially averaged values were then averaged over the depth to each sampler to provide an average volumetric moisture content for use in calculations involving each sampler. These data and calculations are presented in Appendix C.

The higher observed pore water velocities indicate that some mechanism of accelerated transport is occurring. The two candidates for this mechanism are anion exclusion and mobile-immobile water. Due to the small clay content in

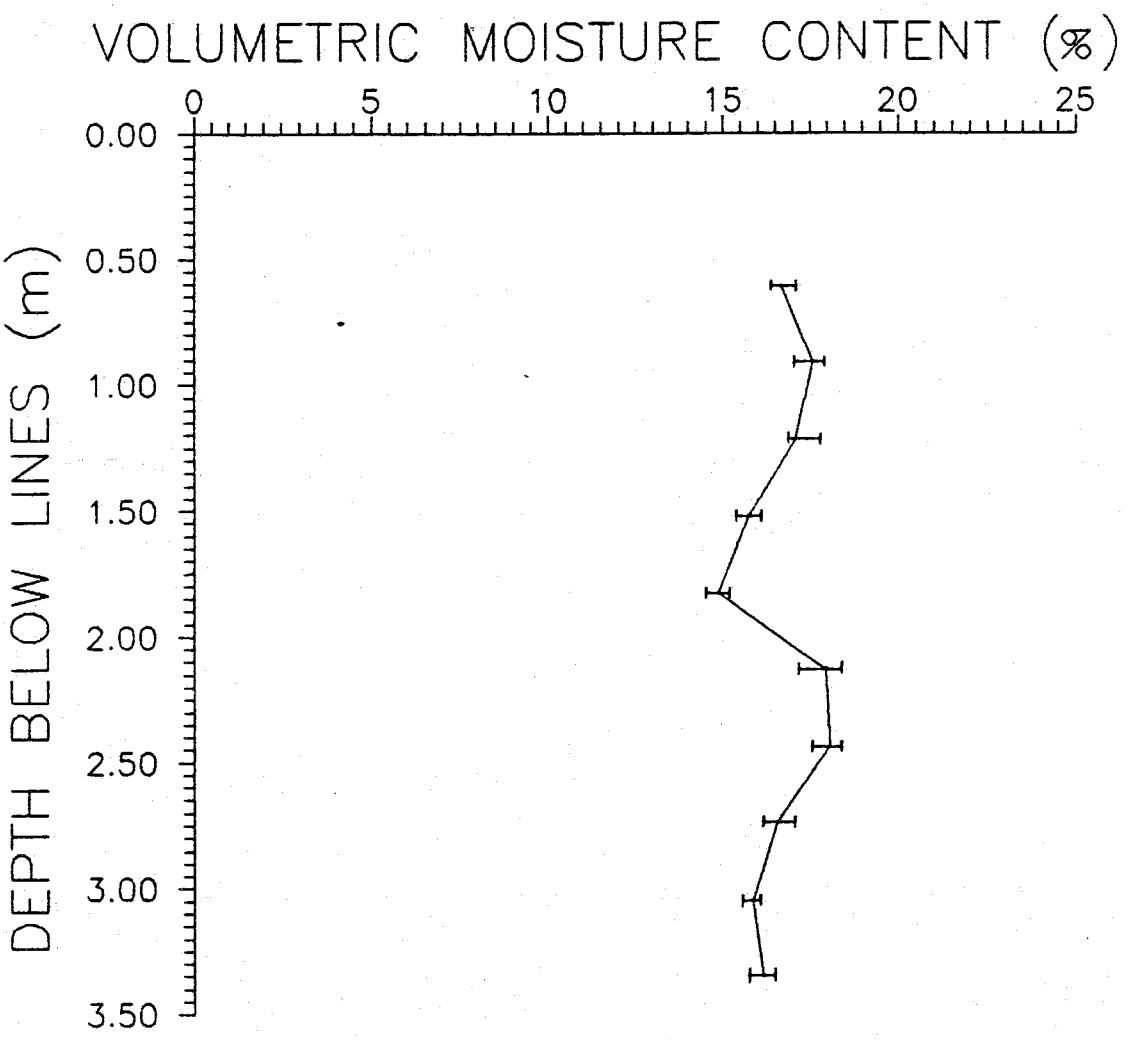

FIGURE 4-16. Volumetric moisture content recorded at station 15-15 by the neutron probe, averaged over the duration of the tracer experiment. The error bars indicate the maximum and minimum values recorded.

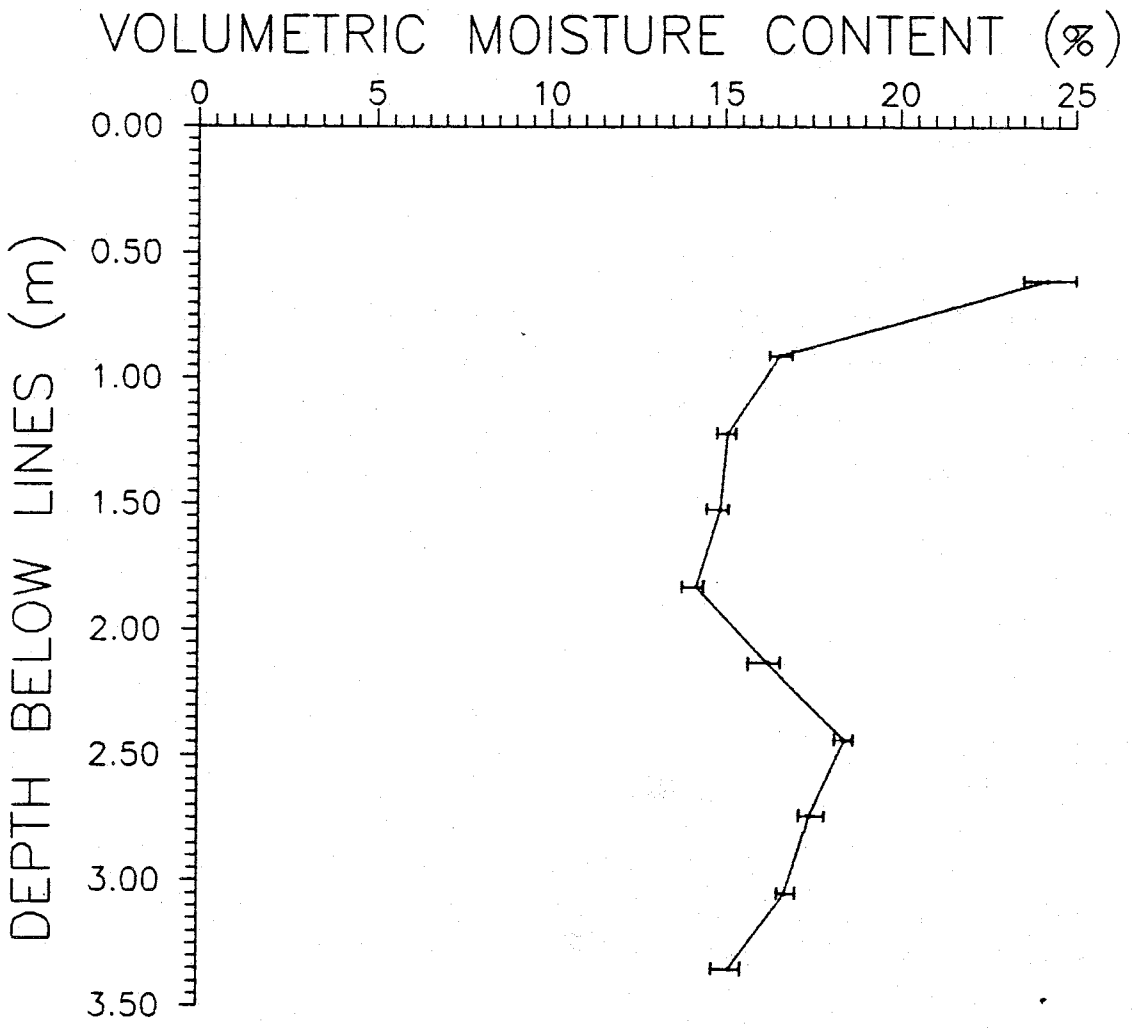

FIGURE 4-17. Volumetric moisture content recorded at station 12-18 by the neutron probe, averaged over the duration of the tracer experiment. The error bars indicate the maximum and minimum values recorded.

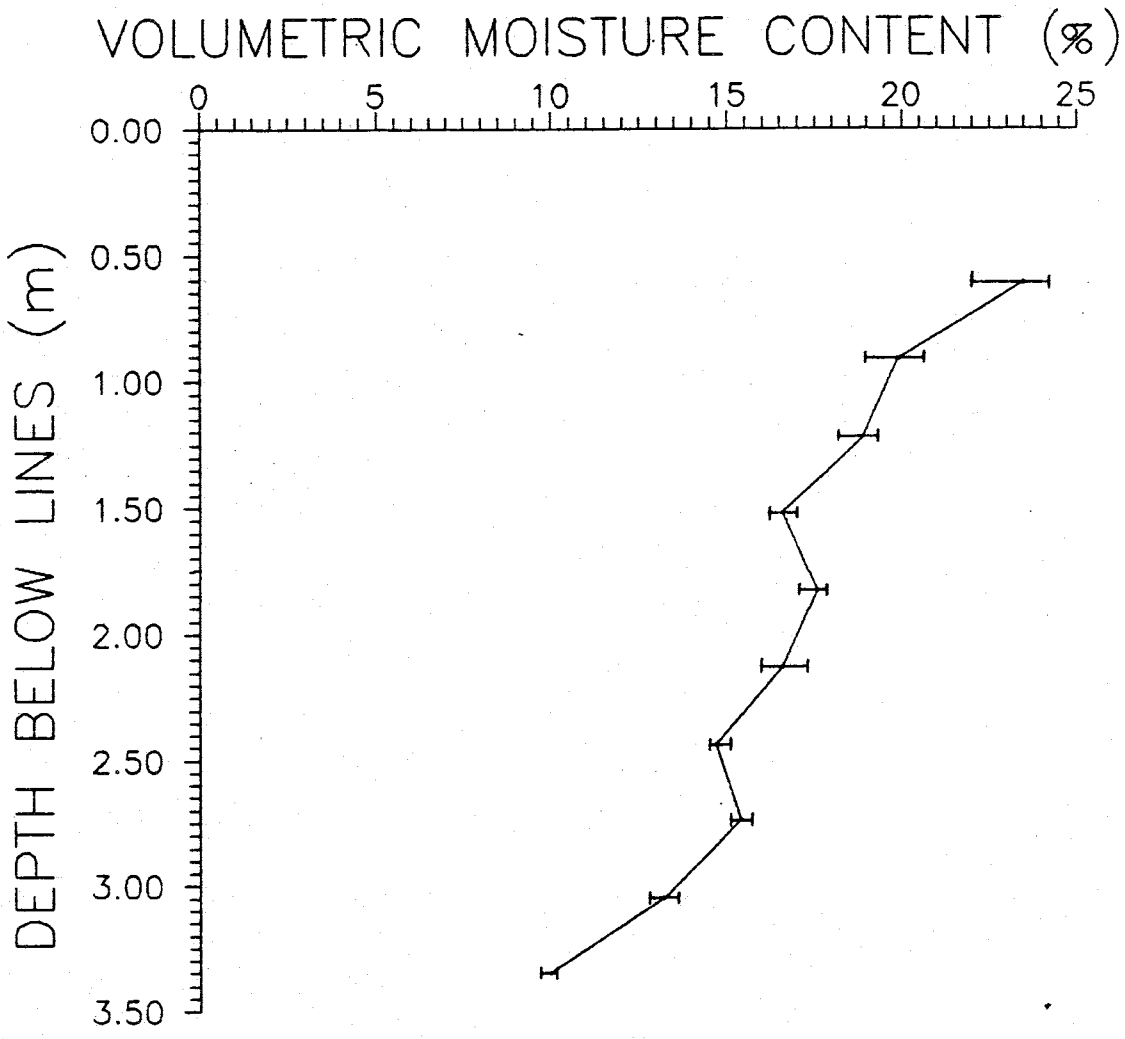

FIGURE 4-18. Volumetric moisture content recorded at station 18-18 by the neutron probe, averaged over the duration of the tracer experiment. The error bars indicate the maximum and minimum values recorded.

the soil at the samplers' location it was believed that little, or no, anion exclusion was occurring.

To check if anion exclusion was occurring at the site, two unsaturated laboratory column experiments using soil from near the samplers' location were conducted using anionic bromide and tritium as tracers. If anion exclusion was occurring, then the bromide would breakthrough prior to the tritium. These experiments were described in Chapter 3, and the results were presented earlier in this chapter. These results indicate that significant anion exclusion was occurring in the soil from the site, which is surprising, due to the small clay content of the alluvial facies zone at the site.

The observed BTCs from the field were then analyzed by CXTFIT, this time including the anion exclusion observed in the laboratory columns. These results are presented in Table 4-5. For these cases, the retardation factor for sampler G was assumed to be equal to that observed in column #1 (R = 0.837), while the retardation factors for samplers H and I were assumed to be equal to the average of those observed in columns 1 and 2. This parameter was held constant, along with the input pulse, and v and D were fitted to the observed BTC data. The resulting values of v an D can also be obtained by multiplying the assumed retardation factors times the values listed in Table 4-3.

The BTCs for samplers G, H, and I were also analyzed using the mobile-immobile water model of CXTFIT. Figures

TABLE 4-5. FITTED PARAMETERS OF THE BROMIDE TRANSPORT EXPERIMENT OBTAINED FROM CXTFIT USING THE CLASSICAL ONE-DIMENSION ADVECTION-DISPERSION EQUATION (EQUATION 2.27), WITH RETARDATION FACTORS OBTAINED FROM THE LABORATORY COLUMN EXPERIMENTS

SAMPLER	z(cm)	R	T_0(day)	v(cm/day)	D(cm²/day)	α_l
G	107	0.837	9.03	4.94	96.65	19.6
H	244	0.786	6.54	5.40	37.07	6.86
I	320	0.786	6.81	4.75	46.70	9.83

z = DEPTH BELOW DRIP LINES.
R = RETARDATION FACTOR. DETERMINED FROM LABORATORY COLUMN EXPERIMENTS. FIXED PARAMETER.
T_0 = PULSE LENGTH. DETERMINED FROM MASS RECOVERY. FIXED PARAMETER.
v = PORE WATER VELOCITY. FITTED PARAMETER.
D = COEFFICIENT OF HYDRODYNAMIC DISPERSION. FITTED PARAMETER.
α_l = LONGITUDINAL DISPERSIVITY = D/v.

4-19 through 4-21 show the BTCs for samplers G, H, and I with fitted curves generated by applying model No. 4 of CXTFIT: two-site/two-region with flux concentrations (the mobile-immobile water model, Equations 2.41 and 2.42). This model fits an analytical solution to Equations 2.41 and 2.42 to the given data points. The analytical model was based on the assumptions that the extracted samples represented flux-averaged concentrations, the initial bromide concentration in both the mobile and the immobile phases was zero

$$C_m(x,0) = C_{im}(x,0) = 0 \qquad (4.3)$$

the upper boundary condition was of the third type

$$-D_1 \frac{\partial C_m}{\partial t} + v_m C_m \Big|_{x=0} \begin{cases} vC_0 & 0 < t \leq t_0 \\ 0 & t > t_0 \end{cases} \qquad (4.4)$$

the system was semi-infinite

$$\frac{\partial C_m}{\partial t}(\infty,t) = 0 \qquad (4.5)$$

and the tracer was applied as a pulse. Note that the fitted curves follow the data points better than the previously fitted curves generated from the 1-D ADE without mobile-immobile water. The tailing of the observed BTCs is particularly well fitted.

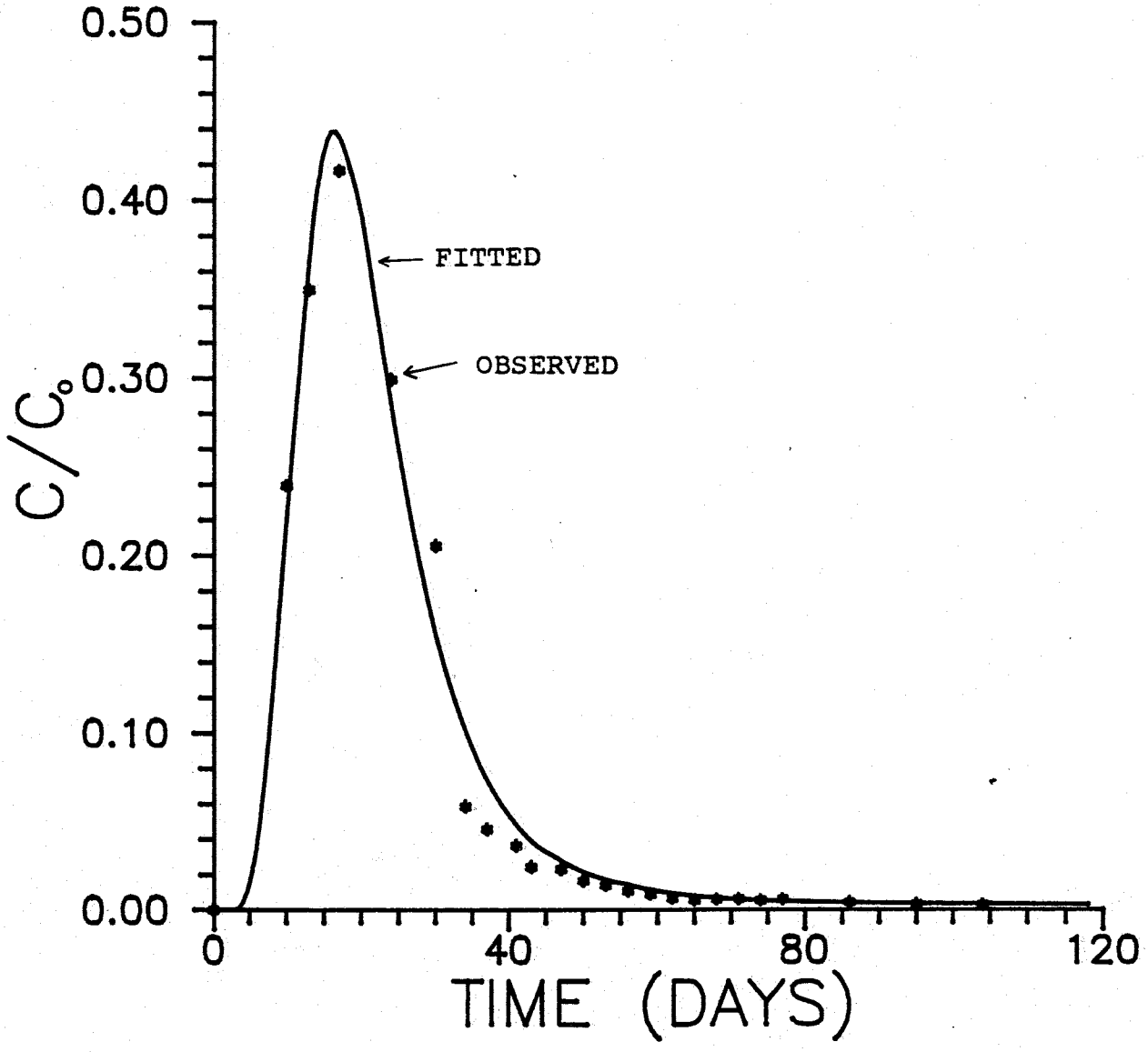

FIGURE 4-19. Bromide breakthrough curve for sampler G. The fitted curve was obtained using the mobile-immobile water model (model number 4) of CXTFIT.

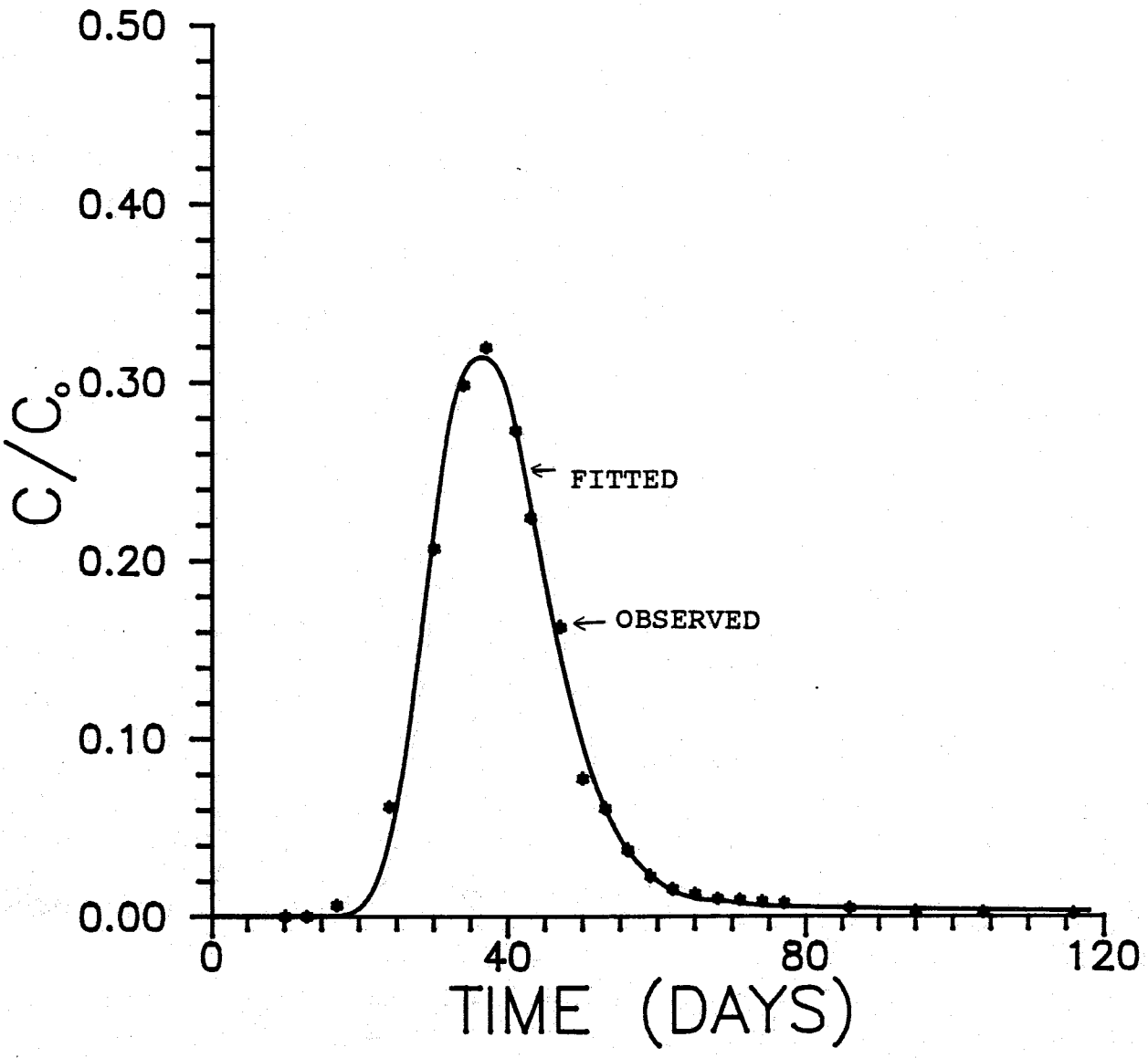

FIGURE 4-20. Bromide breakthrough curve for sampler H. The fitted curve was obtained using the mobile-immobile water model (model number 4) of CXTFIT.

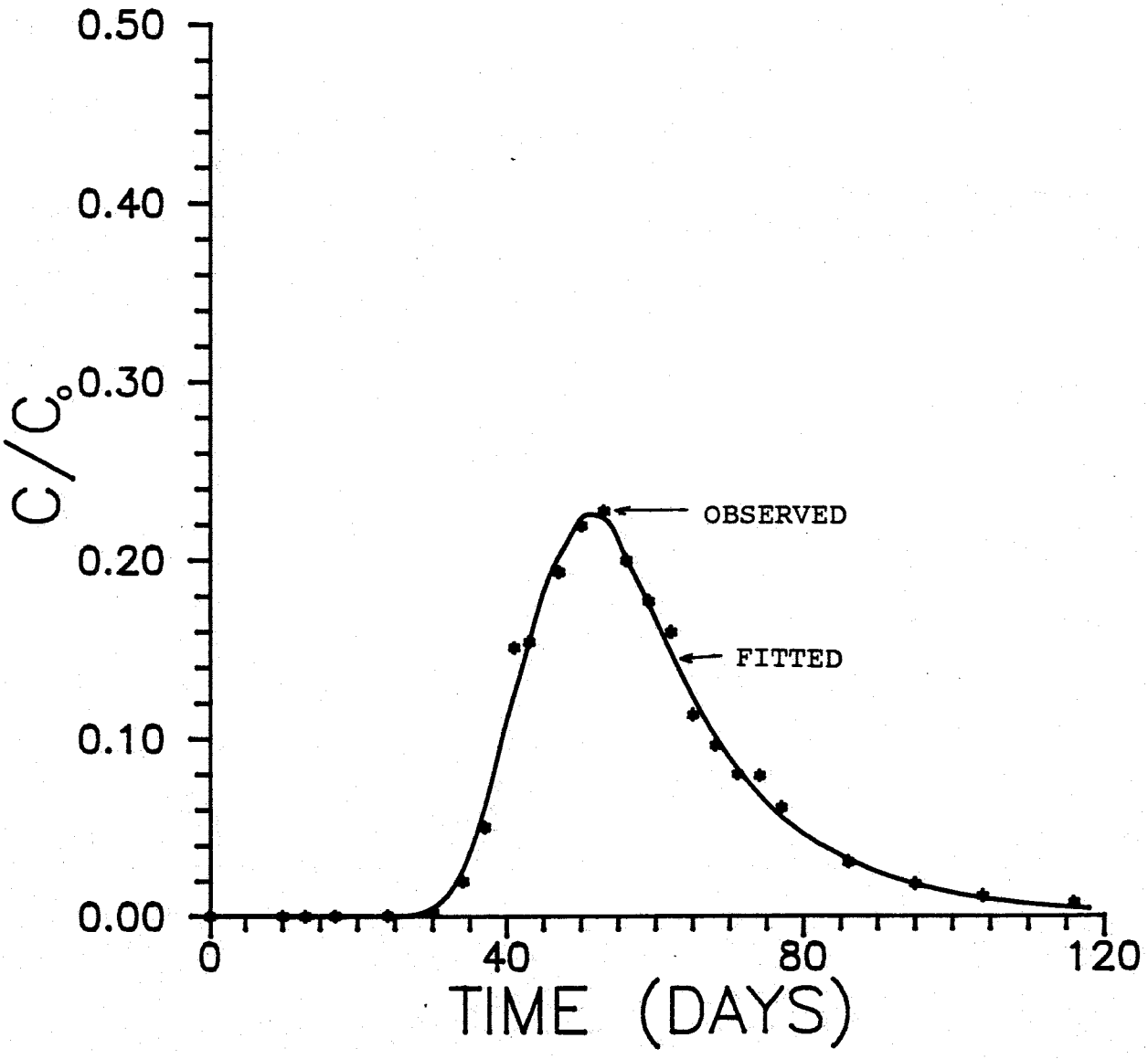

FIGURE 4-21. Bromide breakthrough curve for sampler I. The fitted curve was obtained using the mobile-immobile water model (model number 4) of CXTFIT.

The fitted transport parameters obtained with CXTFIT using the mobile-immobile water model are presented in Table 4-6. For this case, the model parameters which were held constant were the retardation factor (same as in Table 4-5), the input pulse (calculated from the BTCs), and the calculated (from known experimental parameters) pore water velocities. The parameters D, ω, and β were then fitted to the observed BTC data.

The parameter ω (Equation 2.48) is a dimensionless term which relates the mass transfer of solute between the mobile and the immobile phases, the distance of solute transport, and the applied flux rate. From this equation the mass transfer coefficient, ϵ, can be calculated. The parameter β, also dimensionless, is defined as

$$\beta = \frac{\theta_m + f\rho K_d}{\theta + \rho K_d} \qquad (4.6)$$

where f = the fraction of the sorption sites which equilibrate with the mobile liquid phase.

For the case of nonreactive tracers such as bromide, K_d = 0, and Equation 4.3 reduces to

$$\beta = \frac{\theta_m}{\theta} = \phi \text{ (Equation 2.43)} \qquad (4.7)$$

TABLE 4-6. FITTED AND CALCULATED PARAMETERS OF THE BROMIDE FIELD TRANSPORT EXPERIMENT OBTAINED FROM CXTFIT USING THE MOBILE-IMMOBILE WATER EQUATION (EQUATIONS 2.41 AND 2.42)

FIXED PARAMETERS

SAMPLER	z(cm)	R	T_0(day)	v'(cm/day)
G	107	0.84	9.03	3.64
H	244	0.79	6.54	3.94
I	320	0.79	6.81	4.08

FITTED PARAMETERS

SAMPLER	D_m(cm²/day)	β	ω
G	60.10	0.684	0.082
H	21.89	0.714	0.075
I	29.53	0.825	0.161
AVE.	37.18	0.741	0.106

CALCULATED PARAMETERS

SAMPLER	θ_m	θ_{im}	v_m	α_{lm}	ϵ(day^{-1})
G	0.129	0.059	5.32	11.3	5.25×10^{-4}
H	0.124	0.050	5.52	3.96	2.11×10^{-4}
I	0.139	0.029	4.93	5.99	3.45×10^{-4}
AVE.	0.131	0.046	5.26	7.08	3.60×10^{-4}

D_m = COEFFICIENT OF HYDRODYNAMIC DISPERSION OF THE MOBILE WATER ZONE.
θ_m = VOLUMETRIC MOISTURE CONTENT OF THE MOBILE WATER ZONE.
θ_{im} = VOLUMETRIC MOISTURE CONTENT OF THE IMMOBILE ZONE.
v_m = PORE WATER VELOCITY OF THE MOBILE WATER ZONE.
α_{lm} = LONGITUDINAL DISPERSIVITY OF THE MOBILE WATER ZONE.
ϵ = MASS TRANSFER COEFFICIENT BETWEEN THE MOBILE AND THE IMMOBILE ZONES.

From this equation the volumetric moisture content of the mobile and immobile phases, and subsequently, the pore water velocity and the dispersivity of the mobile zone can be calculated. While it has been shown earlier in this chapter that the actual value of K_d for bromide at the site is less than 0, for the purposes of estimating these parameters it is assumed that Equation 4.7 is applicable. Table 4-6 presents these calculated values.

This analysis suggests that approximately 26% of the water in the unsaturated zone in the vicinity of these samplers exists as immobile water. The average mass transfer coefficient, ϵ, is two to three orders of magnitude smaller than other values observed in the literature (van Genuchten and Wierenga, 1977; De Smedt et al., 1986), 3.60×10^{-4} day^{-1}, indicating that mass and tracer movement between the mobile and the immobile zones occurs very slowly. Comparison of parameters for the classical advection-dispersion model (including anion exclusion) and the mobile-immobile water model (also including anion exclusion) reveals an average pore water velocity of 5.03 cm/day versus 5.26 cm/day, an average coefficient of hydrodynamic dispersion of 60.14 cm^2/day versus 37.18 cm^2/day, and an average dispersivity of 12.1 cm versus 7.08 cm, respectively. It must be noted that the above parameters for the mobile-immobile water model are representative of the mobile zone only, so that drawing

meaningful conclusions from comparing the above values is difficult.

Another mechanism, due to the nature of the experimental apparatus used, may also have contributed to the accelerated transport of bromide observed at the site. This is illustrated in Figure 4-22. Water being delivered to the site from the drip emitters may flow down and outward in flow fields resembling expanding cones of moisture with depth. In this mechanism, the pore water velocity would be greatest at the top of the cone, and become progressively less as a fluid particle travelled "downcone". This is due to the fact that, in this model, the cross-sectional area of the flow field increases with depth.

Verification that this mechanism is operating may be achieved by examining the ratio of the fitted pore water velocity (from Table 4-5) to the calculated pore water velocity (from Table 4-4), v/v'. If this mechanism is operating, this ratio should approach unity as depth increases. The values of this ratio for samplers G, H, and I are 1.36, 1.37, and 1.16, respectively. These values do suggest that this mechanism is occurring.

As a result of the analysis of the field BTCs by CXTFIT, along with the results of the laboratory column experiments, it is concluded that the accelerated transport observed at the site resulted from both anion exclusion and mobile-immobile water flow. The expanding flow cone model

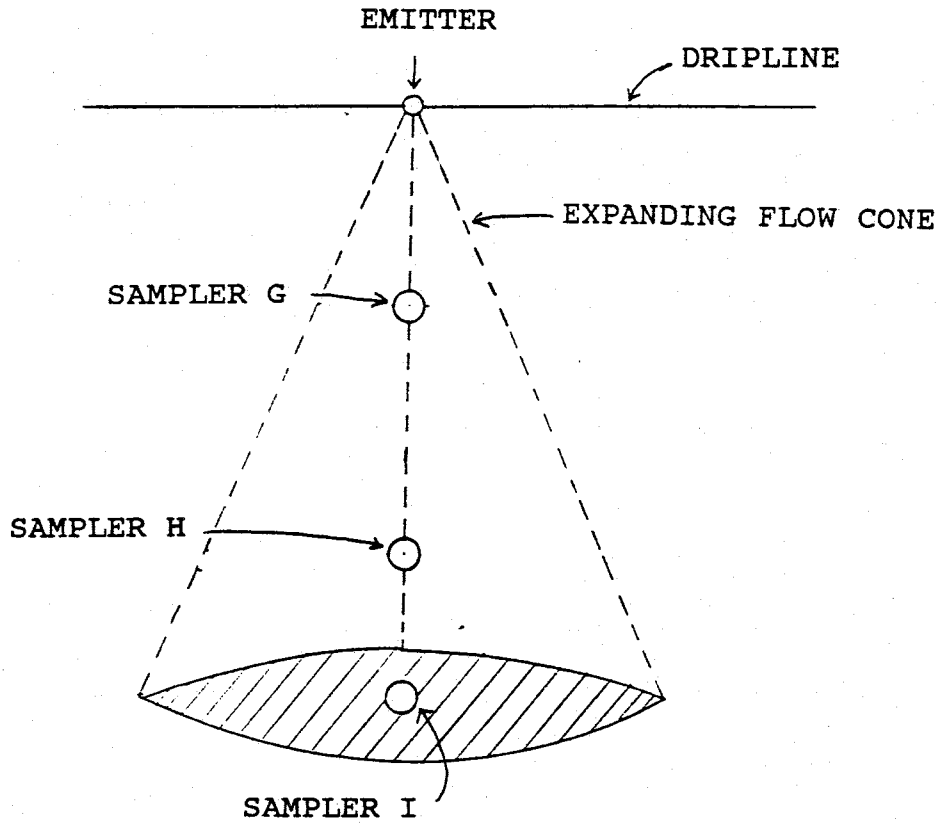

FIGURE 4-22. "Expanding cone" model. As water delivered to the site leaves the drip emitters, it may flow down and outward as an expanding cone, resulting in decreasing fluid velocity with depth.

may also have contributed to the observed accelerated transport.

The results of this unsaturated field solute transport experiment were compared (Figure 4-23) to other similar field experiments conducted at various vertical scales (Table 2-1, Figure 2-6). The dispersivities attained from this experiment were generally greater than those from the others. This is probably due to the greater amount of heterogeneity and stratification present at the New Mexico Tech field site, than at the other sites. Warrick's (1971) site consisted of a uniform clay loam. Van de Pols's (1974) was a layered soil of 70-cm of silty clay over a medium sand. Kies' (1981) consisted of various small layers of silts and sands, with some clays. Elabd et al.'s (1988) also consisted of various layers of silts and sands.

What is particularly interesting is the high value of dispersivity displayed by sampler G. It is completely opposite of the trend shown by samplers H, and I. It is expected that the dispersivity for G should be in the range of 2 to 4 cm, if the scale dependence of dispersivity were to hold. These anomalous values (including high values for the pulse length and the coefficient of hydrodynamic dispersion) for sampler G may be explained by Figure 4-24. Since G is the closest (107 cm versus 244 and 320 cm for H and I, respectively) to the source of the three samplers, the flow paths to it are of a more three-dimensional nature than the flow to the deeper samplers. The apparently

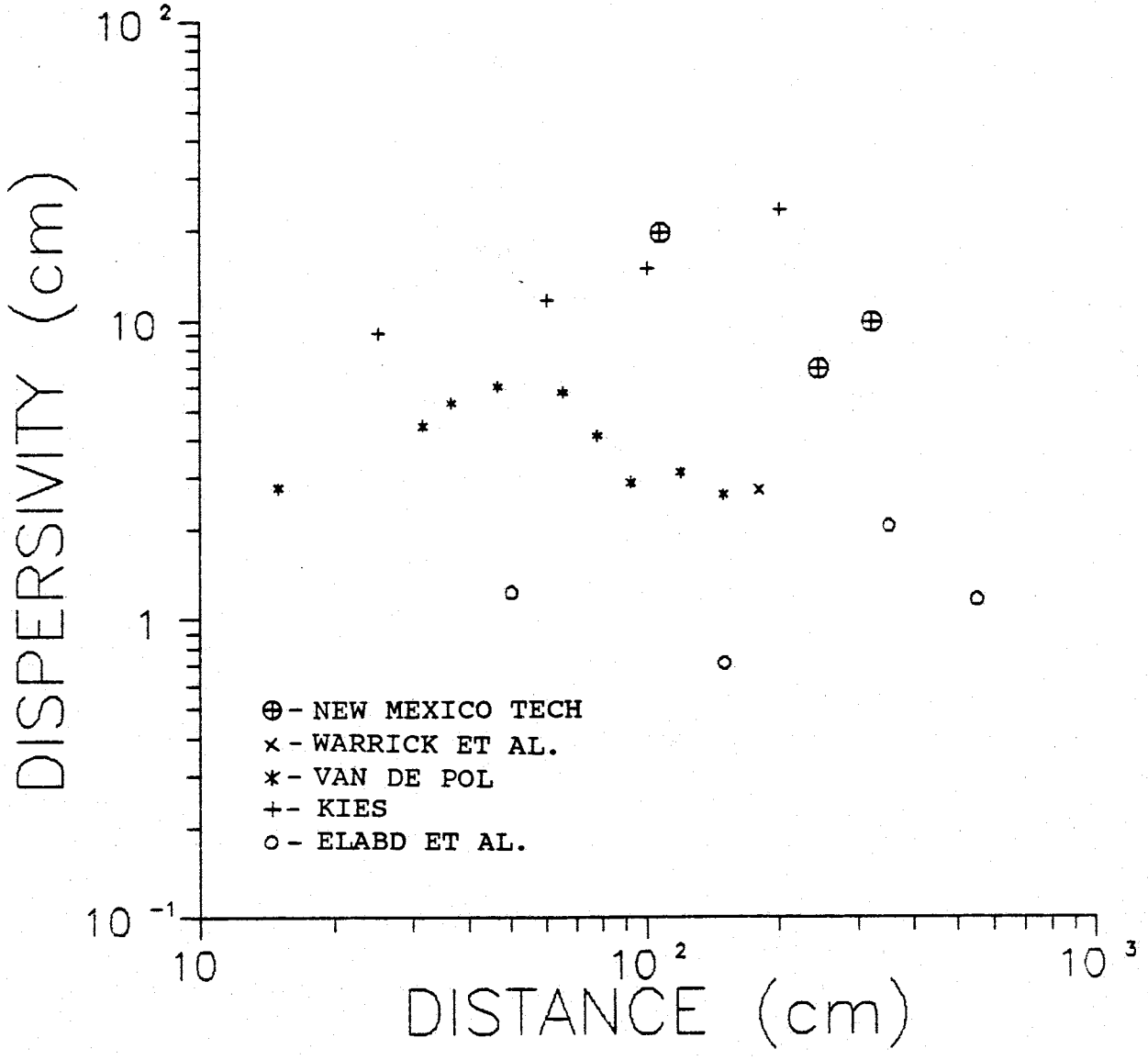

FIGURE 4-23. Dispersivity versus transport distant from various unsaturated solute transport field studies listed in Table 2-1. The circled crosses represent values attained from the New Mexico Tech field site. (After McElroy, 1987).

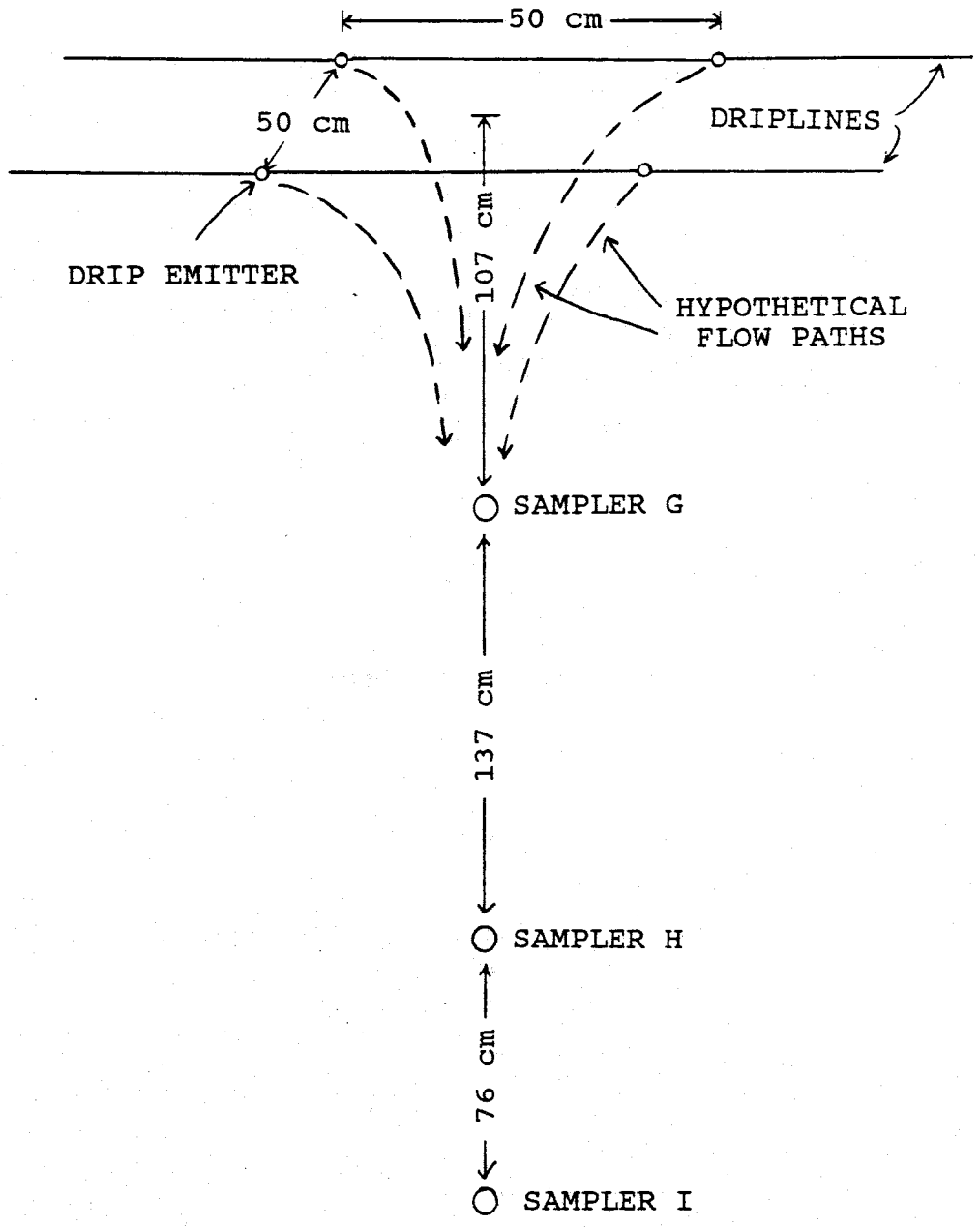

FIGURE 4-24. Three-dimensional representation of samplers G, H, and I in relation to the drip lines and drip emitters.

anomalous values result then from applying a one-dimensional model (CXTFIT) to what is probably a three-dimensional case.

V. SUMMARY AND CONCLUSIONS

A long-term field experiment was conducted on the campus of the New Mexico Institute of Mining and Technology from January of 1987 to May of 1989. The field site is situated in an old arroyo channel which has been diked off from runoff events. The soil horizon is very stratified and heterogeneous, consisting of an upper zone of alluvial silts and sands with interspersed cobble layers, and a lower zone of well sorted fine to coarse fluvial sands.

Water was applied at a rate which was one percent that of the lowest saturated hydraulic conductivity found at the site. A 10 meter by 10 meter plot was irrigated by means of agricultural drip lines. The experiment was designed to simulate seepage from a waste impoundment into the unsaturated zone. Water movement was monitored by neutron logging and a system of tensiometers.

The goals of the experiment were to 1.) investigate the importance of lateral movement of seepage in the unsaturated zone due to soil stratification and heterogeneity; 2.) determine the capability of existing analytical and numerical models to predict water and tracer movement in the unsaturated zone; 3.) develop practical guidelines for sampling and characterizing hydraulic properties in the unsaturated zone; and 4.) evaluate the dispersive and sorptive characteristics and other solute parameters of the site. This report did not attempt to address all of these goals.

Part of the experiment consisted of the injection of a 6.3 day pulse of bromide into the system and monitoring its movement in both the vertical and horizontal directions. Complete breakthrough curves were obtained beneath the plot and analyzed using the non-linear least squares curve fitting model CXTFIT (Parker and van Genuchten, 1984a). Two unsaturated solute transport experiments were also conducted in laboratory columns using soil from the site. The field conditions were simulated in these columns as closely as possible.

From these experiments, the following conclusions are drawn:

1. Wetting front and tracer movement at the field site are controlled by anisotropy and differences in hydraulic properties at stratigraphic interfaces. Significant lateral movement of water and solute was observed. Bromide was detected as much as 6 meters outside the plot at a depth of 5.6 meters, after approximately 150 days.

2. The accelerated transport of bromide observed at the site was due to both the presence of mobile-immobile water and anion exclusion. Approximately 26% of the soil water in the vicinity of samplers G, H, and I existed as immobile water. Mass and solute transfer between the mobile and the

immobile phases at the site occurred very slowly, with an average mass transfer coefficient of 3.60×10^{-4} day^{-1}. Retardation factors around 0.8 were obtained from the unsaturated column experiments, indicating significant anion exclusion was occurring at the site. This is surprising, due to the low clay content of the soil in the upper alluvial zone at the site.

3. The mobile-immobile water model of solute transport described the transport of bromide observed at the site very well. Retardation factors used in this model were less than 1.0, so that anion exclusion was included in the simulations. The CXTFIT generated fitted curves matched the observed data very well, especially the extended tailing of the breakthrough curves.

4. Dispersivity values obtained from applying the one-dimensional advection-dispersion equation to the observed breakthrough curves correlated well with values obtained from other unsaturated solute transport field studies described in the literature. The values obtained from the field site are generally slightly larger than values from the other studies at this scale. This is probably due to the stratified, heterogeneous nature of the site.

5. The data obtained from this experiment will be useful for the validation of multi-dimensional numerical models of flow and transport in the unsaturated zone. There now exists a large data base of results from this experiment quantifying wetting front movement and solute transport both vertically and horizontally. By comparing these actual results with a model's predictions it will be possible to refine and validate the model. Most, if not all, existing numerical models dealing with this subject have not been validated against actual field data. It is desirable to accomplish this so that the predictive capabilities of numerical models to determine the amount and extent of seepage from mine tailings and other waste storage facilities into the unsaturated zone may be known.

There is currently additional work being conducted at the site. The flux was increased an order of magnitude and further propagation of the wetting front was observed. Three piezometers were installed to monitor changes in the water table elevation resulting from recharge from the water application. About 60 additional porous cup samplers were installed, both in the wetted area and adjacent to it. The dripline system was sectioned into quarters with various plumbing fittings and different anionic tracers were injected into each quarter. Bromide was again injected into the entire site. Samples were collected from

the porous cup samplers at a frequency of three times daily, and are currently being analyzed.

Future work planned for the site includes turning off the water and monitoring the drainage and redistribution of the soil moisture content. Extensive site characterization is also planned.

One of the major questions arising from this investigation is the actual amount of anion exclusion occurring at the site. Since the site is extremely heterogeneous, the values obtained from the laboratory column experiments are probably not valid for use throughout the site. It would be interesting to conduct another tracer experiment utilizing bromide and, if the proper State and Federal regulatory permission could be obtained, tritium, so that the amount of anion exclusion could be quantified throughout the site.

If the experiment were to be repeated, several improvements could be made. A shelter could be erected around the entire site and the climate controlled so that weather related factors such as solar radiation, air temperature, precipitation, etc. would not be a problem. This would negate the need for the hay layer (as insulation), so that nitrate masking of bromide would not occur. The driplines could then be placed on the soil surface (or slightly below it), so that they would be readily accessible to check for emitter clogging. A more sophisticated means of controlling the volume of water

delivered to the driplines during each cycle could be used, ensuring a constant flux rate.

REFERENCES

Anderson, M.P. 1984. Movement of contaminants in groundwater: groundwater transport - advection and dispersion. In Studies in Geophysics: Groundwater Contamination. National Academy Press, Washington D.C.

Biggar, J.W., and D.R. Nielsen. 1962. Miscible displacement: II. Behavior of tracers. Soil Science Society of America Proceedings 26:125-128.

Bowman, R.S. 1984. Analysis of soil extracts for inorganic and organic tracer anions via high-performance liquid chromatography. Journal of Chromatography 285:467-477.

Bowman, R.S., and R.C. Rice. 1986. Accelerated herbicide leaching resulting from preferential flow phenomena and its implications for ground water contamination. p.413-425. In Proceedings of the Conference on Southwestern Ground Water Issues, Phoenix, AZ. October 20-22, 1986. National Water Well Association, Dublin, OH.

Boyle, F.W. Jr., H. Elabd., and P.J. Wierenga. 1988. Effect of initial water content on evaluation of laboratory column studies using the convection-dispersion equation. In P.J. Wierenga and D. Bachelet (ed.) Validation of Flow and Transport Models for the Unsaturated Zone: Conference Proceedings; May 22-25, 1988 Ruidoso, New Mexico. Research Report 88-SS-04. Department of Agronomy and Horticulture, New Mexico State University, Las Cruces, N.M. 1988.

Carman, P.C. 1937. Fluid flow through a granular bed. Transactions of the Institute of Chemical Engineers. 15:150-156.

Cassel, D.K., M. Th. van Genuchten, and P.J. Wierenga. 1975. Predicting anion movement in disturbed and undisturbed soils. Soil Science Society of America Journal 39:1015-1019.

Coats, K.H., and B.D. Smith. 1964. Dead-end pore volume and dispersion in porous media. Society of Petroleum Engineers Journal 4:73-84.

Crosby, J.W., D.L. Johnstone, C.H. Drake, and R.L. Fenton. 1968. Migration of pollutants in a glacial outwash environment. Water Resources Research 4:1095-1114.

Crosby, J.W., D.L. Johnstone, and R.L. Fenton. 1971. Migration of pollutants in a glacial outwash environment 2. Water Resources Research 7:204-208.

De Marsily, G. 1986. Quantitative Hydrogeology. Academic Press, San Diego, CA.

De Smedt, F., F. Wauters, and J. Sevilla. 1986. Study of tracer movement through unsaturated sand. Journal of Hydrology 85:169-181.

De Smedt, F., and P.J. Wierenga. 1979. A generalized solution for solute flow in soils with mobile and immobile water. Water Resources Research 15:1137-1141.

De Smedt, F., and P.J. Wierenga. 1979. Mass transfer in porous media with immobile water. Journal of Hydrology 41:59-67.

De Smedt, F., and P.J. Wierenga. 1984. Solute transfer through columns of glass beads. Water Resources Research 20:225-232.

Elabd, H., I. Porro, and P.J. Wierenga. 1988. Estimation of Field Transport Parameters using the convection dispersion equation. In P.J. Wierenga and D. Bachelet (ed.) Validation of Flow and Transport Models for the Unsaturated Zone: Conference Proceedings; May 22-25, 1988 Ruidoso, New Mexico. Research Report 88-SS-04. Department of Agronomy and Horticulture, New Mexico State University, Las Cruces, N.M. 1988.

Elprince, A.M., and P.R. Day. 1977. Fitting solute breakthrough equations to data using two adjustable parameters. Soil Science Society of America Journal 41:39-41.

Elrick, D.E., K.T. Erh, and H.K. Krupp. 1966. Applications of miscible displacement techniques to soils. Water Resources Research 2:717-727.

Freeze, R.A., and J.A. Cherry. 1979. Groundwater. Prentice-Hall, Englewood Cliffs, NJ.

Gaudet, J.P., H. Jegat, G. Vachaud, and P.J. Wierenga. 1977. Solute transfer, with exchange between mobile and stagnant water, through unsaturated sand. Soil Science Society of America Journal 41:665-671.

Gupta, R.K., R.J. Millington, and A. Klute. 1973. Hydrodynamic dispersion in unsaturated porous media. II. The stagnant zone concept and the dispersion coefficient. Journal of Indian Society of Soil Science. 21(2):121-128.

Heerman, S.E. 1986. A laboratory experiment of axisymmetrical infiltration into a layered soil. Unpublished M.S. Independent Study Paper. New Mexico Institute of Mining and Technology, Socorro, NM.

Hildebrand, M.A., and D.M. Himmelbau. 1977. Transport of nitrate ion in unsteady unsaturated flow in porous media. A.I.Ch. Engineering Journal 23:326-335.

James, R.V., and J. Rubin. 1986. Transport of chloride ion in a water-unsaturated soil exhibiting anion exclusion. Soil Science Society of America Journal 50:1142-1149.

Jaynes, D.B., R.C. Rice, and R.S. Bowman. 1988. Independent calibration of a deterministic - stochastic model for field-scale solute transport: results from two field experiments. In P.J. Wierenga and D. Bachelet (ed.) Validation of Flow and Transport Models for the Unsaturated Zone: Conference Proceedings; May 22-25, 1988 Ruidoso, New Mexico. Research Report 88-SS-04. Department of Agronomy and Horticulture, New Mexico State University, Las Cruces, N.M. 1988.

Jury, W.A. 1982. Simulation of solute transport using a transfer function model. Water Resources Research 18:363-368.

Jury, W.A., L.H. Stolzy, and P. Shouse. 1982. A field test of the transfer function model for predicting solute transport. Water Resources Research 18:369-375.

Kies, B. 1981. Solute transport in unsaturated field soil and in groundwater. Ph.D. dissertation, Department of Agronomy, New Mexico State University, Las Cruces, NM.

Krupp, H.K., and D.E. Elrick. 1968. Miscible displacement in an unsaturated glass bead medium. Water Resources Research 4:809-815.

Lapidus, L., and N.R. Amundson. 1952. Mathematics of adsorption in beds. VI. The effects of longitudinal diffusion in ion exchange and chromatographic columns. Journal of Physical Chemistry 56:984-988.

Lindstrom, F.T., R. Hague, V.H. Freed, and L. Boersma. 1967. Theory on the movement of some herbicides in soils: linear diffusion and convection of chemicals in soils. Journal of Environmental Science and Technology 1:561-565.

Mansell, R.S., H.M. Selim, P. Kanchanusut, J.M. Davidson, and J.G.A. Fiskell. 1977. Experimental and simulated transport of phosphorous through sandy soils. Water Resources Research 13:189-194.

Mattson, E.D. 1989. Field simulation of waste impoundment seepage in the vadose zone: experiment design and two-dimensional modeling. Unpublished M.S. Independent Study Paper, New Mexico Institute of Mining and Technology, Socorro, NM.

McCord, J.T., and D.B. Stephens. 1987. Lateral moisture flow beneath a sandy hillslope without an apparent impeding layer. Hydrological Processes 1:225-238.

McElroy, D.L. 1987. The scale dependence of dispersivity in unsaturated mill tailings. Unpublished M.S. Independent Study Paper, New Mexico Institute of Mining and Technology, Socorro, NM.

Miller, D.E.. 1963. Lateral flow as a source of error in moisture retention studies. Soil Science Society of America Proceedings 27:716-717.

Mualem, Y. 1984. Soil anisotropy of unsaturated soils. Soil Science Society of America Journal 48:505-509.

Neumann, S.P., and L.A. Davis. 1983. UNSAT2. U.S. Nuclear Regulatory Commission Technical Report NUREG-CR-3390.

Nielsen, D.R., and J.W. Biggar. 1961. Miscible displacement in soils: I. Experimental information. Soil Science Society of America Proceedings 25:1-5.

Nielsen, D.R., and J.W. Biggar. 1962. Miscible displacement: III. Theoretical considerations. Soil Science Society of America Proceedings 27:216-221.

Nielsen, D.R., M. Th. van Genuchten, and J.W. Biggar. 1986. Water flow and solute transport processes in the unsaturated zone. Water Resources Research 22:89S-108S.

Palmquist, W.N., and A.I. Johnson. 1962. Vadose flow in layered and non-layered materials. USGS Professional Paper 450-C:C142-143.

Parker, J.C., and M. Th. van Genuchten. 1984a. Determining transport parameters from laboratory and field tracer experiments. Virginia Agricultural Experiment Station Bulletin 84-3. Virginia Polytechnic Instititute and State University, Blacksburg, VA.

Parker, J.C., and M. Th. van Genuchten. 1984b. Flux-averaged and volume-averaged concentrations in continuum approaches to solute transport. Water Resources Research 20:866-872.

Parsons, A.M. 1988. Field simulation of waste impoundment seepage in the vadose zone: site characterization and one-dimensional analytical modeling. Unpublished M.S. Independent Study Paper, New Mexico Institute of Mining and Technology, Socorro, NM.

Rifai, M.N.E., W.J. Kaufman, and D.K. Todd. 1956. Dispersion phenomena in laminar flow through porous media, Sanitary Engineering Research Lab., University of California at Berkely. Inst. Eng. Res. Ser. no. 93(2).

Rouston, R.C., W.H. Price, D.J. Brown, and K.R. Fecht. 1979. High level waste leakage from the 241-T-106 tank at Hanford. Rockwell International Report RHO-ST-14, Richland, WA.

Scheideger, A.E. 1961. General theory of dispersion in porous media. Journal of Geophysical Research. 66:3273-3278.

Schulin, R., P.J. Wierenga, H. Fluhler, and J. Leuenberger. 1987. Solute transport through a stony soil. Soil Science Society of America Journal 51:36-42.

Skibitzkie, H.E., and G.M. Robinson. 1963. Dispersion of groundwater flowing through heterogeneous materials. U.S. Geological Survey Professional Paper 386-B.

Slichter, C.S. 1905. Field measurements of the rate of movement of underground water. U.S. Geological Survey Water Supply Paper 140, pp. 9-85.

Springer, E.P., H.R. Fuentes, and W.L. Polzer. 1989. Intermediate-scale experiments to describe solute transport: experimental design and one-dimensional analyses. Water Resources Research (In Press).

Stephens, D.B., and S.E. Heerman. 1988. Dependence of anisotropy on saturation in a stratified sand. Water Resources Research 24:770-778.

Turner, G.A. 1972. Heat and Concentration Waves. Academic Press, New York, NY.

Van de Pol, R.M. 1974. Solute movement in a layered field soil. M.S. Thesis, Department of Agronomy, New Mexico State University, Las Cruces, NM.

Van Genuchten, M. Th. 1980. Determining transport parameters from solute displacement experiments. Research Report No. 118. U.S. Salinity Laboratory, Riverside, CA.

Van Genuchten, M. Th., and W.J. Alves. 1982. Analytical solutions of the one-dimensional convective-dispersive solute transport equation. U.S. Dept. of Agriculture, Agricultural Research Service Technical Bulletin No. 1661. U.S. Government Printing Office, Washington, DC.

Van Genuchten, M. Th., J.C. Parker, and J.B. Kool. 1987. Analysis and prediction of water and solute transport in a large lysimeter. In Springer, E.P., and H.R. Fuentes (ed.) Modeling study of solute transport in the unsaturated zone. Los Alamos National Laboratory, Los Alamos, NM.

Van Genuchten, M. Th., and P.J. Wierenga. 1976. Mass transfer studies in sorbing porous media. 1. Analytical solutions. Soil Science Society of America Journal 40:473-480.

Van Genuchten, M. Th., and P.J. Wierenga. 1977. Mass transfer studies in sorbing porous media. 2. Experimental evaluation with tritium. Soil Science Society of America Journal 41:272-278.

Van Genuchten, M. Th., P.J. Wierenga, and G.A. O'Connor. 1977. Mass transfer studies in sorbing porous media. 3. Experimental evaluation with 2,4,5-T. Soil Science Society of America Journal 41:278-285.

Van Genuchten, M. Th., and P.J. Wierenga. 1986. Solute dispersion coefficients and retardation factors. In A. Klute (ed.) Methods of Soil Analysis. Part 1. Physical and Mineralogical Methods. 2nd ed. American Society of Agronomy, Madison, WI. pp. 1025-1054.

Warrick, A.W., J.W. Biggar, and D.R. Nielsen. 1971. Simultaneous solute and water transfer for an unsaturated soil. Water Resources Research 7:1216-1225.

Wierenga, P.J. 1977. Solute distribution profiles computed with steady-state and transient water movement models. Soil Science Society of America Journal 41:1050-1055.

Wierenga, P.J., and M. Th. van Genuchten. 1989. Solute transport through small and large unsaturated columns. Ground Water 27:35-42.

Wilson, J.L., and L.W. Gelhar. 1974. Dispersive mixing in a partially saturated porous medium. Technical Report 191, Ralph M. Parsons Laboratory for Water Resources and Hydrodynamics, Massachusetts Institute of Technology, Cambridge, MA.

Yeh, G.T. 1987. FEMWATER. Oak Ridge National Laboratory Technical Report ORNL-5567.

Yeh, J.T.C., L.W. Gelhar, and A.L. Gutjahr. 1985. Stochastic analysis of unsaturated flow in heterogeneous soils 2. Statistically anisotropic media with variable α. Water Resources Research 21:457-464.

Yule, D.F., and W.R. Gardner. 1978. Longitudinal and transverse dispersion coefficients in unsaturated plainfield sand. Water Resources Research 14:582-588.

APPENDIX A

BROMIDE CONCENTRATION (PPM) VERSUS TIME FOR EACH SAMPLER USED IN THE BROMIDE TRACER EXPERIMENT.

BROMIDE TRANSPORT EXPERIMENT

INJECTION PERIOD: FEB 25 TO MAR 2, 1988

INITIAL CONCENTRATION: 435 ppm
VOLUME INJECTED: 5867 LITERS (1550 gal)

COORDINATES:		(14,10)	(14,10)	(14,12)	(14,12)
DEPTH BELOW LINES (m):		1.14	1.59	0.83	1.38
DISTANCE FROM LINES (m):		0.98	1.12	----	----
		A	B	C	D
DATE	EXP DAY				
2/29/88	3		0.00	0.00	
3/7/88	10		0.00	0.00	
3/10/88	13		0.00	0.00	
3/14/88	17		0.00	0.15	0.00
3/21/88	24		0.00	26.41	
3/27/88	30			83.73	
3/31/88	34				
4/3/88	37				
4/7/88	41				
4/9/88	43				
4/13/88	47				
4/16/88	50		1.45		48.63
4/19/88	53			17.37	42.84
4/22/88	56			11.00	27.18
4/25/88	59		5.39	5.83	21.50
4/28/88	62		8.86	5.10	17.93
5/1/88	65		12.71	4.25	11.31
5/4/88	68		17.51	2.86	9.27
5/7/88	71		23.84	3.97	6.16
5/10/88	74		27.50	2.96	6.82
5/13/88	77		29.63	2.29	4.72
5/16/88	80		33.41		
5/19/88	83		33.94		
5/22/88	86		32.30	1.05	2.48
5/25/88	89		32.60		
5/28/88	92		33.15		
5/31/88	95		30.37	0.99	1.01
6/3/88	98		30.68		
6/6/88	101				
6/9/88	104		27.27	0.33	0.97
6/14/88	109		26.93		
6/17/88	112		26.32		
6/21/88	116		25.37	0.37	0.47
6/24/88	119		24.83		
6/27/88	122		24.17		
6/30/88	125		23.77		
7/3/88	128		23.20		
7/6/88	131		21.70		

COORDINATES:		(14,10)	(14,10)	(14,12)	(14,12)
DEPTH BELOW LINES (m):		1.14	1.59	0.83	1.38
DISTANCE FROM LINES (m):		0.98	1.12	----	----
		A	B	C	D
DATE	EXP DAY				
7/9/88	134		20.71		
7/12/88	137		19.56		
7/15/88	140		17.98		
7/19/88	144		16.36		
7/22/88	147		15.95		
7/25/88	150		14.98		
7/28/88	153		13.14		
7/31/88	156		10.15		
8/3/88	159		9.97		
8/6/88	162		9.34		
8/9/88	165		9.11		
8/12/88	168		8.25		
8/15/88	171		8.53		
8/18/88	174		8.29		
8/21/88	177		6.97		
8/24/88	180		6.74		
8/27/88	183		6.14		
8/30/88	186		5.56		
9/4/88	191		5.44		
9/8/88	195		5.49		
9/13/88	200		5.27		
9/16/88	203		4.63		
9/20/88	207		4.91		
9/23/88	210		5.06		
9/26/88	213		4.60		
9/30/88	217		4.73		
10/3/88	220		4.69		
10/5/88	222				
10/6/88	223		4.65		
10/11/88	228		4.71		
10/14/88	231		4.51		
10/17/88	234		4.17		
10/20/88	237		4.22		
10/24/88	241				
10/27/88	244		4.31		
10/31/88	248		4.07		
11/8/88	256				
11/19/88	267				
11/22/88	270		3.69		
12/1/88	279				
12/11/88	289		3.15		
12/20/88	298				
12/23/88	301				
12/27/88	305		2.29		
1/6/89	315				

COORDINATES:		(14,10)	(14,10)	(14,12)	(14,12)
DEPTH BELOW LINES (m):		1.14	1.59	0.83	1.38
DISTANCE FROM LINES (m):		0.98	1.12	----	----
		A	B	C	D
DATE	EXP DAY				
1/9/89	318		2.35		
1/16/89	325		1.87		
1/19/89	328				
1/23/89	332		1.98		
1/26/89	335				
1/30/89	339		1.79		
2/2/89	342				
2/5/89	345				
2/8/89	348				
2/11/89	351				
2/14/89	354				
2/17/89	357				
2/21/89	361				
2/28/89	368		1.64		

COORDINATES:		(15,21)	(16,17)	(15,27)	(14,17)
DEPTH BELOW LINES (m):		1.37	1.07	2.44	3.20
DISTANCE FROM LINES (m):		0.93	----	----	----
		F	G	H	I
DATE	EXP DAY				
2/29/88	3				
3/7/88	10		104.04	0.00	0.00
3/10/88	13		152.02	0.00	0.00
3/14/88	17		181.12	2.74	0.09
3/21/88	24	0.00	130.00	26.78	0.14
3/27/88	30		89.20	89.87	0.92
3/31/88	34		25.32	129.75	8.59
4/3/88	37		19.69	138.90	21.85
4/7/88	41		15.68	118.61	65.68
4/9/88	43		10.44	97.44	67.07
4/13/88	47		9.91	70.70	84.06
4/16/88	50		7.04	33.60	95.36
4/19/88	53	0.00	6.01	26.30	98.90
4/22/88	56		4.57	16.12	86.81
4/25/88	59		3.74	9.76	76.85
4/28/88	62		2.72	6.63	69.37
5/1/88	65		2.25	5.46	49.19
5/4/88	68		2.54	4.25	41.78
5/7/88	71		2.55	4.03	34.69
5/10/88	74		2.25	3.65	34.32
5/13/88	77	0.41	2.53	3.26	26.52
5/16/88	80				
5/19/88	83	0.79			
5/22/88	86	1.52	1.77	2.01	13.20
5/25/88	89	2.97			
5/28/88	92	4.70			
5/31/88	95	6.90	1.37	1.26	7.81
6/3/88	98	10.78			
6/6/88	101	14.35			
6/9/88	104	19.05	1.19	1.00	4.86
6/14/88	109	25.10			
6/17/88	112	28.40			
6/21/88	116	32.84	0.98	0.79	3.29
6/24/88	119	36.73			
6/27/88	122	39.49			
6/30/88	125	41.16	0.85		2.43
7/3/88	128	44.28			
7/6/88	131	43.61			

COORDINATES:		(15,21)	(16,17)	(15,27)	(14,17)
DEPTH BELOW LINES (m):		1.37	1.07	2.44	3.20
DISTANCE FROM LINES (m):		0.93	----	----	----
		F	G	H	I
DATE	EXP DAY				
7/9/88	134	42.17	0.91		
7/12/88	137	41.50			
7/15/88	140	38.48			
7/19/88	144	34.36			
7/22/88	147	31.43			
7/25/88	150	28.20			
7/28/88	153	25.96			
7/31/88	156	17.86			
8/3/88	159	16.85			
8/6/88	162	14.81			
8/9/88	165				
8/12/88	168	12.89			
8/15/88	171	11.38			
8/18/88	174	10.38			
8/21/88	177	9.20			
8/24/88	180	7.99	0.51		
8/27/88	183				
8/30/88	186	5.71			
9/4/88	191		0.42		
9/8/88	195	4.27			
9/13/88	200				
9/16/88	203	3.49			
9/20/88	207				
9/23/88	210	3.10			
9/26/88	213		0.23		
9/30/88	217	2.69			
10/3/88	220				
10/5/88	222				
10/6/88	223				
10/11/88	228	3.98			
10/14/88	231				
10/17/88	234				
10/20/88	237				
10/24/88	241				
10/27/88	244				
10/31/88	248				
11/8/88	256				
11/19/88	267				
11/22/88	270				
12/1/88	279				
12/11/88	289				
12/20/88	298				
12/23/88	301				
12/27/88	305				
1/6/89	315				

COORDINATES:		(15,21)	(16,17)	(15,27)	(14,17)
DEPTH BELOW LINES (m):		1.37	1.07	2.44	3.20
DISTANCE FROM LINES (m):		0.93	----	----	----
		F	G	H	I
DATE	EXP DAY				
1/9/89	318				
1/16/89	325	0.14			
1/19/89	328				
1/23/89	332				
1/26/89	335				
1/30/89	339				
2/2/89	342				
2/5/89	345				
2/8/89	348				
2/11/89	351				
2/14/89	354				
2/17/89	357				
2/21/89	361				
2/28/89	368				

COORDINATES:		(11,10)	(14,15)	(15,6)	(26,15)
DEPTH BELOW LINES (m):		2.47	1.58	6.21	5.42
DISTANCE FORM LINES (m):		0.67	----	5.67	5.89
		J	K	L	M
DATE	EXP DAY				
2/29/88	3				
3/7/88	10				
3/10/88	13				
3/14/88	17				
3/21/88	24				
3/27/88	30				
3/31/88	34	0.00			
4/3/88	37	0.00			
4/7/88	41	0.00			
4/9/88	43	0.00			
4/13/88	47				
4/16/88	50	0.00	74.65		
4/19/88	53		76.80		
4/22/88	56		71.29		
4/25/88	59		56.61		
4/28/88	62		45.63		
5/1/88	65		36.65		
5/4/88	68		29.63		
5/7/88	71	0.50	29.51		
5/10/88	74		27.11		
5/13/88	77	1.10	22.66		
5/16/88	80		20.4		
5/19/88	83	2.62	17.9		
5/22/88	86	4.63	16.23		
5/25/88	89	5.99	13.41		
5/28/88	92		12.69		
5/31/88	95	8.97	10.21		
6/3/88	98	11.77	9.67		
6/6/88	101	15.30	8.6		
6/9/88	104	16.59	7.14		0.50
6/14/88	109	20.55	6.58		
6/17/88	112	22.96	5.44		
6/21/88	116	25.89	4.61		
6/24/88	119	24.44			
6/27/88	122	26.83			
6/30/88	125	28.53	4.11		
7/3/88	128	29.66			
7/6/88	131	27.30			

COORDINATES:		(11,10)	(14,15)	(15,6)	(26,15)
DEPTH BELOW LINES (m):		2.47	1.58	6.21	5.42
DISTANCE FORM LINES (m):		0.67	----	5.67	5.89
		J	K	L	M
DATE	EXP DAY				
7/9/88	134	23.79	3.27		
7/12/88	137	27.95			
7/15/88	140	26.17			
7/19/88	144	25.70	2.44		1.02
7/22/88	147	24.55			
7/25/88	150	22.21			
7/28/88	153	18.94	1.84		1.17
7/31/88	156	20.23			
8/3/88	159	17.41			
8/6/88	162	15.02	1.22		1.51
8/9/88	165	16.3			
8/12/88	168	15.65			
8/15/88	171	14.02			2.23
8/18/88	174				
8/21/88	177	12.49			
8/24/88	180			0.32	2.75
8/27/88	183	10.53			
8/30/88	186				
9/4/88	191	8.14			3.43
9/8/88	195				
9/13/88	200	6.56			
9/16/88	203			0.33	4.79
9/20/88	207				
9/23/88	210	5.38			
9/26/88	213				7.26
9/30/88	217				
10/3/88	220	4.44			
10/5/88	222				
10/6/88	223				7.66
10/11/88	228	4.20			7.93
10/14/88	231				
10/17/88	234				8.59
10/20/88	237	3.73			
10/24/88	241				
10/27/88	244				8.80
10/31/88	248	3.33			
11/8/88	256				9.47
11/19/88	267				9.76
11/22/88	270				
12/1/88	279				9.88
12/11/88	289				10.07
12/20/88	298				9.74
12/23/88	301			0.73	
12/27/88	305				
1/6/89	315			0.82	

COORDINATES:		(11,10)	(14,15)	(15,6)	(26,15)
DEPTH BELOW LINES (m):		2.47	1.58	6.21	5.42
DISTANCE FORM LINES (m):		0.67	----	5.67	5.89
		J	K	L	M
DATE	EXP DAY				
1/9/89	318	1.16		0.80	10.08
1/16/89	325			0.84	9.84
1/19/89	328	1.15		0.90	10.60
1/23/89	332			0.93	10.21
1/26/89	335			0.94	9.60
1/30/89	339	1.02			9.64
2/2/89	342				9.92
2/5/89	345			1.04	9.84
2/8/89	348			1.14	9.68
2/11/89	351			1.04	9.54
2/14/89	354				9.46
2/17/89	357			1.08	9.46
2/21/89	361				
2/28/89	368	1.14		1.28	8.74
3/6/89	374			1.29	8.60
3/12/89	380				8.26
3/24/89	392				7.77
3/30/89	398				7.28
4/4/89	403				7.07
4/10/89	409				6.75
4/17/89	416				6.43
4/24/89	423				5.96
5/1/89	430				5.78

COORDINATES:		(15,26)	(4,15)
DEPTH BELOW LINES (m):		6.31	6.12
DISTANCE FORM LINES (m):		5.69	5.87
		N	O
DATE	EXP DAY		
2/29/88	3		
3/7/88	10		
3/10/88	13		
3/14/88	17		
3/21/88	24		
3/27/88	30		
3/31/88	34		
4/3/88	37		
4/7/88	41		
4/9/88	43		
4/13/88	47		
4/16/88	50		
4/19/88	53		
4/22/88	56		
4/25/88	59		
4/28/88	62		
5/1/88	65		
5/4/88	68		
5/7/88	71		
5/10/88	74		
5/13/88	77		
5/16/88	80		
5/19/88	83		
5/22/88	86		
5/25/88	89		
5/28/88	92		
5/31/88	95		
6/3/88	98		
6/6/88	101		
6/9/88	104	0.31	
6/14/88	109		
6/17/88	112		
6/21/88	116		
6/24/88	119		
6/27/88	122		
6/30/88	125		
7/3/88	128		
7/6/88	131		

COORDINATES:		(15,26)	(4,15)
DEPTH BELOW LINES (m):		6.31	6.12
DISTANCE FORM LINES (m):		5.69	5.87
		N	O
DATE	EXP DAY		
7/9/88	134		
7/12/88	137		
7/15/88	140		
7/19/88	144		
7/22/88	147		
7/25/88	150		
7/28/88	153		
7/31/88	156		
8/3/88	159		
8/6/88	162		
8/9/88	165		
8/12/88	168		
8/15/88	171		
8/18/88	174		
8/21/88	177		
8/24/88	180		
8/27/88	183		
8/30/88	186		
9/4/88	191		
9/8/88	195		
9/13/88	200		
9/16/88	203		
9/20/88	207		
9/23/88	210		
9/26/88	213		
9/30/88	217		
10/3/88	220		
10/5/88	222		
10/6/88	223		
10/11/88	228		
10/14/88	231		
10/17/88	234		
10/20/88	237		
10/24/88	241		
10/27/88	244		
10/31/88	248		
11/8/88	256		
11/19/88	267		
11/22/88	270		
12/1/88	279		
12/11/88	289		
12/20/88	298		
12/23/88	301		
12/27/88	305		
1/6/89	315	1.92	

COORDINATES:		(15,26)	(4,15)
DEPTH BELOW LINES (m):		6.31	6.12
DISTANCE FORM LINES (m):		5.69	5.87
		N	O
DATE	EXP DAY		
1/9/89	318		0.12
1/16/89	325	2.09	0.13
1/19/89	328	3.26	
1/23/89	332	2.85	
1/26/89	335	2.51	
1/30/89	339		0.15
2/2/89	342		
2/5/89	345	2.34	
2/8/89	348	2.37	
2/11/89	351	2.35	
2/14/89	354		
2/17/89	357	2.36	
2/21/89	361	2.50	
2/28/89	368	2.40	
3/6/89	374	2.59	
3/12/89	380		
3/24/89	392		
3/30/89	398		
4/4/89	403		
4/10/89	409		
4/17/89	416		
4/24/89	423		
5/1/89	430		

APPENDIX B

BROMIDE AND TRITIUM COLUMN DATA.

UNSATURATED COLUMN EXPERIMENTS

COLUMN 1

FRACTION	SAMPLE VOLUME	COLLECTION TIME (HR)	% OF PORE VOLUME	PV SUM
1-1	10.35	16.08	0.079	0.079
1-2	8.82	16.00	0.079	0.158
1-3	NC	16.00	0.079	0.237
1-4	8.95	16.00	0.079	0.316
1-5	9.26	16.00	0.079	0.395
1-6	NC	16.00	0.079	0.474
1-7	8.93	16.00	0.079	0.553
1-8	9.55	16.00	0.079	0.632
1-9	NC	16.00	0.079	0.711
1-10	1.92	3.20	0.016	0.727
1-11	3.96	4.00	0.020	0.746
1-12	2.55	4.00	0.020	0.766
1-13	NC	4.00	0.020	0.786
1-14	2.17	4.00	0.020	0.806
1-15	2.12	4.00	0.020	0.825
1-16	NC	4.00	0.020	0.845
1-17	2.15	4.00	0.020	0.865
1-18	2.05	4.00	0.020	0.885
1-19	NC	4.00	0.020	0.904
1-20	2.12	4.00	0.020	0.924
1-21	2.21	4.00	0.020	0.944
1-22	NC	4.00	0.020	0.964
1-23	2.21	4.00	0.020	0.983
1-24	2.11	4.00	0.020	1.003
1-25	NC	4.00	0.020	1.023
1-26	2.16	4.00	0.020	1.042
1-27	1.63	2.85	0.014	1.057
1-28	2.59	4.00	0.020	1.076
1-29	2.24	4.00	0.020	1.096
1-30	NC	4.00	0.020	1.116
1-31	2.14	4.00	0.020	1.136
1-32	2.29	4.00	0.020	1.155
1-33	NC	4.00	0.020	1.175
1-34	2.20	4.00	0.020	1.195
1-35	2.19	4.00	0.020	1.214
1-36	NC	4.00	0.020	1.234
1-37	2.24	4.00	0.020	1.254
1-38	NC	3.78	0.019	1.273
1-39	2.43	4.00	0.020	1.292
1-40	2.41	4.00	0.020	1.312

FRACTION	SAMPLE VOLUME	COLLECTION TIME (HR)	% OF PORE VOLUME	PV SUM
1-41	NC	4.00	0.020	1.332
1-42	2.24	4.00	0.020	1.352
1-43	2.12	4.00	0.020	1.371
1-44	NC	4.00	0.020	1.391
1-45	2.06	4.00	0.020	1.411
1-46	2.18	4.00	0.020	1.431
1-47	NC	4.00	0.020	1.450
1-48	2.16	4.00	0.020	1.470
1-49	2.12	4.00	0.020	1.490
1-50	NC	4.00	0.020	1.510
1-51	2.22	4.00	0.020	1.529
1-52	2.10	4.00	0.020	1.549
1-53	NC	4.00	0.020	1.569
1-54	2.15	4.00	0.020	1.589
1-55	2.27	4.00	0.020	1.608
1-56	NC	4.00	0.020	1.628
1-57	2.52	4.00	0.020	1.648
1-58	0.06	0.12	0.001	1.648
1-59	NC	0.00	0.000	1.648
1-60	7.63	12.00	0.059	1.708
1-61	6.36	12.00	0.059	1.767
1-62	NC	12.00	0.059	1.826
1-63	6.81	12.00	0.059	1.885
1-64	7.07	12.00	0.059	1.944
1-65	NC	12.00	0.059	2.004
1-66	3.31	5.33	0.026	2.030

NC = NOT COLLECTED

COLUMN 1

FRACTION	MIDPOINT	C/C. Br	C/C. H	NORM Br
1-1	0.0395	0.786	0.0008	
1-2	0.1185	0.620	0.0008	0.000
1-3	0.1975			
1-4	0.2764	0.394	0.0008	0.000
1-5	0.3554	0.326	0.0008	
1-6	0.4344			
1-7	0.5134	0.267	0.0011	
1-8	0.5923	0.257	0.0045	0.000
1-9	0.6713			
1-10	0.7187	0.271	0.0547	0.014
1-11	0.7365	0.514		0.257
1-12	0.7562	0.621	0.1321	0.364
1-13	0.7759			
1-14	0.7957	0.707	0.1860	0.450
1-15	0.8154	0.773	0.2177	0.516
1-16	0.8352			
1-17	0.8549	0.858	0.2798	0.601
1-18	0.8747	0.880		0.623
1-19	0.8944			
1-20	0.9141	0.901	0.3826	0.644
1-21	0.9339	0.910	0.4214	0.653
1-22	0.9536			
1-23	0.9734	0.927	0.4904	0.670
1-24	0.9931	1.019		
1-25	1.0129			
1-26	1.0326	0.911	0.6000	0.654
1-27	1.0495	0.927		0.670
1-28	1.0664			
1-29	1.0862	0.848	0.6167	0.591
1-30	1.1059			
1-31	1.1256	0.722	0.6312	0.465
1-32	1.1454	0.660		0.403
1-33	1.1651			
1-34	1.1849	0.529	0.6423	0.272
1-35	1.2046	0.462		0.205
1-36	1.2244			
1-37	1.2441	0.355	0.5997	0.098
1-38	1.2633			
1-39	1.2825			
1-40	1.3022	0.308	0.4429	0.051

FRACTION	MIDPOINT	C/C. Br	C/C. H	NORM Br
1-41	1.3220			
1-42	1.3417			
1-43	1.3615	0.289	0.3536	0.032
1-44	1.3812			
1-45	1.4010			
1-46	1.4207	0.272	0.2792	0.015
1-47	1.4405			
1-48	1.4602			
1-49	1.4799	0.266	0.2086	0.009
1-50	1.4997			
1-51	1.5194			
1-52	1.5392		0.1542	
1-53	1.5589			
1-54	1.5787			
1-55	1.5984	0.254	0.1113	0.000
1-56	1.6181			
1-57	1.6379		0.0863	
1-58	1.6481			
1-59	1.6483			
1-60	1.6780	0.261	0.0596	0.000
1-61	1.7372		0.0388	
1-62	1.7964			
1-63	1.8557		0.0174	
1-64	1.9149		0.0118	
1-65	1.9741			
1-66	2.0169		0.0066	

COLUMN 2

FRACTION	SAMPLE VOLUME	COLLECTION TIME (HR)	% OF PORE VOLUME	PV SUM
2-1	9.42	16.08	0.093	0.093
2-2	8.33	16.00	0.093	0.186
2-3	8.38	16.00	0.093	0.278
2-4	8.66	16.00	0.093	0.371
2-5	8.68	16.00	0.093	0.463
2-6	9.35	16.00	0.093	0.556
2-7	10.59	16.00	0.093	0.648
2-8	10.71	16.00	0.093	0.741
2-9	10.58	16.00	0.093	0.833
2-10	2.21	3.20	0.019	0.852
2-11	2.87	4.00	0.023	0.875
2-12	2.37	4.00	0.023	0.898
2-13	2.26	4.00	0.023	0.921
2-14	2.20	4.00	0.023	0.944
2-15	2.22	4.00	0.023	0.967
2-16	2.39	4.00	0.023	0.991
2-17	2.49	4.00	0.023	1.014
2-18	2.45	4.00	0.023	1.037
2-19	2.42	4.00	0.023	1.060
2-20	2.48	4.00	0.023	1.083
2-21	2.46	4.00	0.023	1.106
2-22	2.68	4.00	0.023	1.129
2-23	2.61	4.00	0.023	1.153
2-24	2.57	4.00	0.023	1.176
2-25	2.60	4.00	0.023	1.199
2-26	2.57	4.00	0.023	1.222
2-27	1.88	2.85	0.016	1.238
2-28	2.87	4.00	0.023	1.262
2-29	2.46	4.00	0.023	1.285
2-30	2.44	4.00	0.023	1.308
2-31	2.39	4.00	0.023	1.331
2-32	2.54	4.00	0.023	1.354
2-33	2.41	4.00	0.023	1.377
2-34	2.74	4.00	0.023	1.400
2-35	2.62	4.00	0.023	1.424
2-36	2.61	4.00	0.023	1.447
2-37	2.57	4.00	0.023	1.470
2-38	2.65	3.78	0.022	1.492
2-39	2.26	4.00	0.023	1.515
2-40	2.11	4.00	0.023	1.538

FRACTION	SAMPLE VOLUME	COLLECTION TIME (HR)	% OF PORE VOLUME	PV SUM
2-41	2.03	4.00	0.023	1.561
2-42	2.15	4.00	0.023	1.584
2-43	1.93	4.00	0.023	1.607
2-44	1.97	4.00	0.023	1.630
2-45	2.06	4.00	0.023	1.654
2-46	2.23	4.00	0.023	1.677
2-47	2.13	4.00	0.023	1.700
2-48	1.83	4.00	0.023	1.723
2-49	1.86	4.00	0.023	1.746
2-50	1.78	4.00	0.023	1.769
2-51	1.88	4.00	0.023	1.792
2-52	1.80	4.00	0.023	1.816
2-53	1.74	4.00	0.023	1.839
2-54	1.86	4.00	0.023	1.862
2-55	2	4.00	0.023	1.885
2-56	2.01	4.00	0.023	1.908
2-57	2.15	0.12	0.001	1.909
2-58	0.11	12.00	0.069	1.978
2-59	NC	0.00	0.000	1.978
2-60	8.1	12.00	0.069	2.048
2-61	7.25	12.00	0.069	2.117
2-62	7.83	12.00	0.069	2.186
2-63	7.57	12.00	0.069	2.256
2-64	7.95	12.00	0.069	2.325
2-65	7.75	12	0.069	2.395
2-66	3.66	5.33	0.031	2.425

COLUMN 2

FRACTION	MIDPOINT	C/C. Br	C/C. H	NORM Br
2-1	0.0465	0.164	0.0015	0
2-2	0.1393			
2-3	0.2318			
2-4	0.3243	0.154	0.0012	0
2-5	0.4169	0.161	0.0018	0.007
2-6	0.5094	0.215	0.0086	0.055
2-7	0.6020	0.381	0.0439	0.221
2-8	0.6945	0.597	0.1315	0.437
2-9	0.7870	0.774	0.263	0.614
2-10	0.8426			
2-11	0.8634	0.814	0.3655	0.654
2-12	0.8865	0.783	0.3786	0.623
2-13	0.9097			
2-14	0.9328	0.739	0.4092	0.579
2-15	0.9559			
2-16	0.9791	0.645	0.4765	0.485
2-17	1.0022			
2-18	1.0253	0.554	0.5031	0.394
2-19	1.0485			
2-20	1.0716	0.497	0.5091	0.337
2-21	1.0947			
2-22	1.1179	0.405	0.5095	0.245
2-23	1.1410	0.369		0.209
2-24	1.1641	0.332		0.172
2-25	1.1873	0.313		0.153
2-26	1.2104	0.269	0.4444	0.109
2-27	1.2302	0.247		0.087
2-28	1.2500			
2-29	1.2732	0.222	0.3728	0.062
2-30	1.2963			
2-31	1.3194	0.153	0.3244	
2-32	1.3426			
2-33	1.3657	0.177	0.2888	0.017
2-34	1.3888			
2-35	1.4120	0.164	0.2367	0.004
2-36	1.4351			
2-37	1.4582	0.141	0.1979	0.000
2-38	1.4807			
2-39	1.5032		0.1452	
2-40	1.5264			

FRACTION	MIDPOINT	C/C. Br	C/C. H	NORM Br
2-41	1.5495			
2-42	1.5726		0.1116	
2-43	1.5958			
2-44	1.6189	0.155		0.000
2-45	1.6420		0.0821	
2-46	1.6652			
2-47	1.6883			
2-48	1.7114		0.0527	
2-49	1.7346			
2-50	1.7577			
2-51	1.7809		0.038	
2-52	1.8040	0.156		0.000
2-53	1.8271			
2-54	1.8503		0.025	
2-55	1.8734			
2-56	1.8965			
2-57	1.9084		0.0186	
2-58	1.9435			
2-59	1.9782			
2-60	2.0129	0.150	0.0146	0.000
2-61	2.0823		0.0107	
2-62	2.1517			
2-63	2.2211		0.0063	
2-64	2.2905			
2-65	2.3599			
2-66	2.4100			

APPENDIX C

VOLUMETRIC MOISTURE CONTENT DATA FOR THE THREE NEUTRON MONITORING STATIONS SURROUNDING SAMPLERS G, H, AND I, AND CALCULATION OF MOISTURE CONTENTS FOR SAMPLERS G, H, AND I.

STATION 15-15
VOLUMETRIC MOISTURE CONTENT DATA DURING BROMIDE TRACER EXPERIMENT

DATE		2/14/88	2/24/88	4/4/88	4/20/88	4/28/88
TIME		1500	1715	1542	1620	1305
MCHI		0.98	1.12	0.85	1.00	0.87
STANDARD CT		10221	10204	10353	10375	10368
EXPERIMENTAL DAYS		-10.8	-0.7	39.2	55.3	63.1
DPTH BE DATUM(M	DEPTH (FT)					
0.55	1.0					
0.86	2.0					
1.01	2.5					
1.16	3.0	23.3	23.3	22.4	23.1	22.9
1.32	3.5					
1.47	4.0	16.9		16.5		16.6
1.62	4.5					
1.77	5.0	17.9	17.8	17.1	17.7	
1.93	5.5					
2.08	6.0	17.4		17.1		16.9
2.23	6.5					
2.38	7.0	16.1	15.9	16.0	15.9	
2.54	7.5					
2.69	8.0	15.2		14.8		15.0
2.84	8.5					
2.99	9.0	18.2	18.2	17.4	17.9	
3.15	9.5					
3.30	10.0	18.4		18.2		18.4
3.45	10.5					
3.60	11.0	16.3	16.8	16.7	16.7	
3.76	11.5					
3.91	12.0	15.9		15.6		16.1
4.06	12.5					
4.21	13.0	16.3	16.4	16.4	16.5	

STATION 15-15
VOLUMETRIC MOISTURE CONTENT DATA DURING BROMIDE TRACER EXPER

DATE		5/5/88	5/12/88	5/19/88	5/26/88
TIME		1615	1230	1635	1450
MCHI		1.03	1.00	0.81	0.95
STANDARD CT		10356	10345	10337	10305
EXPERIMENTAL DAYS		70.3	77.1	84.3	91.2
DPTH BELOW DATUM(M)	DEPTH (FT)				
0.55	1.0				
0.86	2.0				
1.01	2.5				
1.16	3.0	22.9	23.2	23.0	23.0
1.32	3.5				
1.47	4.0	17.1	16.9	17.0	16.6
1.62	4.5				
1.77	5.0	17.5		17.8	
1.93	5.5				
2.08	6.0		17.2		17.2
2.23	6.5				
2.38	7.0	15.8		15.8	
2.54	7.5				
2.69	8.0		14.9		14.8
2.84	8.5				
2.99	9.0	18.3		18.4	
3.15	9.5				
3.30	10.0		18.1		18.0
3.45	10.5				
3.60	11.0	16.5		17.1	
3.76	11.5				
3.91	12.0		16.1		16.1
4.06	12.5				
4.21	13.0	16.1		16.4	

STATION 15-15
VOLUMETRIC MOISTURE CONTENT DATA DURING BROMIDE TRACER EXPERIMENT

DATE		6/3/88	6/9/88	6/17/88	
TIME		1135	1200	750	
MCHI		0.99	0.89	0.78	
STANDARD CT		10367	10346	10293	
EXPERIMENTAL DAYS		99.1	105.1	112.9	
DPTH BELOW DATUM(M)	DEPTH (FT)				
0.55	1.0				
0.86	2.0				
1.01	2.5				
1.16	3.0	22.6	22.7	22.6	AVE
1.32	3.5				
1.47	4.0	16.5	16.5	16.4	16.7
1.62	4.5				
1.77	5.0	17.6		17.1	17.6
1.93	5.5				
2.08	6.0		16.7		17.1
2.23	6.5				
2.38	7.0	15.4		15.6	15.8
2.54	7.5				
2.69	8.0		14.6		14.9
2.84	8.5				
2.99	9.0	18.0		17.2	18.0
3.15	9.5				
3.30	10.0		17.6		18.1
3.45	10.5				
3.60	11.0	16.5		16.2	16.6
3.76	11.5				
3.91	12.0		15.8		15.9
4.06	12.5				
4.21	13.0	16.0		15.8	16.2

STATION 12-18
VOLUMETRIC MOISTURE CONTENT DATA DURING BROMIDE TRACER EXPERIMENT

DATE		2/14/88	2/26/88	4/4/88	4/20/88	4/28/88
TIME		1400	1130	1630	1745	1145
MCHI		0.98	1.09	0.85	1.00	0.87
STANDARD CT		10221	10145	10353	10375	10368
EXPERIMENTAL DAYS		-10.8	1.1	39.3	55.3	63.1
DPTH BE DATUM(M	DEPTH (FT)					
0.55	1.0					
0.86	2.0					
1.01	2.5					
1.16	3.0	30.0	29.8	27.1	28.4	28.6
1.32	3.5					
1.47	4.0	25.0	24.6	24.3		24.4
1.62	4.5					
1.77	5.0	16.9		16.3	16.8	
1.93	5.5					
2.08	6.0		15.0	15.1		15.1
2.23	6.5					
2.38	7.0	15.1		14.9	15.1	
2.54	7.5					
2.69	8.0		14.2	13.8		14.4
2.84	8.5					
2.99	9.0	16.2		15.7	16.5	
3.15	9.5					
3.30	10.0		18.7	18.7		18.7
3.45	10.5					
3.60	11.0	17.3		17.4	17.7	
3.76	11.5					
3.91	12.0		17.0	16.7		16.6
4.06	12.5					
4.21	13.0	15.2		15.1	15.5	

STATION 12-18
VOLUMETRIC MOISTURE CONTENT DATA DURING BROMIDE TRACER EXPERIMENT

DATE		5/5/88	5/12/88	5/19/88	5/26/88
TIME		1500	1120	1650	1425
MCHI		1.03	1.00	0.81	0.95
STANDARD CT		10356	10345	10337	10305
EXPERIMENTAL DAYS		70.2	77.1	84.3	91.2
DPTH BE DATUM(M	DEPTH (FT)				
0.55	1.0				
0.86	2.0				
1.01	2.5				
1.16	3.0	27.9	28.5	28.1	28.4
1.32	3.5				
1.47	4.0	24.5	24.2	24.3	24.0
1.62	4.5				
1.77	5.0	16.7		16.7	
1.93	5.5				
2.08	6.0		15.3		15.1
2.23	6.5				
2.38	7.0	15.0		14.7	
2.54	7.5				
2.69	8.0		14.4		14.2
2.84	8.5				
2.99	9.0	16.2		16.6	
3.15	9.5				
3.30	10.0		18.6		18.2
3.45	10.5				
3.60	11.0	17.9		17.9	
3.76	11.5				
3.91	12.0		17.1		16.9
4.06	12.5				
4.21	13.0	15.4		15.1	

STATION 12-18
VOLUMETRIC MOISTURE CONTENT DATA DURING BROMIDE TRACER EXPERIMENT

DATE		6/3/88	6/9/88	6/17/88	
TIME		1035	1125	820	
MCHI		0.99	0.89	0.78	
STANDARD CT		10367	10346	10293	
EXPERIMENTAL DAYS		99.0	105.1	112.9	
DPTH BE DATUM(M	DEPTH (FT)				
0.55	1.0				
0.86	2.0				
1.01	2.5				
1.16	3.0	28.2	27.7	27.1	AVE
1.32	3.5				
1.47	4.0	23.7	23.8	23.5	24.2
1.62	4.5				
1.77	5.0	16.4		16.4	16.6
1.93	5.5				
2.08	6.0		14.8		15.1
2.23	6.5				
2.38	7.0	14.7		14.5	14.9
2.54	7.5				
2.69	8.0		14.2		14.2
2.84	8.5				
2.99	9.0	16.6		16.4	16.3
3.15	9.5				
3.30	10.0		18.3		18.5
3.45	10.5				
3.60	11.0	17.2		17.4	17.5
3.76	11.5				
3.91	12.0		16.7		16.8
4.06	12.5				
4.21	13.0	15.2		14.7	15.2

TION 18-18
UMETRIC MOISTURE CONTENT DATA DURING BROMIDE TRACER EXPERIMENT

E	2/14/88	2/24/88	4/4/88	4/20/88	4/28/88
E	1415	1805	1640	1825	1215
I	0.98	1.12	0.85	1.00	0.87
NDARD CT	10221	10204	10353	10375	10368
ERIMENTAL DAYS	-10.8	-0.7	39.3	55.3	63.1
H BE DEPTH					
UM(M (FT)					
.55 1.0					
.86 2.0					
.01 2.5					
.16 3.0	36.0	37.5	34.2	36.3	35.9
.32 3.5					
.47 4.0	23.3	23.7	22.0		23.4
.62 4.5					
.77 5.0	20.2		19.0	20.6	
.93 5.5					
.08 6.0		19.3	18.2		19.1
.23 6.5					
.38 7.0	17.0		16.8	16.8	
.54 7.5					
.69 8.0		17.8	17.1		17.8
.84 8.5					
.99 9.0	16.8		16.5	17.3	
.15 9.5					
.30 10.0		15.1	14.5		14.8
.45 10.5					
.60 11.0	15.5		15.7	15.7	
.76 11.5					
.91 12.0		13.2	13.4		13.6
.06 12.5					
.21 13.0	10.1		9.8	10.1	

STATION 18-18
VOLUMETRIC MOISTURE CONTENT DATA DURING BROMIDE TRACER EX

DATE		5/5/88	5/12/88	5/19/88	5/26/88
TIME		1530	1145	1626	1440
MCHI		1.03	1.00	0.81	0.95
STANDARD CT		10356	10345	10337	10305
EXPERIMENTAL DAYS		70.2	77.1	84.3	91.2
DPTH BE DATUM(M	DEPTH (FT)				
0.55	1.0				
0.86	2.0				
1.01	2.5				
1.16	3.0	35.7	35.4	35.4	35.6
1.32	3.5				
1.47	4.0	23.6	24.2	24.0	23.8
1.62	4.5				
1.77	5.0	20.2		20.0	
1.93	5.5				
2.08	6.0		19.3		18.6
2.23	6.5				
2.38	7.0	16.4		16.6	
2.54	7.5				
2.69	8.0		17.7		17.8
2.84	8.5				
2.99	9.0	16.6		16.6	
3.15	9.5				
3.30	10.0		14.6		14.7
3.45	10.5				
3.60	11.0	15.4		15.4	
3.76	11.5				
3.91	12.0		13.0		12.8
4.06	12.5				
4.21	13.0	10.1		10.0	

STATION 18-18
VOLUMETRIC MOISTURE CONTENT DATA DURING BROMIDE TRACER EXPER

DATE		6/3/88	6/9/88	6/17/88	
TIME		1100	1140	805	
MCHI		0.99	0.89	0.78	
STANDARD CT		10367	10346	10293	
EXPERIMENTAL DAYS		99.0	105.1	112.9	
DPTH BELOW DATUM(M)	DEPTH (FT)				
0.55	1.0				
0.86	2.0				
1.01	2.5				
1.16	3.0	35.1	34.5	34.5	AVE
1.32	3.5				
1.47	4.0	23.6	23.4	23.2	23.5
1.62	4.5				
1.77	5.0	20.0		19.6	19.9
1.93	5.5				
2.08	6.0		18.6		18.9
2.23	6.5				
2.38	7.0	16.5		16.2	16.6
2.54	7.5				
2.69	8.0		17.2		17.6
2.84	8.5				
2.99	9.0	16.7		16.0	16.6
3.15	9.5				
3.30	10.0		14.7		14.7
3.45	10.5				
3.60	11.0	15.1		15.1	15.4
3.76	11.5				
3.91	12.0		13.1		13.2
4.06	12.5				
4.21	13.0	9.7		10.0	10.0

VOLUMETRIC WATER CONTENTS FOR SAMPLERS G, H, AND I

	TIME AVERAGED MOISTURE CONTENTS			
DEPTH (ft)	STATION 15-15	STATION 12-18	STATION 18-18	$\bar{\theta}$
4	16.7	24.2	23.5	21.5
5	17.6	16.6	19.9	18.0
6	17.1	15.1	18.9	17.0
7	15.8	14.9	16.6	15.8
8	14.9	14.2	17.6	15.6
9	18.0	16.3	16.6	17.0
10	18.1	18.5	14.7	17.1
11	16.6	17.5	15.4	16.5
12	15.9	16.8	13.2	15.3
13	16.2	15.2	10.0	13.8

SAMPLER G (DEPTH = 5.5 ft)

DEPTH	$\bar{\theta}$
4	21.5
5	18.0
6	17.0
AVE	18.8

SAMPLER H (DEPTH = 10.0 ft)

4	21.5
5	18.0
6	17.0
7	15.8
8	15.6
9	17.0
10	17.1
AVE	17.4

SAMPLER I (DEPTH = 12.5 ft)

4	21.5
5	18.0
6	17.0
7	15.8
8	15.6
9	17.0
10	17.1
11	16.5
12	15.3
13	13.8
AVE	16.8

APPENDIX D

CALCULATION OF APPLIED FLUX RATE AT SAMPLERS G, H, AND I, AND FLOW METER DATA.

CALCULATION OF APPLIED FLUX RATE AT SAMPLERS G, H, AND I

During the course of the tracer experiment, 8.98 gal/hr, on average, was pumped to the drip lines. This value is from the totalizing flow meter inside the trailer, which recorded the total amount of water pumped.

The section of the plot in which samplers G, H, and I are located received 24.0% of the total. This value comes from calculations involving the other 7 meters in the drip line system. Figure D-1 shows the location of the meters.

$$(0.24)(8.98 \text{ gal/hr}) = 2.155 \text{ gal/hr}$$

$$(2.155 \text{ gal/hr})(3.785 \text{ l/gal})(24 \text{ hr/day})(1000 \text{ cm}^3/\text{l}) =$$

$$1.958 \times 10^5 \text{ cm}^3/\text{day}$$

There are 6 drip lines in this section.

$$6/21 = 0.2857$$

$$(0.2857)(100 \text{ M}^2) = 28.57 \text{ M}^2$$

$$= 2.857 \times 10^5 \text{ cm}^2$$

Therefore, the applied flux is

$$(1.958 \times 10^5 \text{ cm}^3/\text{day}) \div (2.857 \times 10^5 \text{ cm}^2) = 0.685 \text{ cm/day}$$

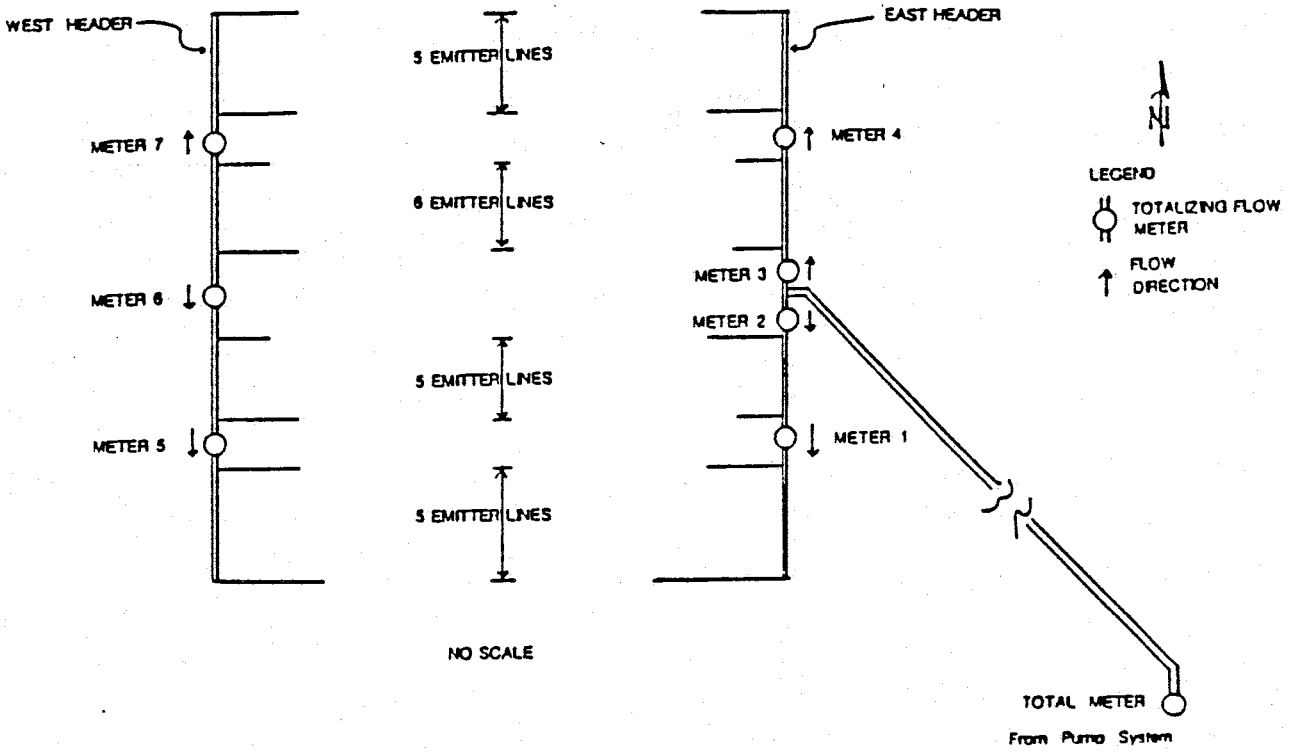

FIGURE D-1. Schematic showing the location of the eight totalizing flow meters used to monitor the distribution of water throughout the dripline system.

METERED FLOW INSIDE THE DRIPLINE SYSTEM
DURING THE BROMIDE TRANSPORT EXPERIMENT

DATE :	2/24/88	2/25/88	2/28/88	3/2/88	3/6/88
TIME :	13.00	10.00	15.00	16.00	14.00
TOTAL :	361307.12	361329.5	362080	362799.19	363619.58
METER 1 :	9569.21	9577.61	9722.97	9861.53	10020
METER 2 :	91242.18	91259.97	91632.93	91992.52	92405.6
METER 3 :	60114.7	60127.8	60531.1	60915.6	61357.81
METER 4 :	9621.3	9625.8	9766.8	9901.36	10057.5
METER 5 :	2779.49	2782.72	2827.42	2871.55	2921.7
METER 6 :	680.44	680.27	689.7	699.11	710.5
METER 7 :	2441.48	2444.2	2483.99	2522.48	2565.33
BROMIDE					
EXP. DAYS :	-0.83	0.04	3.25	6.30	10.21
EXP. DAYS :	392.21	393.08	396.29	399.33	403.25
# OFRUNS :		1	77	73	94
DELTA/RUN (1)					
TOTAL :		22.38	9.75	9.85	8.73
METER 1 :		8.40	1.89	1.90	1.69
METER 2 :		17.79	4.84	4.93	4.39
METER 3 :		13.10	5.24	5.27	4.70
METER 4 :		4.50	1.83	1.84	1.66
METER 5 :		3.23	0.58	0.60	0.53
METER 6 :		-0.17	0.12	0.13	0.12
METER 7 :		2.72	0.52	0.53	0.46
CUMULATIVE					
TOTAL (2)		22.38	9.91	9.87	9.44
METER 1 :		8.40	1.97	1.93	1.84
METER 2 :		17.79	5.01	4.96	4.75
METER 3 :		13.10	5.34	5.30	5.07
METER 4 :		4.50	1.87	1.85	1.78
METER 5 :		3.23	0.61	0.61	0.58
METER 6 :		-0.17	0.12	0.12	0.12
METER 7 :		2.72	0.54	0.54	0.51
PER RUN (3)					
% TOTAL :		138.03	103.43	103.46	104.25
SOUTH :		17.62	4.97	5.05	4.52
NORTH :		13.27	5.12	5.14	4.58
SS5 :		11.63	2.47	2.50	2.22
S5 :		5.99	2.50	2.55	2.30
N6 :		6.05	2.77	2.77	2.47
NN5 :		7.22	2.35	2.37	2.12
CUMULATIVE (4)					
% TOTAL :		138.03	104.43	103.97	104.07
SOUTH :		17.62	5.13	5.09	4.87
NORTH :		13.27	5.22	5.17	4.95
SS5 :		11.63	2.59	2.54	2.42
S5 :		5.99	2.54	2.54	2.45
N6 :		6.05	2.81	2.78	2.66
NN5 :		7.22	2.41	2.39	2.29

DATE	: 2/24/88	2/25/88	2/28/88	3/2/88	3/6/88
PER RUN					
PER LINE (5)					
1-5	:	2.33	0.49	0.50	0.44
6-10	:	1.20	0.50	0.51	0.46
11-16	:	1.01	0.46	0.46	0.41
17-21	:	1.44	0.47	0.47	0.42
1-10	:	1.76	0.50	0.51	0.45
11-21	:	1.21	0.47	0.47	0.42
PER RUN % (6)					
1-5	:	38.9	25.7	25.7	25.5
6-10	:	20.0	26.0	26.2	26.4
11-16	:	16.9	24.0	23.7	23.7
17-21	:	24.2	24.4	24.4	24.4
1-10	:	59.4	51.6	52.0	52.0
11-21	:	40.6	48.4	48.0	48.0
CUMULATIVE (7)					
1-5	:	2.33	0.52	0.51	0.48
6-10	:	1.20	0.51	0.51	0.49
11-16	:	1.01	0.47	0.46	0.44
17-21	:	1.44	0.48	0.48	0.46
1-10	:	1.76	0.51	0.51	0.49
11-21	:	1.21	0.47	0.47	0.45
CUMULATIVE % (8)					
1-5	:	38.9	26.2	26.0	25.8
6-10	:	20.0	25.7	26.0	26.1
11-16	:	16.9	23.7	23.7	23.7
17-21	:	24.2	24.4	24.4	24.4
1-10	:	59.4	51.9	52.0	52.0
11-21	:	40.6	48.1	48.0	48.0

(1): GALLONS PER RUN FOR EACH METER FOR TIME BETWEEN CURRENT AND PREVIOUS READINGS
(2): AVERAGE NUMBER OF GALLONS PER RUN FOR EACH METER DURING THE COURSE OF THE BROMIDE INJECTION EXPERIMENT
(3): GALLONS PER RUN FOR EACH SECTION OF PLOT FOR TIME BETWEEN CURRENT AND PREVIOUS READINGS
(4): AVERAGE NUMBER OF GALLONS PER RUN FOR EACH SECTION OF PLOT DURING COURSE OF THE BROMIDE INJECTION EXPERIMENT
(5): GALLONS PER RUN FOR EACH LINE IN EACH SECTION OF PLOT FOR TIME BETWEEN CURRENT AND PREVIOUS READINGS
(6): PERCENTAGE OF FLOW TO EACH SECTION OF PLOT FOR TIME BETWEEN CURRENT AND PREVIOUS READINGS
(7): GALLONS PER RUN FOR EACH LINE IN EACH SECTION OF PLOT DURING COURSE OF BROMIDE INJECTION EXPERIMENT
(8): PERCENTAGE OF FLOW TO EACH SECTION OF PLOT DURING COURSE OF BROMIDE INJECTION EXPERIMENT

DATE	:	3/8/88	3/10/88	3/12/88	3/14/88	3/17/88
TIME	:	13.00	11.00	16.00	13.00	14.00
TOTAL	:	364026.33	364430.16	364890.35	365296.3	365933.88
METER 1	:	10098.61	10176.1	10266.31	10342	10466.76
METER 2	:	92610.83	92813.7	93059.68	93247.85	93573.62
METER 3	:	61577.46	61794.68	62047.63	62260.21	62600.51
METER 4	:	10134.53	10210.46	10299.18	10373.55	10492.8
METER 5	:	2947.1	2972.23	3000.9	3024.62	3064.95
METER 6	:	716.5	722.4	728.9	734.32	742.71
METER 7	:	2586.73	2607.97	2632.61	2653.65	2687.48
BROMIDE						
EXP. DAYS	:	12.18	14.09	16.31	18.18	21.23
EXP. DAYS	:	405.21	407.13	409.33	411.21	414.25
# OFRUNS	:	47	46	53	45	73
DELTA/RUN (1)						
TOTAL	:	8.65	8.78	8.68	9.02	8.73
METER 1	:	1.67	1.68	1.70	1.68	1.71
METER 2	:	4.37	4.41	4.64	4.18	4.46
METER 3	:	4.67	4.72	4.77	4.72	4.66
METER 4	:	1.64	1.65	1.67	1.65	1.63
METER 5	:	0.54	0.55	0.54	0.53	0.55
METER 6	:	0.13	0.13	0.12	0.12	0.11
METER 7	:	0.46	0.46	0.46	0.47	0.46
CUMULATIVE						
TOTAL (2)		9.30	9.24	9.15	9.14	9.08
METER 1	:	1.81	1.79	1.78	1.77	1.76
METER 2	:	4.68	4.65	4.64	4.60	4.58
METER 3	:	5.00	4.97	4.94	4.92	4.88
METER 4	:	1.76	1.74	1.73	1.72	1.71
METER 5	:	0.57	0.57	0.57	0.56	0.56
METER 6	:	0.12	0.12	0.12	0.12	0.12
METER 7	:	0.50	0.49	0.49	0.49	0.48
PER RUN (3)						
% TOTAL	:	104.46	104.03	108.42	98.72	104.47
SOUTH	:	4.49	4.54	4.76	4.30	4.58
NORTH	:	4.55	4.59	4.65	4.60	4.55
SS5	:	2.21	2.23	2.24	2.21	2.26
S5	:	2.28	2.31	2.52	2.09	2.32
N6	:	2.45	2.48	2.51	2.48	2.45
NN5	:	2.09	2.11	2.14	2.12	2.10
CUMULATIVE (4)						
% TOTAL	:	104.13	104.11	104.67	104.06	104.12
SOUTH	:	4.81	4.77	4.77	4.72	4.70
NORTH	:	4.88	4.84	4.81	4.79	4.76
SS5	:	2.38	2.36	2.35	2.33	2.32
S5	:	2.42	2.41	2.42	2.39	2.38
N6	:	2.63	2.61	2.59	2.58	2.56
NN5	:	2.25	2.23	2.22	2.21	2.19

DATE	:	3/8/88	3/10/88	3/12/88	3/14/88	3/17/88
PER RUN PER LINE (5)						
1-5	:	0.44	0.45	0.45	0.44	0.45
6-10	:	0.46	0.46	0.50	0.42	0.46
11-16	:	0.41	0.41	0.42	0.41	0.41
17-21	:	0.42	0.42	0.43	0.42	0.42
1-10	:	0.45	0.45	0.48	0.43	0.46
11-21	:	0.41	0.42	0.42	0.42	0.41
PER RUN % (6)						
1-5	:	25.6	25.6	24.9	26.0	25.9
6-10	:	26.4	26.5	28.0	24.6	26.6
11-16	:	23.7	23.7	23.3	24.4	23.4
17-21	:	24.3	24.2	23.8	25.0	24.1
1-10	:	52.1	52.1	53.0	50.7	52.5
11-21	:	47.9	47.9	47.0	49.3	47.5
CUMULATIVE (7)						
1-5	:	0.48	0.47	0.47	0.47	0.46
6-10	:	0.48	0.48	0.48	0.48	0.48
11-16	:	0.44	0.43	0.43	0.43	0.43
17-21	:	0.45	0.45	0.44	0.44	0.44
1-10	:	0.48	0.48	0.48	0.47	0.47
11-21	:	0.44	0.44	0.44	0.44	0.43
CUMULATIVE % (8)						
1-5	:	25.8	25.8	25.6	25.7	25.7
6-10	:	26.2	26.2	26.5	26.3	26.3
11-16	:	23.7	23.7	23.6	23.7	23.7
17-21	:	24.4	24.3	24.3	24.3	24.3
1-10	:	52.0	52.0	52.1	52.0	52.1
11-21	:	48.0	48.0	47.9	48.0	47.9

(1): GALLONS PER RUN FOR EACH METER FOR TIME BETWEEN CURRENT AND PREVIOUS READINGS

(2): AVERAGE NUMBER OF GALLONS PER RUN FOR EACH METER DURING THE COURSE OF THE BROMIDE INJECTION EXPERIMENT

(3): GALLONS PER RUN FOR EACH SECTION OF PLOT FOR TIME BETWEEN CURRENT AND PREVIOUS READINGS

(4): AVERAGE NUMBER OF GALLONS PER RUN FOR EACH SECTION OF PLOT DURING COURSE OF THE BROMIDE INJECTION EXPERIMENT

(5): GALLONS PER RUN FOR EACH LINE IN EACH SECTION OF PLOT FOR TIME BETWEEN CURRENT AND PREVIOUS READINGS

(6): PERCENTAGE OF FLOW TO EACH SECTION OF PLOT FOR TIME BETWEEN CURRENT AND PREVIOUS READINGS

(7): GALLONS PER RUN FOR EACH LINE IN EACH SECTION OF PLOT DURING COURSE OF BROMIDE INJECTION EXPERIMENT

(8): PERCENTAGE OF FLOW TO EACH SECTION OF PLOT DURING COURSE OF BROMIDE INJECTION EXPERIMENT

DATE	:	3/20/88	3/23/88	3/26/88	3/29/88	3/31/88
TIME	:	12.00	14.00	14.00	12.00	16.00
TOTAL	:	365970.27	366671.37	367349.9	368010.29	368501.78
METER 1	:	10472.03	10607.9	10738.6	10865.89	10960.32
METER 2	:	93587.31	93941.3	94283.43	94616.7	94865.02
METER 3	:	62624.3	63003.7	63370.92	63728.13	63994.2
METER 4	:	10501.64	10631.64	10759.08	10879.72	10970.13
METER 5	:	3066.85	3110.6	3152.35	3193.04	3224.24
METER 6	:	742.71	753.8	763.75	773.2	779.2
METER 7	:	2693.6	2731.65	2768.34	2807.06	2835.08
BROMIDE						
EXP. DAYS	:	24.14	27.21	30.21	33.13	35.31
EXP. DAYS	:	417.17	420.25	423.25	426.17	428.33
# OFRUNS	:	70	74	72	70	52
DELTA/RUN (1)						
TOTAL	:	0.52	9.47	9.42	9.43	9.45
METER 1	:	0.08	1.84	1.82	1.82	1.82
METER 2	:	0.20	4.78	4.75	4.76	4.78
METER 3	:	0.34	5.13	5.10	5.10	5.12
METER 4	:	0.13	1.76	1.77	1.72	1.74
METER 5	:	0.03	0.59	0.58	0.58	0.60
METER 6	:	0.00	0.15	0.14	0.14	0.12
METER 7	:	0.09	0.51	0.51	0.55	0.54
CUMULATIVE						
TOTAL (2)		8.05	8.21	8.33	8.43	8.49
METER 1	:	1.56	1.59	1.61	1.63	1.64
METER 2	:	4.05	4.13	4.19	4.24	4.28
METER 3	:	4.33	4.42	4.49	4.55	4.58
METER 4	:	1.52	1.55	1.57	1.58	1.59
METER 5	:	0.50	0.51	0.51	0.52	0.52
METER 6	:	0.11	0.11	0.11	0.12	0.12
METER 7	:	0.44	0.44	0.45	0.46	0.46
PER RUN (3)						
% TOTAL	:	103.00	104.61	104.54	104.56	104.66
SOUTH	:	0.20	4.93	4.89	4.90	4.89
NORTH	:	0.34	4.98	4.96	4.97	5.00
SS5	:	0.10	2.43	2.40	2.40	2.42
S5	:	0.09	2.51	2.49	2.50	2.47
N6	:	0.13	2.71	2.68	2.69	2.72
NN5	:	0.21	2.27	2.28	2.28	2.28
CUMULATIVE (4)						
% TOTAL	:	104.11	104.17	104.21	104.25	104.28
SOUTH	:	4.16	4.25	4.31	4.36	4.39
NORTH	:	4.22	4.31	4.38	4.43	4.46
SS5	:	2.05	2.10	2.13	2.15	2.17
S5	:	2.10	2.15	2.18	2.21	2.23
N6	:	2.27	2.32	2.36	2.39	2.41
NN5	:	1.96	1.99	2.02	2.04	2.06

DATE	:	3/20/88	3/23/88	3/26/88	3/29/88	3/31/88
PER RUN PER LINE (5)						
1-5	:	0.02	0.49	0.48	0.48	0.48
6-10	:	0.02	0.50	0.50	0.50	0.49
11-16	:	0.02	0.45	0.45	0.45	0.45
17-21	:	0.04	0.45	0.46	0.46	0.46
1-10	:	0.02	0.49	0.49	0.49	0.49
11-21	:	0.03	0.45	0.45	0.45	0.45
PER RUN % (6)						
1-5	:	19.9	25.7	25.5	25.5	25.6
6-10	:	18.1	26.5	26.5	26.5	26.2
11-16	:	20.4	23.8	23.8	23.8	24.0
17-21	:	41.5	24.0	24.2	24.2	24.1
1-10	:	38.8	52.2	52.0	52.0	51.8
11-21	:	61.2	47.8	48.0	48.0	48.2
CUMULATIVE (7)						
1-5	:	0.41	0.42	0.43	0.43	0.43
6-10	:	0.42	0.43	0.44	0.44	0.45
11-16	:	0.38	0.39	0.39	0.40	0.40
17-21	:	0.39	0.40	0.40	0.41	0.41
1-10	:	0.42	0.42	0.43	0.44	0.44
11-21	:	0.38	0.39	0.40	0.40	0.41
CUMULATIVE % (8)						
1-5	:	25.7	25.7	25.6	25.6	25.6
6-10	:	26.3	26.3	26.3	26.3	26.3
11-16	:	23.6	23.7	23.7	23.7	23.7
17-21	:	24.4	24.4	24.4	24.3	24.3
1-10	:	52.0	52.0	52.0	52.0	52.0
11-21	:	48.0	48.0	48.0	48.0	48.0

(1): GALLONS PER RUN FOR EACH METER FOR TIME BETWEEN CURRENT AND PREVIOUS READINGS
(2): AVERAGE NUMBER OF GALLONS PER RUN FOR EACH METER DURING THE COURSE OF THE BROMIDE INJECTION EXPERIMENT
(3): GALLONS PER RUN FOR EACH SECTION OF PLOT FOR TIME BETWEEN CURRENT AND PREVIOUS READINGS
(4): AVERAGE NUMBER OF GALLONS PER RUN FOR EACH SECTION OF PLOT DURING COURSE OF THE BROMIDE INJECTION EXPERIMENT
(5): GALLONS PER RUN FOR EACH LINE IN EACH SECTION OF PLOT FOR TIME BETWEEN CURRENT AND PREVIOUS READINGS
(6): PERCENTAGE OF FLOW TO EACH SECTION OF PLOT FOR TIME BETWEEN CURRENT AND PREVIOUS READINGS
(7): GALLONS PER RUN FOR EACH LINE IN EACH SECTION OF PLOT DURING COURSE OF BROMIDE INJECTION EXPERIMENT
(8): PERCENTAGE OF FLOW TO EACH SECTION OF PLOT DURING COURSE OF BROMIDE INJECTION EXPERIMENT

DATE	:	4/3/88	4/6/88	4/8/88	4/11/88	4/13/88
TIME	:	13.00	15.00	11.00	15.00	12.00
TOTAL	:	368797.5	369473.57	369894.69	370613.02	371034.9
METER 1	:	11016.26	11146.69	11227.38	11364.7	11444.96
METER 2	:	95014.41	95357.63	95570.99	95934.81	96148.27
METER 3	:	64154.23	64520.72	64748.4	65136.28	65364.48
METER 4	:	11024.74	11147.9	11224.75	11354.29	11432.32
METER 5	:	3243.51	3288.39	3315.82	3361.81	3389.4
METER 6	:	780.9	788.66	794.32	803.1	807.7
METER 7	:	2853.79	2894.74	2919.29	2962.5	2986.5
BROMIDE						
EXP. DAYS	:	38.18	41.26	43.11	46.26	48.13
EXP. DAYS	:	431.21	434.29	436.13	439.29	441.17
# OFRUNS	:	69	74	44	76	45
DELTA/RUN (1)						
TOTAL	:	4.29	9.14	9.57	9.45	9.38
METER 1	:	0.81	1.76	1.83	1.81	1.78
METER 2	:	2.17	4.64	4.85	4.79	4.74
METER 3	:	2.32	4.95	5.17	5.10	5.07
METER 4	:	0.79	1.66	1.75	1.70	1.73
METER 5	:	0.28	0.61	0.62	0.61	0.61
METER 6	:	0.02	0.10	0.13	0.12	0.10
METER 7	:	0.27	0.55	0.56	0.57	0.53
CUMULATIVE						
TOTAL (2)		8.17	8.25	8.30	8.38	8.42
METER 1	:	1.58	1.59	1.60	1.62	1.62
METER 2	:	4.12	4.16	4.18	4.23	4.25
METER 3	:	4.41	4.45	4.48	4.52	4.54
METER 4	:	1.53	1.54	1.55	1.56	1.57
METER 5	:	0.51	0.51	0.52	0.52	0.53
METER 6	:	0.11	0.11	0.11	0.11	0.11
METER 7	:	0.45	0.46	0.46	0.47	0.47
PER RUN (3)						
% TOTAL	:	104.63	104.98	104.73	104.65	104.69
SOUTH	:	2.19	4.74	4.98	4.90	4.85
NORTH	:	2.29	4.85	5.05	4.99	4.97
SS5	:	1.09	2.37	2.46	2.41	2.40
S5	:	1.10	2.37	2.52	2.49	2.45
N6	:	1.23	2.63	2.74	2.72	2.70
NN5	:	1.06	2.22	2.30	2.27	2.27
CUMULATIVE (4)						
% TOTAL	:	104.29	104.35	104.37	104.39	104.40
SOUTH	:	4.23	4.26	4.29	4.34	4.36
NORTH	:	4.30	4.34	4.37	4.41	4.43
SS5	:	2.09	2.11	2.12	2.14	2.15
S5	:	2.14	2.16	2.17	2.20	2.21
N6	:	2.32	2.34	2.36	2.38	2.39
NN5	:	1.98	2.00	2.01	2.03	2.04

DATE	:	4/3/88	4/6/88	4/8/88	4/11/88	4/13/88
PER RUN						
PER LINE (5)						
1-5	:	0.22	0.47	0.49	0.48	0.48
6-10	:	0.22	0.47	0.50	0.50	0.49
11-16	:	0.21	0.44	0.46	0.45	0.45
17-21	:	0.21	0.44	0.46	0.45	0.45
1-10	:	0.22	0.47	0.50	0.49	0.48
11-21	:	0.21	0.44	0.46	0.45	0.45
PER RUN % (6)						
1-5	:	25.5	25.9	25.7	25.6	25.6
6-10	:	25.7	25.9	26.3	26.4	26.2
11-16	:	24.0	23.9	23.9	24.0	24.0
17-21	:	24.8	24.2	24.1	24.1	24.2
1-10	:	51.2	51.8	52.0	51.9	51.8
11-21	:	48.8	48.2	48.0	48.1	48.2
CUMULATIVE (7)						
1-5	:	0.42	0.42	0.42	0.43	0.43
6-10	:	0.43	0.43	0.43	0.44	0.44
11-16	:	0.39	0.39	0.39	0.40	0.40
17-21	:	0.40	0.40	0.40	0.41	0.41
1-10	:	0.42	0.43	0.43	0.43	0.44
11-21	:	0.39	0.39	0.40	0.40	0.40
CUMULATIVE % (8)						
1-5	:	25.6	25.6	25.6	25.6	25.6
6-10	:	26.3	26.3	26.3	26.3	26.3
11-16	:	23.7	23.7	23.8	23.8	23.8
17-21	:	24.3	24.3	24.3	24.3	24.3
1-10	:	52.0	51.9	52.0	52.0	51.9
11-21	:	48.0	48.1	48.0	48.0	48.1

(1): GALLONS PER RUN FOR EACH METER FOR TIME BETWEEN CURRENT AND PREVIOUS READINGS

(2): AVERAGE NUMBER OF GALLONS PER RUN FOR EACH METER DURING THE COURSE OF THE BROMIDE INJECTION EXPERIMENT

(3): GALLONS PER RUN FOR EACH SECTION OF PLOT FOR TIME BETWEEN CURRENT AND PREVIOUS READINGS

(4): AVERAGE NUMBER OF GALLONS PER RUN FOR EACH SECTION OF PLOT DURING COURSE OF THE BROMIDE INJECTION EXPERIMENT

(5): GALLONS PER RUN FOR EACH LINE IN EACH SECTION OF PLOT FOR TIME BETWEEN CURRENT AND PREVIOUS READINGS

(6): PERCENTAGE OF FLOW TO EACH SECTION OF PLOT FOR TIME BETWEEN CURRENT AND PREVIOUS READINGS

(7): GALLONS PER RUN FOR EACH LINE IN EACH SECTION OF PLOT DURING COURSE OF BROMIDE INJECTION EXPERIMENT

(8): PERCENTAGE OF FLOW TO EACH SECTION OF PLOT DURING COURSE OF BROMIDE INJECTION EXPERIMENT

DATE	:	4/15/88	4/18/88	4/21/88	4/23/88	4/25/88
TIME	:	13.00	16.00	9.00	10.00	15.00
TOTAL	:	371516.13	372263.89	372894.58	373361.09	373861
METER 1	:	11536.45	11678.01	11797.68	11885.24	11978.21
METER 2	:	96391.4	96770.01	97087.4	97320.8	97570.71
METER 3	:	65624.8	66038.49	66368.93	66620.28	66889.94
METER 4	:	11521.6	11658.88	11773.4	11858.19	11948.35
METER 5	:	3420.52	3468.71	3511.65	3541.9	3575.64
METER 6	:	813.68	821.84	825.82	832.24	839.18
METER 7	:	3013.08	3056.25	3096.7	3121.54	3147.33
BROMIDE						
EXP. DAYS	:	50.17	53.29	56.01	58.04	60.27
EXP. DAYS	:	443.21	446.33	449.04	451.08	453.29
# OFRUNS	:	49	75	65	49	53
DELTA/RUN (1)						
TOTAL	:	9.82	9.97	9.70	9.52	9.43
METER 1	:	1.87	1.89	1.84	1.79	1.75
METER 2	:	4.96	5.05	4.88	4.76	4.72
METER 3	:	5.31	5.52	5.08	5.13	5.09
METER 4	:	1.82	1.83	1.76	1.73	1.70
METER 5	:	0.64	0.64	0.66	0.62	0.64
METER 6	:	0.12	0.11	0.06	0.13	0.13
METER 7	:	0.54	0.58	0.62	0.51	0.49
CUMULATIVE						
TOTAL (2)		8.48	8.57	8.62	8.65	8.68
METER 1	:	1.63	1.65	1.66	1.66	1.67
METER 2	:	4.28	4.32	4.35	4.36	4.37
METER 3	:	4.58	4.63	4.65	4.67	4.68
METER 4	:	1.58	1.59	1.60	1.61	1.61
METER 5	:	0.53	0.54	0.54	0.55	0.55
METER 6	:	0.11	0.11	0.11	0.11	0.11
METER 7	:	0.47	0.48	0.49	0.49	0.49
PER RUN (3)						
% TOTAL	:	104.62	105.96	102.72	103.91	103.93
SOUTH	:	5.08	5.16	4.94	4.89	4.85
NORTH	:	5.19	5.41	5.02	5.00	4.96
SS5	:	2.50	2.53	2.50	2.40	2.39
S5	:	2.58	2.63	2.44	2.49	2.46
N6	:	2.83	3.00	2.64	2.76	2.77
NN5	:	2.36	2.41	2.38	2.24	2.19
CUMULATIVE (4)						
% TOTAL	:	104.41	104.52	104.42	104.40	104.38
SOUTH	:	4.39	4.43	4.46	4.47	4.48
NORTH	:	4.47	4.52	4.54	4.56	4.57
SS5	:	2.17	2.19	2.20	2.21	2.22
S5	:	2.22	2.24	2.25	2.26	2.27
N6	:	2.41	2.45	2.46	2.47	2.48
NN5	:	2.05	2.07	2.09	2.09	2.10

DATE	:	4/15/88	4/18/88	4/21/88	4/23/88	4/25/88
PER RUN						
PER LINE (5)						
1-5	:	0.50	0.51	0.50	0.48	0.48
6-10	:	0.52	0.53	0.49	0.50	0.49
11-16	:	0.47	0.50	0.44	0.46	0.46
17-21	:	0.47	0.48	0.48	0.45	0.44
1-10	:	0.51	0.52	0.49	0.49	0.48
11-21	:	0.47	0.49	0.46	0.45	0.45
PER RUN % (6)						
1-5	:	25.5	25.1	26.3	25.5	25.6
6-10	:	26.3	26.1	25.6	26.4	26.3
11-16	:	24.0	24.9	23.1	24.4	24.7
17-21	:	24.1	23.9	25.0	23.7	23.4
1-10	:	51.9	51.2	52.0	51.9	51.8
11-21	:	48.1	48.8	48.0	48.1	48.2
CUMULATIVE (7)						
1-5	:	0.43	0.44	0.44	0.44	0.44
6-10	:	0.44	0.45	0.45	0.45	0.45
11-16	:	0.40	0.41	0.41	0.41	0.41
17-21	:	0.41	0.41	0.42	0.42	0.42
1-10	:	0.44	0.44	0.45	0.45	0.45
11-21	:	0.41	0.41	0.41	0.41	0.42
CUMULATIVE % (8)						
1-5	:	25.6	25.6	25.6	25.6	25.6
6-10	:	26.3	26.3	26.2	26.2	26.2
11-16	:	23.8	23.9	23.8	23.8	23.9
17-21	:	24.3	24.3	24.3	24.3	24.3
1-10	:	51.9	51.9	51.9	51.9	51.9
11-21	:	48.1	48.1	48.1	48.1	48.1

(1): GALLONS PER RUN FOR EACH METER FOR TIME BETWEEN CURRENT AND PREVIOUS READINGS
(2): AVERAGE NUMBER OF GALLONS PER RUN FOR EACH METER DURING THE COURSE OF THE BROMIDE INJECTION EXPERIMENT
(3): GALLONS PER RUN FOR EACH SECTION OF PLOT FOR TIME BETWEEN CURRENT AND PREVIOUS READINGS
(4): AVERAGE NUMBER OF GALLONS PER RUN FOR EACH SECTION OF PLOT DURING COURSE OF THE BROMIDE INJECTION EXPERIMENT
(5): GALLONS PER RUN FOR EACH LINE IN EACH SECTION OF PLOT FOR TIME BETWEEN CURRENT AND PREVIOUS READINGS
(6): PERCENTAGE OF FLOW TO EACH SECTION OF PLOT FOR TIME BETWEEN CURRENT AND PREVIOUS READINGS
(7): GALLONS PER RUN FOR EACH LINE IN EACH SECTION OF PLOT DURING COURSE OF BROMIDE INJECTION EXPERIMENT
(8): PERCENTAGE OF FLOW TO EACH SECTION OF PLOT DURING COURSE OF BROMIDE INJECTION EXPERIMENT

DATE	:	4/27/88	4/30/88	5/3/88	5/5/88	5/9/88
TIME	:	15.00	11.00	13.00	13.00	12.00
TOTAL	:	374312.87	374928.43	375589.27	376050.77	376968.89
METER 1	:	12062.31	12176.56	12300.2	12385.71	12555.42
METER 2	:	97797.12	98104.01	98433.9	98664.35	99122.68
METER 3	:	67134.55	67465.97	67822.98	68070.42	68565.11
METER 4	:	12029.98	12140.27	12259.14	12342.05	12506.82
METER 5	:	3606.35	3649.45	3686.91	3728.29	3790.26
METER 6	:	846.99	857.05	867.29	874.8	888.04
METER 7	:	3172.15	3205.09	3240	3263.63	3313.59
BROMIDE						
EXP. DAYS	:	62.26	65.10	68.17	70.17	74.13
EXP. DAYS	:	455.29	458.13	461.21	463.21	467.17
# OFRUNS	:	48	68	74	48	95
DELTA/RUN (1)						
TOTAL	:	9.41	9.05	8.93	9.61	9.66
METER 1	:	1.75	1.68	1.67	1.78	1.79
METER 2	:	4.72	4.51	4.46	4.80	4.82
METER 3	:	5.10	4.87	4.82	5.16	5.21
METER 4	:	1.70	1.62	1.61	1.73	1.73
METER 5	:	0.64	0.63	0.51	0.86	0.65
METER 6	:	0.16	0.15	0.14	0.16	0.14
METER 7	:	0.52	0.48	0.47	0.49	0.53
CUMULATIVE						
TOTAL (2)		8.70	8.72	8.73	8.76	8.80
METER 1	:	1.67	1.67	1.67	1.67	1.68
METER 2	:	4.39	4.39	4.40	4.41	4.43
METER 3	:	4.70	4.71	4.71	4.72	4.75
METER 4	:	1.61	1.61	1.61	1.62	1.62
METER 5	:	0.55	0.56	0.55	0.56	0.57
METER 6	:	0.11	0.11	0.11	0.12	0.12
METER 7	:	0.49	0.49	0.49	0.49	0.49
PER RUN (3)						
% TOTAL	:	104.24	103.70	103.94	103.55	103.80
SOUTH	:	4.88	4.66	4.60	4.96	4.96
NORTH	:	4.93	4.73	4.69	5.00	5.07
SS5	:	2.39	2.31	2.18	2.64	2.44
S5	:	2.49	2.35	2.42	2.31	2.53
N6	:	2.72	2.62	2.61	2.78	2.81
NN5	:	2.22	2.11	2.08	2.22	2.26
CUMULATIVE (4)						
% TOTAL	:	104.38	104.34	104.33	104.30	104.27
SOUTH	:	4.50	4.51	4.51	4.52	4.55
NORTH	:	4.59	4.59	4.60	4.61	4.63
SS5	:	2.22	2.23	2.22	2.24	2.25
S5	:	2.28	2.28	2.29	2.29	2.30
N6	:	2.49	2.49	2.50	2.51	2.52
NN5	:	2.10	2.10	2.10	2.10	2.11

DATE	4/27/88	4/30/88	5/3/88	5/5/88	5/9/88
PER RUN					
PER LINE (5)					
1-5	0.48	0.46	0.44	0.53	0.49
6-10	0.50	0.47	0.48	0.46	0.51
11-16	0.45	0.44	0.43	0.46	0.47
17-21	0.44	0.42	0.42	0.44	0.45
1-10	0.49	0.47	0.46	0.50	0.50
11-21	0.45	0.43	0.43	0.45	0.46
PER RUN % (6)					
1-5	25.6	25.9	24.6	27.8	25.5
6-10	26.6	26.2	27.3	24.4	26.4
11-16	24.2	24.4	24.6	24.4	24.5
17-21	23.7	23.5	23.5	23.4	23.6
1-10	52.1	52.0	51.9	52.2	51.9
11-21	47.9	48.0	48.1	47.8	48.1
CUMULATIVE (7)					
1-5	0.44	0.45	0.44	0.45	0.45
6-10	0.46	0.46	0.46	0.46	0.46
11-16	0.41	0.42	0.42	0.42	0.42
17-21	0.42	0.42	0.42	0.42	0.42
1-10	0.45	0.45	0.45	0.45	0.45
11-21	0.42	0.42	0.42	0.42	0.42
CUMULATIVE % (8)					
1-5	25.6	25.6	25.6	25.7	25.6
6-10	26.3	26.3	26.3	26.2	26.3
11-16	23.9	23.9	23.9	24.0	24.0
17-21	24.2	24.2	24.2	24.1	24.1
1-10	51.9	51.9	51.9	51.9	51.9
11-21	48.1	48.1	48.1	48.1	48.1

(1): GALLONS PER RUN FOR EACH METER FOR TIME BETWEEN CURRENT AND PREVIOUS READINGS
(2): AVERAGE NUMBER OF GALLONS PER RUN FOR EACH METER DURING THE COURSE OF THE BROMIDE INJECTION EXPERIMENT
(3): GALLONS PER RUN FOR EACH SECTION OF PLOT FOR TIME BETWEEN CURRENT AND PREVIOUS READINGS
(4): AVERAGE NUMBER OF GALLONS PER RUN FOR EACH SECTION OF PLOT DURING COURSE OF THE BROMIDE INJECTION EXPERIMENT
(5): GALLONS PER RUN FOR, EACH LINE IN EACH SECTION OF PLOT FOR TIME BETWEEN CURRENT AND PREVIOUS READINGS
(6): PERCENTAGE OF FLOW TO EACH SECTION OF PLOT FOR TIME BETWEEN CURRENT AND PREVIOUS READINGS
(7): GALLONS PER RUN FOR EACH LINE IN EACH SECTION OF PLOT DURING COURSE OF BROMIDE INJECTION EXPERIMENT
(8): PERCENTAGE OF FLOW TO EACH SECTION OF PLOT DURING COURSE OF BROMIDE INJECTION EXPERIMENT

DATE	:	5/10/88	5/12/88	5/13/88	5/16/88	5/18/88
TIME	:	13.00	14.00	15.00	14.00	13.00
TOTAL	:	377209.55	377680.28	377918.63	378593.29	379040.03
METER 1	:	12599.89	12686.89	12731.12	12857.34	12940.68
METER 2	:	99242.22	99475.9	99594.42	99931.09	100153.89
METER 3	:	68695.41	68950.57	69079.62	69443.17	69683.79
METER 4	:	12550.3	12635.09	12677.94	12796.58	12875.6
METER 5	:	3806.69	3838.49	3854.72	3900.4	3930.19
METER 6	:	891.05	898.02	901.88	909.98	915.39
METER 7	:	3327.03	3353.61	3366.9	3409.16	3436.77
BROMIDE						
EXP. DAYS	:	75.18	77.22	78.26	81.23	83.17
EXP. DAYS	:	468.21	470.25	471.29	474.25	476.21
# OFRUNS	:	25	49	25	71	47
DELTA/RUN (1)						
TOTAL	:	9.63	9.61	9.53	9.50	9.51
METER 1	:	1.78	1.78	1.77	1.78	1.77
METER 2	:	4.78	4.77	4.74	4.74	4.74
METER 3	:	5.21	5.21	5.16	5.12	5.12
METER 4	:	1.74	1.73	1.71	1.67	1.68
METER 5	:	0.66	0.65	0.65	0.64	0.63
METER 6	:	0.12	0.14	0.15	0.11	0.12
METER 7	:	0.54	0.54	0.53	0.60	0.59
CUMULATIVE						
TOTAL (2)		8.81	8.83	8.84	8.87	8.88
METER 1	:	1.68	1.68	1.68	1.69	1.69
METER 2	:	4.43	4.44	4.45	4.46	4.46
METER 3	:	4.76	4.77	4.77	4.79	4.79
METER 4	:	1.62	1.63	1.63	1.63	1.63
METER 5	:	0.57	0.57	0.57	0.57	0.58
METER 6	:	0.12	0.12	0.12	0.12	0.12
METER 7	:	0.49	0.49	0.49	0.50	0.50
PER RUN (3)						
% TOTAL	:	103.81	103.85	103.87	103.79	103.73
SOUTH	:	4.90	4.91	4.90	4.86	4.86
NORTH	:	5.09	5.07	5.01	5.01	5.00
SS5	:	2.44	2.42	2.42	2.42	2.41
S5	:	2.47	2.49	2.48	2.43	2.45
N6	:	2.81	2.79	2.76	2.74	2.74
NN5	:	2.28	2.27	2.25	2.27	2.27
CUMULATIVE (4)						
% TOTAL	:	104.27	104.25	104.25	104.23	104.22
SOUTH	:	4.55	4.56	4.56	4.57	4.58
NORTH	:	4.64	4.65	4.66	4.67	4.68
SS5	:	2.25	2.25	2.26	2.26	2.27
S5	:	2.30	2.31	2.31	2.31	2.32
N6	:	2.52	2.53	2.54	2.54	2.55
NN5	:	2.11	2.12	2.12	2.13	2.13

DATE	:	5/10/88	5/12/88	5/13/88	5/16/88	5/18/88
PER RUN PER LINE (5)						
1-5	:	0.49	0.48	0.48	0.48	0.48
6-10	:	0.49	0.50	0.50	0.49	0.49
11-16	:	0.47	0.47	0.46	0.46	0.46
17-21	:	0.46	0.45	0.45	0.45	0.45
1-10	:	0.49	0.49	0.49	0.49	0.49
11-21	:	0.46	0.46	0.46	0.46	0.45
PER RUN % (6)						
1-5	:	25.6	25.5	25.6	25.7	25.6
6-10	:	25.9	26.1	26.2	25.9	26.0
11-16	:	24.6	24.5	24.4	24.3	24.2
17-21	:	23.9	23.9	23.8	24.1	24.1
1-10	:	51.4	51.6	51.8	51.6	51.6
11-21	:	48.6	48.4	48.2	48.4	48.4
CUMULATIVE (7)						
1-5	:	0.45	0.45	0.45	0.45	0.45
6-10	:	0.46	0.46	0.46	0.46	0.46
11-16	:	0.42	0.42	0.42	0.42	0.42
17-21	:	0.42	0.42	0.42	0.43	0.43
1-10	:	0.46	0.46	0.46	0.46	0.46
11-21	:	0.42	0.42	0.42	0.42	0.43
CUMULATIVE % (8)						
1-5	:	25.6	25.6	25.6	25.6	25.6
6-10	:	26.2	26.2	26.2	26.2	26.2
11-16	:	24.0	24.0	24.0	24.0	24.0
17-21	:	24.1	24.1	24.1	24.1	24.1
1-10	:	51.9	51.9	51.9	51.9	51.9
11-21	:	48.1	48.1	48.1	48.1	48.1

(1): GALLONS PER RUN FOR EACH METER FOR TIME BETWEEN CURRENT AND PREVIOUS READINGS
(2): AVERAGE NUMBER OF GALLONS PER RUN FOR EACH METER DURING THE COURSE OF THE BROMIDE INJECTION EXPERIMENT
(3): GALLONS PER RUN FOR EACH SECTION OF PLOT FOR TIME BETWEEN CURRENT AND PREVIOUS READINGS
(4): AVERAGE NUMBER OF GALLONS PER RUN FOR EACH SECTION OF PLOT DURING COURSE OF THE BROMIDE INJECTION EXPERIMENT
(5): GALLONS PER RUN FOR EACH LINE IN EACH SECTION OF PLOT FOR TIME BETWEEN CURRENT AND PREVIOUS READINGS
(6): PERCENTAGE OF FLOW TO EACH SECTION OF PLOT FOR TIME BETWEEN CURRENT AND PREVIOUS READINGS
(7): GALLONS PER RUN FOR EACH LINE IN EACH SECTION OF PLOT DURING COURSE OF BROMIDE INJECTION EXPERIMENT
(8): PERCENTAGE OF FLOW TO EACH SECTION OF PLOT DURING COURSE OF BROMIDE INJECTION EXPERIMENT

DATE	:	5/21/88	5/23/88	5/25/88	5/27/88	5/30/88
TIME	:	14.00	12.00	13.00	9.00	7.00
TOTAL	:	379750.71	380197.2	380658.72	381067.83	381726.11
METER 1	:	13074.31	13158.2	13244.51	13321.44	13445.44
METER 2	:	100509.78	100733.12	100964.24	101169.29	101499.27
METER 3	:	70064.5	70304.43	70552.5	70771.66	71123.53
METER 4	:	12997.04	13076.59	13156.52	13227.31	13340.8
METER 5	:	3976.59	4005.64	4036.23	4062.72	4105.8
METER 6	:	924.18	930.52	935.89	938.77	945.5
METER 7	:	3485.83	3510.28	3541.41	3569.41	3613.79
BROMIDE						
EXP. DAYS	:	86.21	88.14	90.19	92.01	94.94
EXP. DAYS	:	479.25	481.17	483.21	485.04	487.96
# OFRUNS	:	73	46	49	44	70
DELTA/RUN (1)						
TOTAL	:	9.74	9.71	9.42	9.30	9.40
METER 1	:	1.83	1.82	1.76	1.75	1.77
METER 2	:	4.88	4.86	4.72	4.66	4.71
METER 3	:	5.22	5.22	5.06	4.98	5.03
METER 4	:	1.66	1.73	1.63	1.61	1.62
METER 5	:	0.64	0.63	0.62	0.60	0.62
METER 6	:	0.12	0.14	0.11	0.07	0.10
METER 7	:	0.67	0.53	0.64	0.64	0.63
CUMULATIVE						
TOTAL (2)		8.91	8.93	8.94	8.95	8.96
METER 1	:	1.69	1.70	1.70	1.70	1.70
METER 2	:	4.48	4.49	4.49	4.50	4.50
METER 3	:	4.81	4.82	4.82	4.83	4.83
METER 4	:	1.63	1.63	1.63	1.63	1.63
METER 5	:	0.58	0.58	0.58	0.58	0.58
METER 6	:	0.12	0.12	0.12	0.12	0.12
METER 7	:	0.50	0.51	0.51	0.51	0.51
PER RUN (3)						
% TOTAL	:	103.65	103.76	103.83	103.69	103.58
SOUTH	:	5.00	4.99	4.83	4.73	4.81
NORTH	:	5.09	5.08	4.95	4.92	4.93
SS5	:	2.47	2.46	2.39	2.35	2.39
S5	:	2.53	2.54	2.44	2.38	2.42
N6	:	2.76	2.82	2.69	2.67	2.68
NN5	:	2.34	2.26	2.27	2.25	2.26
CUMULATIVE (4)						
% TOTAL	:	104.20	104.19	104.18	104.17	104.15
SOUTH	:	4.60	4.60	4.61	4.61	4.62
NORTH	:	4.69	4.70	4.70	4.71	4.72
SS5	:	2.27	2.28	2.28	2.28	2.28
S5	:	2.32	2.33	2.33	2.33	2.33
N6	:	2.55	2.56	2.56	2.57	2.57
NN5	:	2.14	2.14	2.14	2.14	2.15

DATE	:	5/21/88	5/23/88	5/25/88	5/27/88	5/30/88
PER RUN						
PER LINE (5)						
1-5	:	0.49	0.49	0.48	0.47	0.48
6-10	:	0.51	0.51	0.49	0.48	0.48
11-16	:	0.46	0.47	0.45	0.45	0.45
17-21	:	0.47	0.45	0.45	0.45	0.45
1-10	:	0.50	0.50	0.48	0.47	0.48
11-21	:	0.46	0.46	0.45	0.45	0.45
PER RUN % (6)						
1-5	:	25.6	25.6	25.6	25.6	25.7
6-10	:	26.3	26.4	26.2	25.8	26.1
11-16	:	23.9	24.5	24.0	24.2	24.0
17-21	:	24.3	23.5	24.3	24.4	24.3
1-10	:	51.9	52.0	51.7	51.4	51.8
11-21	:	48.1	48.0	48.3	48.6	48.2
CUMULATIVE (7)						
1-5	:	0.45	0.46	0.46	0.46	0.46
6-10	:	0.46	0.47	0.47	0.47	0.47
11-16	:	0.43	0.43	0.43	0.43	0.43
17-21	:	0.43	0.43	0.43	0.43	0.43
1-10	:	0.46	0.46	0.46	0.46	0.46
11-21	:	0.43	0.43	0.43	0.43	0.43
CUMULATIVE % (8)						
1-5	:	25.6	25.6	25.6	25.6	25.6
6-10	:	26.2	26.2	26.2	26.2	26.2
11-16	:	24.0	24.0	24.0	24.0	24.0
17-21	:	24.1	24.1	24.1	24.1	24.1
1-10	:	51.9	51.9	51.9	51.9	51.9
11-21	:	48.1	48.1	48.1	48.1	48.1

(1): GALLONS PER RUN FOR EACH METER FOR TIME BETWEEN CURRENT AND PREVIOUS READINGS
(2): AVERAGE NUMBER OF GALLONS PER RUN FOR EACH METER DURING THE COURSE OF THE BROMIDE INJECTION EXPERIMENT
(3): GALLONS PER RUN FOR EACH SECTION OF PLOT FOR TIME BETWEEN CURRENT AND PREVIOUS READINGS
(4): AVERAGE NUMBER OF GALLONS PER RUN FOR EACH SECTION OF PLOT DURING COURSE OF THE BROMIDE INJECTION EXPERIMENT
(5): GALLONS PER RUN FOR EACH LINE IN EACH SECTION OF PLOT FOR TIME BETWEEN CURRENT AND PREVIOUS READINGS
(6): PERCENTAGE OF FLOW TO EACH SECTION OF PLOT FOR TIME BETWEEN CURRENT AND PREVIOUS READINGS
(7): GALLONS PER RUN FOR EACH LINE IN EACH SECTION OF PLOT DURING COURSE OF BROMIDE INJECTION EXPERIMENT
(8): PERCENTAGE OF FLOW TO EACH SECTION OF PLOT DURING COURSE OF BROMIDE INJECTION EXPERIMENT

DATE	:	6/2/88	6/5/88	6/7/88	6/8/88	6/10/88
TIME	:	12.00	15.00	7.00	8.00	7.00
TOTAL	:	382445.01	383142.64	383530.92	383765.66	384215.83
METER 1	:	13581.11	13712.3	13785.25	13829.3	13913.7
METER 2	:	101859.75	102210.58	102405.2	102522.32	102747.3
METER 3	:	71508.58	71882.83	72090.6	72215.62	72455.82
METER 4	:	13464.16	13584.4	13651.34	13692.18	13769.8
METER 5	:	4152.78	4197.79	4222.66	4237.5	4265.75
METER 6	:	953.4	961.13	965.69	968.69	973.74
METER 7	:	3663.15	3719.95	3735.25	3750.26	3779.58
BROMIDE						
EXP. DAYS	:	98.14	101.25	102.93	103.98	105.94
EXP. DAYS	:	491.17	494.29	495.96	497.00	498.96
# OFRUNS	:	77	75	40	25	47
DELTA/RUN (1)						
TOTAL	:	9.34	9.30	9.71	9.39	9.58
METER 1	:	1.76	1.75	1.82	1.76	1.80
METER 2	:	4.68	4.68	4.87	4.68	4.79
METER 3	:	5.00	4.99	5.19	5.00	5.11
METER 4	:	1.60	1.60	1.67	1.63	1.65
METER 5	:	0.61	0.60	0.62	0.59	0.60
METER 6	:	0.10	0.10	0.11	0.12	0.11
METER 7	:	0.64	0.76	0.38	0.60	0.62
CUMULATIVE						
TOTAL (2)		8.97	8.99	9.00	9.00	9.01
METER 1	:	1.70	1.70	1.71	1.71	1.71
METER 2	:	4.51	4.51	4.52	4.52	4.53
METER 3	:	4.84	4.84	4.85	4.85	4.85
METER 4	:	1.63	1.63	1.63	1.63	1.63
METER 5	:	0.58	0.58	0.58	0.58	0.58
METER 6	:	0.12	0.12	0.12	0.12	0.12
METER 7	:	0.52	0.53	0.52	0.52	0.53
PER RUN (3)						
% TOTAL	:	103.70	103.93	103.63	103.15	103.33
SOUTH	:	4.78	4.78	4.98	4.80	4.89
NORTH	:	4.90	4.89	5.08	4.88	5.00
SS5	:	2.37	2.35	2.45	2.36	2.40
S5	:	2.41	2.43	2.53	2.45	2.50
N6	:	2.65	2.53	3.02	2.65	2.73
NN5	:	2.24	2.36	2.06	2.23	2.28
CUMULATIVE (4)						
% TOTAL	:	104.13	104.13	104.12	104.11	104.09
SOUTH	:	4.62	4.63	4.63	4.64	4.64
NORTH	:	4.72	4.73	4.73	4.73	4.74
SS5	:	2.29	2.29	2.29	2.29	2.29
S5	:	2.34	2.34	2.34	2.34	2.35
N6	:	2.57	2.57	2.58	2.58	2.58
NN5	:	2.15	2.16	2.16	2.16	2.16

DATE	:	6/2/88	6/5/88	6/7/88	6/8/88	6/10/88
PER RUN						
PER LINE (5)						
1-5	:	0.47	0.47	0.49	0.47	0.48
6-10	:	0.48	0.49	0.51	0.49	0.50
11-16	:	0.44	0.42	0.50	0.44	0.45
17-21	:	0.45	0.47	0.41	0.45	0.46
1-10	:	0.48	0.48	0.50	0.48	0.49
11-21	:	0.45	0.44	0.46	0.44	0.45
PER RUN % (6)						
1-5	:	25.7	25.4	25.6	25.5	25.4
6-10	:	26.1	26.3	26.5	26.5	26.4
11-16	:	23.9	22.8	26.4	23.9	24.1
17-21	:	24.3	25.5	21.5	24.2	24.1
1-10	:	51.8	51.8	51.9	52.0	51.8
11-21	:	48.2	48.2	48.1	48.0	48.2
CUMULATIVE (7)						
1-5	:	0.46	0.46	0.46	0.46	0.46
6-10	:	0.47	0.47	0.47	0.47	0.47
11-16	:	0.43	0.43	0.43	0.43	0.43
17-21	:	0.43	0.43	0.43	0.43	0.43
1-10	:	0.46	0.46	0.46	0.46	0.46
11-21	:	0.43	0.43	0.43	0.43	0.43
CUMULATIVE % (8)						
1-5	:	25.6	25.6	25.6	25.6	25.6
6-10	:	26.2	26.2	26.2	26.2	26.2
11-16	:	24.0	24.0	24.0	24.0	24.0
17-21	:	24.1	24.2	24.1	24.1	24.1
1-10	:	51.9	51.9	51.9	51.9	51.9
11-21	:	48.1	48.1	48.1	48.1	48.1

(1): GALLONS PER RUN FOR EACH METER FOR TIME BETWEEN CURRENT AND PREVIOUS READINGS
(2): AVERAGE NUMBER OF GALLONS PER RUN FOR EACH METER DURING THE COURSE OF THE BROMIDE INJECTION EXPERIMENT
(3): GALLONS PER RUN FOR EACH SECTION OF PLOT FOR TIME BETWEEN CURRENT AND PREVIOUS READINGS
(4): AVERAGE NUMBER OF GALLONS PER RUN FOR EACH SECTION OF PLOT DURING COURSE OF THE BROMIDE INJECTION EXPERIMENT
(5): GALLONS PER RUN FOR EACH LINE IN EACH SECTION OF PLOT FOR TIME BETWEEN CURRENT AND PREVIOUS READINGS
(6): PERCENTAGE OF FLOW TO EACH SECTION OF PLOT FOR TIME BETWEEN CURRENT AND PREVIOUS READINGS
(7): GALLONS PER RUN FOR EACH LINE IN EACH SECTION OF PLOT DURING COURSE OF BROMIDE INJECTION EXPERIMENT
(8): PERCENTAGE OF FLOW TO EACH SECTION OF PLOT DURING COURSE OF BROMIDE INJECTION EXPERIMENT

DATE	:	6/13/88	6/15/88
TIME	:	11.00	9.00
TOTAL	:	384960.43	385221.82
METER 1	:	14063.32	14112.89
METER 2	:	103115.74	103244.59
METER 3	:	72854.2	72995.3
METER 4	:	13898.85	13944.59
METER 5	:	4359.9	4377.8
METER 6	:	1019.9	1025.68
METER 7	:	3811.08	3827.63
BROMIDE			
EXP. DAYS	:	109.11	111.00
EXP. DAYS	:	502.13	504.04
# OFRUNS	:	76	46
DELTA/RUN (1)			
TOTAL	:	9.80	5.68
METER 1	:	1.97	1.08
METER 2	:	4.85	2.80
METER 3	:	5.24	3.07
METER 4	:	1.70	0.99
METER 5	:	1.24	0.39
METER 6	:	0.61	0.13
METER 7	:	0.41	0.36
CUMULATIVE			
TOTAL (2)		9.03	8.98
METER 1	:	1.72	1.71
METER 2	:	4.53	4.51
METER 3	:	4.87	4.84
METER 4	:	1.63	1.62
METER 5	:	0.60	0.60
METER 6	:	0.13	0.13
METER 7	:	0.52	0.52
PER RUN (3)			
% TOTAL	:	102.98	103.27
SOUTH	:	5.46	2.93
NORTH	:	4.63	2.94
SS5	:	3.21	1.47
S5	:	2.25	1.46
N6	:	2.52	1.59
NN5	:	2.11	1.35
CUMULATIVE (4)			
% TOTAL	:	104.06	104.05
SOUTH	:	4.66	4.63
NORTH	:	4.74	4.71
SS5	:	2.32	2.31
S5	:	2.34	2.33
N6	:	2.58	2.56
NN5	:	2.16	2.14

DATE	:	6/13/88	6/15/88
PER RUN			
PER LINE (5)			
1-5	:	0.64	0.29
6-10	:	0.45	0.29
11-16	:	0.42	0.26
17-21	:	0.42	0.27
1-10	:	0.55	0.29
11-21	:	0.42	0.27
PER RUN % (6)			
1-5	:	33.2	26.2
6-10	:	23.2	26.1
11-16	:	21.7	23.6
17-21	:	21.8	24.2
1-10	:	56.4	52.3
11-21	:	43.6	47.7
CUMULATIVE (7)			
1-5	:	0.46	0.46
6-10	:	0.47	0.47
11-16	:	0.43	0.43
17-21	:	0.43	0.43
1-10	:	0.47	0.46
11-21	:	0.43	0.43
CUMULATIVE % (8)			
1-5	:	25.9	25.9
6-10	:	26.1	26.1
11-16	:	24.0	24.0
17-21	:	24.0	24.0
1-10	:	52.0	52.0
11-21	:	48.0	48.0

(1): GALLONS PER RUN FOR EACH METER FOR TIME B
AND PREVIOUS READINGS
(2): AVERAGE NUMBER OF GALLONS PER RUN FOR EAC
THE COURSE OF THE BROMIDE INJECTION EXPER
(3): GALLONS PER RUN FOR EACH SECTION OF PLOT
BETWEEN CURRENT AND PREVIOUS READINGS
(4): AVERAGE NUMBER OF GALLONS PER RUN FOR EAC
PLOT DURING COURSE OF THE BROMIDE INJECTI
(5): GALLONS PER RUN FOR EACH LINE IN EACH SEC
TIME BETWEEN CURRENT AND PREVIOUS READING
(6): PERCENTAGE OF FLOW TO EACH SECTION OF PLO
BETWEEN CURRENT AND PREVIOUS READINGS
(7): GALLONS PER RUN FOR EACH LINE IN EACH SEC
DURING COURSE OF BROMIDE INJECTION EXPERI
(8): PERCENTAGE OF FLOW TO EACH SECTION OF PLO
COURSE OF BROMIDE INJECTION EXPERIMENT

APPENDIX E

FORTRAN LISTING OF TRAP2 CODE.

```
C       THIS PROGRAM CALCULATES THE AREA UNDER A SET OF DATA POINTS
C       BY FIRST FITTING A POLYNOMIAL TO THE DATA POINTS USING CUBIC
C       SPLINE INTERPOLATION, AND SECONDLY,  PERFORMING NUMERICAL
C       INTEGRATION ON THE POLYNOMIAL BY SIMPSON'S RULE.
C
C       PROGRAM WRITTEN BY JAMES A.BEACH. 4/10/89
C
        character*80 filin,filout
        common/data/ X(0:100),A(0:100),H(0:100),ALF(0:100),C(0:100),
     * PP(0:5000),RL(0:100),RMU(0:100),Z(0:100),B(0:100),D(0:100),
     * PRED(5000)
        COMMON/INT/ NPR,NOBS
C
        write(*,*)'enter the output file'
        read(*,'(a)')filout
        OPEN(91,FILE=FILOUT,STATUS='UNKNOWN')
C
        call cubic
        call area
C
        STOP
        END
C
        SUBROUTINE AREA
C=============================================================  SUBROUTINE AREA
C
C       SUBROUTINE TO CALCULATE AREA UNDER A CURVE THROUGH SIMPSON'S RULE
C=============================================================================
        common/data/ X(0:100),A(0:100),H(0:100),ALF(0:100),C(0:100),
     * PP(0:5000),RL(0:100),RMU(0:100),Z(0:100),B(0:100),D(0:100),
     * PRED(5000)
        COMMON/INT/ NPR,NOBS
C
        SUM=0.
        BMA=X(NOBS-1)-X(0)
        DO 100 I=2,NPR-1
             SUM=SUM+(2.*PRED(I))
100     CONTINUE
        ENDS=PRED(1)+PRED(NPR)
        RMASS =.5*(ENDS + SUM)*BMA/NPR
        WRITE(*,*)' TOTAL MASS =',RMASS
        WRITE(91,*) ' TOTAL MASS =',RMASS
        RETURN
        END
C
        SUBROUTINE CUBIC
C=============================================================  SUBROUTINE CUBIC
C
C       SUBROUTINE TO PERFORM CUBIC SPLINE INTERPOLATION
C=============================================================================
        common/data/ X(0:100),A(0:100),H(0:100),ALF(0:100),C(0:100),
     * PP(0:5000),RL(0:100),RMU(0:100),Z(0:100),B(0:100),D(0:100),
     * PRED(5000)
        COMMON/INT/ NPR,NOBS

        CHARACTER *70 FILIN,STUFF
        ITASK=4
        WRITE(*,*)' ENTER THE DATA FILE NAME'
```

```
      Read(*,'(A)')FILIN
      OPEN(90,FILE=FILIN,STATUS='OLD')
      WRITE(91,*)' CALCULATIONS FROM DATA CONTAINED IN FILE :',FILIN
      WRITE(*,*)' ENTER TEXT TO HELP YOU IDENTIFY THIS RUN'
      READ(*,'(A)')STUFF
      WRITE(91,*)STUFF
      WRITE(91,*)'
      WRITE(*,*)'       INPUT DATA'
      WRITE(91,*)'            INPUT DATA'
      DO 100 I=0,100
        READ(90,*,END=101)X(I),A(I)
        WRITE(*,*)I+1,X(I),A(I)
        WRITE(91,*)X(I),A(I)
100   CONTINUE
101   NPTS=I-1
      NOBS=NPTS+1
      WRITE(*,*)'  NUMBER OF OBSERVATIONS =',NOBS
      DO 200 I=0,NPTS-1
         H(I)=X(I+1)-X(I)
200   CONTINUE
      IF(ITASK.EQ.5)THEN
          WRITE(*,*)' ENTER DERIVATIVE AT X(0) AND X(NPTS)'
          READ(*,*)FP0,FPN
          ALF(0)=(3.*(A(1)-A(0))/H(0)) - 3.*FP0
          ALF(NPTS)=3.*FPN-(3.*(A(NPTS)-A(NPTS-1))/H(NPTS-1))
      ENDIF
      DO 300 I=1,NPTS-1
         ALF(I)=3.*(A(I+1)*H(I-1)-A(I)*(X(I+1)-X(I-1))+A(I-1)*H(I))
     *                /(H(I-1)*H(I))
300   CONTINUE
C
      IF(ITASK.EQ.4)THEN
           rl(0)=1.
           RMU(0)=0.
           Z(0)=0.
      ELSEIF(ITASK.EQ.5)THEN
           rl(0)=2.*H(0)
           RMU(0)=.5
           Z(0)=ALF(0)/rl(0)
      ENDIF
C
      DO 400 I=1,NPTS-1
          rl(I)=(2.*(X(I+1)-X(I-1)))-(H(I-1)*RMU(I-1))
          RMU(I)=H(I)/rl(I)
          Z(I)=(ALF(I)-H(I-1)*Z(I-1))/rl(I)
400   CONTINUE
      IF(ITASK.EQ.4)THEN
           rl(NPTS)=1.
           C(NPTS)=0.
           Z(NPTS)=0.
      ELSEIF(ITASK.EQ.5)THEN
          rl(NPTS)=H(NPTS-1)*(2.-RMU(NPTS-1))
          Z(NPTS)=(ALF(NPTS)-H(NPTS-1)*Z(NPTS-1))/rl(NPTS)
          C(NPTS)=Z(NPTS)
      ENDIF

      DO 500 J=NPTS-1,0,-1
          C(J)=Z(J)-RMU(J)*C(J+1)
```

```
            B(J)=(A(J+1)-A(J))/H(J)-((H(J)*(C(J+1)+2.*C(J)))/3.)
            D(J)=(C(J+1)-C(J))/(3.*H(J))
  500   CONTINUE
        DO 600 K=0,NPTS-1
            WRITE(*,1005)K,X(K),A(K),B(K),C(K),D(K)
  600   CONTINUE
C
          WRITE(*,*)'ENTER THE # OF DIVISIONS FOR CUBIC SPLINE'
          WRITE(*,*)'    BETWEEN EACH OBSERVATION'
          READ(*,*)IB
           NPR=NOBS*IB
           DELX = (X(NPTS)-X(0))/NPR
           PP(0)=X(0)-DELX
           DO 725 IJ=1,NPR
             PP(IJ)=PP(IJ-1)+DELX
              DO 700 K=0,NPTS
                IF(PP(IJ).GE.X(K).AND.PP(IJ).LT.X(K+1)) THEN
                  KP=K
                ENDIF
  700           CONTINUE
         PRED(IJ)=A(KP)+B(KP)*(PP(IJ)-X(KP))+(C(KP)*(PP(IJ)-X(KP))**2)+
     *              (D(KP)*(PP(IJ)-X(KP))**3)
  725     CONTINUE
  1010    FORMAT(8G10.3)
  1005    FORMAT(I6,5(G11.3,1X))
        RETURN
        END
C
```